

A STUDY OF SILICON-BASED MATERIALS
AS MATRICES
FOR
MALDI-TOF MS

**A STUDY OF SILICON-BASED MATERIALS
AS MATRICES
FOR
MATRIX-ASSISTED LASER DESORPTION/IONIZATION-TIME-OF-FLIGHT
MASS SPECTROMETRY**

**By
SANELA MARTIC, B.Sc.**

**A Thesis submitted to
The School of Graduate Studies
in Partial Fulfillment of the Requirements
for the degree:
Master of Science**

McMaster University

© Copyright by Sanela Martic, August 2005

MASTER OF SCIENCE (2005)

McMASTER UNIVERSITY

(Chemistry)

Hamilton, Ontario

TITLE: **A Study of Silicon-Based Materials as
Matrices for Matrix-Assisted Laser
Desorption/Ionization Time-of-Flight Mass
Spectrometry**

AUTHOR: **Sanela Martic, B.Sc. (Bishop's University)**

SUPERVISOR: **Dr. M.A. Brook**

NUMBER OF PAGES: **xvi, 148**

Abstract

This thesis provides examples of new solid supports for Matrix-Assisted Laser Desorption Ionization Time-of-Flight (MALDI-TOF) in two parts.

Firstly, mesoporous and macroporous silicas were developed as new supports for the elimination of low mass interference signals in the mass spectrum. Due to the complexity of the system, a variety of factors were studied, such as sol gel morphology, matrix crystallization, polymeric molecular weight and concentration. It was observed that the mesoporous silicas and higher matrix crystallization were advantageous for optimal signal intensity and signal-to-background ratio.

Secondly, due to the inconsistencies in the literature apropos the role of the matrix in MALDI process, we have developed chemically modified compounds and studied these as alternative MALDI matrices. It was concluded that for optimal free matrix performance, the phenolic groups were desirable while crystallization was not required. Moreover, a highly selective covalently linked silicon-based matrix was developed, which yielded a superior signal-to-background ratio at moderate signal intensities. A chemical nature of matrix and sol gel processing methodology used were the relevant factors to be considered when optimizing a tethered matrix. It was demonstrated that requirements for free and surface-bound matrices were different; hence, suggesting the drastic difference in their operating mechanisms during MALDI process.

ACKNOWLEDGMENT

I would like to thank Dr. M.A. Brook for the opportunity to work in his lab and for all the valuable guidance and encouragement he has given me throughout the period of my research and during writing of this thesis. In addition, I would like to thank Natural Sciences and Engineering Research Council of Canada (NSERC) and MDS Sciex for financial support. Special thanks are given to Dr. Noemi Nagy for her valuable scientific contributions and suggestions.

Thanks to all my co-workers over the past two years for providing me with valuable help and a most friendly atmosphere.

Dr. Yan Gao	Dr. Yang Chen
Lihua Liu	Dr. Zheng Zhang
Hazem Amarne	Dr. Amro Ragheb
Dr. Ferdinand Gonzaga	Dave Thompson
Weian Zhao	Forrest (Li) Gan
Lucy Ye	

Finally, I would like to express my sincerest thanks to my family and to John for their infinite generosity and understanding.

Dragi tata i mama, voljela bih da vam se zahvalim što ste odlučili da se naselite u Kanadi. Zbog vašeg nesebičnog čina, moje i Marijanine želje se ispunjavaju. Na nama je sad da vam vratimo, na neki način, to što ste vi nama prožuli svih ovih godina. Nadam se da ću, kroz ovaj život, uspjeti da zadovoljim sve vaše nade i da ponosno ispunim ulogu kćerke koju vi želite.

Table of Contents

Abstract	iii
Acknowledgment	iv
Table of Contents	v
List of Tables	ix
List of Figures	xi
List of Schemes	xiv
List of Abbreviations	xv
CHAPTER 1. INTRODUCTION	17
1.1 MALDI-TOF Overview	17
1.2 The Role of Matrix in UV-MALDI	18
1.3 MALDI Limitations and Solutions	20
1.3.1 Inorganic Matrix Approach	21
1.3.2 Surface-Based Approach	22
1.4 Research Goals	26
1.5 Outline of the Thesis	27
1.6 References	27
CHAPTER 2. HIGH SURFACE AREA MALDI-TOF SUPPORTS	31
2.1 Introduction	31
2.2 Results	34
2.2.1 Standard MALDI Protocol	38
2.2.2 Matrix in Silica Films	41

2.2.2.1	DHB in Meso/macroporous Silica	41
2.2.2.2	DHB in PEO-Free Mesoporous Silica	43
2.2.3	Matrix on Silica Films	47
2.2.3.1	Porous Silica (treated and untreated)	47
2.2.3.2	Other Matrices on Meso/macroporous Silica	54
2.2.4	Location of the Analyte	56
2.2.5	Spot-to-Spot Reproducibility	57
2.3	Discussion	58
2.3.1	Matrix Crystallinity	58
2.3.2	Effect of Incorporating DHB in Mesoporous Silica	59
2.3.3	Effect of Silica on Signal Intensity (DHB and analyte placed on top)	61
2.4	Conclusions	63
2.5	Experimental Procedure	63
2.5.1	Chemicals	63
2.5.2	Sol Gel Preparation	64
2.5.3	Formation of the MALDI Support Film	66
2.5.4	MALDI Sample Preparation	67
2.5.5	MALDI Instrumentation	69
2.5.6	Characterization Studies	69
2.6	References	70
CHAPTER 3. HIGHLY SELECTIVE TETHERED MALDI MATRIX		73
3.1	Introduction	73

3.2 Results and Discussions	77
3.2.1 Synthesis	77
3.2.2 Synthetic Methods Used	78
3.2.3 UV Studies	81
3.2.4 Crystal Formation and Morphology of Synthetic Matrices	86
3.2.5 Effect of Functionality on MALDI	90
3.2.6 Silicon-Containing MALDI-TOF Matrices	98
3.2.7 Nature of Binding to the MALDI Surfaces	99
3.3 Summary	105
3.4 Conclusions	106
3.5 Experimental Section	106
3.5.1 Chemicals	106
3.5.2 Characterization	107
3.5.3 Synthesis of Protected Matrices	108
3.5.3.1 Methyl 2,5-dihydroxybenzoate, 19	108
3.5.3.2 3-Allyloxy-4-hydroxybenzaldehyde; 4-allyloxy-3-hydroxybenzaldehyde, 18 ; 3,4-diallyloxybenzaldehyde, 7	109
3.5.3.3 3-Allyloxy-4-hydroxy-methyl cinnamate; 4-allyloxy-3-hydroxy-methyl cinnamate, 12 ; 3,4-diallyloxy-methyl cinnamate, 11	111
3.5.3.4 <i>N</i> -Allyl-2,5-dihydroxy-benzamide, 15	112
3.5.3.5 <i>N</i> -Allyl-3-cyano-3-(4-hydroxy-phenyl)acrylamide, 8	114

3.5.3.6	<i>N</i> -Allyl-3,4-dihydroxybenzamide, 9	115
3.5.3.7	Methyl-4-hydroxy-3-methoxybenzoate, 21	116
3.5.3.8	Ethyl-4-allyloxy-3-methoxybenzoate, 22	117
3.5.3.9	Methyl-3,4-dihydroxycinnamate, 14	118
3.5.3.10	<i>N</i> -Allyl-2,5-dibenzylbenzamide, 23	119
3.5.4	Synthesis of Sol Gel Precursors	120
3.5.4.1	6-Hydroxy- <i>N</i> -(3-propyltriethoxysilyl)-phthalamic acid; 3-Hydroxy- <i>N</i> -(3-propyltriethoxysilyl)-phthalamic acid, 2	120
3.5.4.2	Ethyl-3-methoxy-4-(3-propyltriethoxysilyl)benzoate, 1	121
3.5.4.3	<i>N</i> -(3-Triethoxypropylsilyl)-2,5-dihydroxybenzoate, 5	122
3.5.4.4	<i>N</i> -(3-Triethoxypropylsilyl)-2,5,-dibenzylbenzamide, 6	123
3.5.4.5	(<i>N</i> -(3-Triethoxysilylpropyl)- <i>N'</i> -(7-(4-methylcoumarin)) ureido (TSPCU), 3	124
3.5.5	Sol Gel Preparation	125
3.5.6	MALDI Preparation	127
3.5.7	MALDI-TOF Experiments	127
3.6	References	129
CHAPTER 4.	CASE STUDY OF SILICON-BASED MATRIX	131
4.1	Introduction	131
4.2	Results	132
4.3	Summary	143
4.4	References	144

List of Tables

Table 2-1. The conditions of TEOS:DHB sol gels.	36
Table 2-2. The conditions of TEOS:DHB:PEO macroporous sol gels.	36
Table 2-3. The conditions of TEOS-PEO sol gels (heated).	37
Table 2-4. The conditions of TEOS-PEO macroporous sol gels (washed).	38
Table 2-5. Average signal intensities and signal-to-background ratios as a function of meso/macroporous sol gel compositions with entrained DHB and residual PEO.	42
Table 2-6. Average signal intensities and signal-to-background ratios as a function of mesoporous sol gel composition with entrained DHB.	45
Table 2-7. Spot-to-spot reproducibility in MALDI of DHB versus TEOS:DHB:PEO 1:0.042:0 hybrid.	47
Table 2-8. Average signal intensity for silica with (untreated) and without (heat treated)a residual PEO (DHB on top).	49
Table 2-9. Average signal intensities and signal-to-background ratios as a function of mesoporosity (washed silica, DHB on top)a.	53
Table 2-10. Analyte entrained in silica:DHB:PEO sol.	56
Table 3-1. UV values of synthesized organic matrices, 0.120 mM.	82
Table 3-2. Optical micrographs of standard MALDI matrices and their derivatives.	87
Table 3-3. MALDI analyte signal intensity observed for series of MALDI matrices.	94

Table 3-4. Covalently linked matrices as TQ resins in terms of their MALDI performance.

99

List of Figures

Figure 2-1. Micrographs of silicas, optionally containing DHB.	34
Figure 2-2. MALDI MS of glu-fibrinopeptide, haloperidol, trimethoprim and fluorescein with DHB (@ 0.129 M).	40
Figure 2-3 . MALDI MS of glu-fib, TMP, haloperidol, fluorescein using mesoporous silica TEOS:DHB:400 PEO 1:0.081:0.057 molar ratio.	43
Figure 2-4. UV study of TEOS:DHB sol solutions.	44
Figure 2-5. MALDI MS of glu-fibrinopeptide, haloperidol, trimethoprim and fluorescein with mesoporous silica TEOS:DHB:PEO 1:0.042:0 molar ratio.	46
Figure 2-6. MALDI MS of glu-fib, haloperidol, TMP, fluorescein with mesoporous silica TEOS:DHB:PEO 1:0.77:0.	46
Figure 2-7. MALDI MS of Glu-fib, TMP, haloperidol and fluorescein using heat treated porous silica TEOS:DHB:100kPEO 1:0:2x10 ⁻⁴ (DHB on top).	48
Figure 2-8. IR study of various PEO/DHB sol solutions.	50
Figure 2-9. UV studies of PEO/DHB solutions as a function of PEO molecular weight.	51
Figure 2-10. MALDI MS of glu-fib, TMP, haloperidol and fluorescein using untreated porous TEOS:DHB:PEO 1:0:2x10 ⁻⁴ molar ratio (DHB on top).	52
Figure 2-11. MALDI spectra using optimal macroporous silica with residual PEO present with matrix on top: caffeic acid ((a) free and b) over porous silica); CHCA ((a) free and b) over porous silica).	55

Figure 2-12. Optical images of variable TEOS:DHB:PEO hybrids with varying TEOS concentration: a) 1.66×10^{-4} mol/mL; b) 9×10^{-3} mol/mL; c) 1.66×10^{-4} mol/mL, (20x magnification).	59
Figure 2-13. MALDI MS of glu-fib, TMP, haloperidol, fluorescein using untreated mesoporous silica TEOS:DHB:400PEO 1:0:0.018 (DHB on top).	62
Figure 3-1. Synthetic scheme proposed for phenolic allylation and subsequent hydrosilylation to give 1 .	78
Figure 3-2. Synthetic approach utilizing for 3-hydroxyphthalic anhydride to give 2 .	79
Figure 3-3. Synthesis of triethoxysilylated coumarin to give 3 .	79
Figure 3-4. Synthetic scheme for carboxylic allylation via amide formation and hydrosilylation to give 5 .	80
Figure 3-5. The triethoxysilylated compounds 1 , 5 and 6 .	80
Figure 3-6. Challenges associated with hydrosilylation reactions of 7 , 8 and 9 .	81
Figure 3-7. UV of DHB derivatives.	84
Figure 3-8. UV of CA derivatives.	84
Figure 3-9. UV of HMBA derivatives, 0.12 mM.	85
Figure 3-10. MALDI MS of glu-fib, TMP, haloperidol and fluorescein using: a) DHB, b) CHCA and c) CA matrix.	92
Figure 3-11. Spectroscopic study of AMC 13 and TSPCU 3 : a) UV absorbance, b) Fluorescence emission.	100
Figure 3-12. MALDI MS of TSPCU sol gel under various conditions: a) TSPCU as T resin (basic conditions), b) TSPCU as T resin (acidic conditions) (pH=1-2), c) AMC.	102

Figure 3-13. MALDI MS using monolayer of triethoxysilyl phthalamic acid (compound 2.) as T resin.	104
Figure 3-14. MALDI MS using compound 5 as TQ resin.	105
Figure 3-15. Schematic of MALDI Instrument.	128
Figure 4-1. MALDI MS using a) DHB, b) T resin, c) Compound 3/TEOS TQ resin, d) Cured silica with Compound 3 as MALDI support (analyte on top).	134
Figure 4-2. Average signal intensity using compound 1 as T, TQ resin or when coated over silica.	136
Figure 4-3. UV spectra of the compounds from Scheme 4-1.	137
Figure 4-4. Fluorescence spectra of the compounds from Scheme 4-1.	138
Figure 4-5. Optical micrographs of a) 4-hydroxy-3-methoxybenzoic acid, b) compound 21 and c) compound 22	140
Figure 4-6: Optical microscope images: a) Compound 1 T resin, b) TQ resin, c) silica coated with 1.	141

List of Schemes

Scheme 1-1. Polymers with a) UV absorbing molecules and b) covalently tethered biomolecule.	25
Scheme 2-1. Structure of fluorescein, trimethoprim and haloperidol.	39
Scheme 3-1. Formation of TQ resins.	102
Scheme 4-1. Synthesis of triethoxysilylated derivative.	133

List of Abbreviations

MALDI-TOF	Matrix-assisted laser desorption ionization time of flight
CHCA	α -cyano-4-hydroxy-cinnamic acid
2,5-DHB, DHB	2,5-dihydroxybenzoic acid
TMP	Trimethoprim
Glu-fib	Glu ¹ -fibrinopeptide B
DMF	Dimethylformamide
ESI	Electrospray ionization
¹³ C NMR	Carbon Nuclear Magnetic Resonance Spectroscopy
CI	Chemical Ionization
¹ H NMR	Proton Nuclear Magnetic Resonance Spectroscopy
IR	Infrared Spectroscopy
MS	Mass Spectrometry
m/z	Mass to Charge Ratio of an Ion (Mass Spectrometry)
UV	Ultraviolet

1 CHAPTER 1. INTRODUCTION

1.1 MALDI Overview

Since the development of matrix-assisted laser desorption (MALDI) mass spectrometry in late 80's,¹ numerous advances have been made in order to expand its applicability and usability. Generally, MALDI is less demanding with respect to the purity of the sample than the ESI (electrospray ionization) technique. Other advantages such as lack of signal suppression, presence of predominantly singly charged ions (i.e., relatively simple spectra), higher sensitivity, tolerance for salts and impurities, and wide mass range (~300 kDa) make this method highly desirable for rapid and automated qualitative analysis.

Typically, UV-MALDI involves the use of an organic UV-absorbing molecule which co-crystallizes with the analyte, absorbs UV laser light and effectively transfers energy to analyte, and in turn leads to analyte desorption and ionization. MALDI has been successfully employed in the study of biomolecules (peptides, proteins, oligonucleotides, nucleic acids, carbohydrates etc.) and synthetic polymers. In general, a large excess of matrix to sample (from 100:1 to 10000:1) is used, since the matrix serves as the primary (and highly efficient) absorber of the UV laser radiation and breaks down rapidly, expanding into the gas phase.² Although the choice of matrix is generally a product of trial and error, several characteristics are believed to be necessary for good MALDI performance of the matrix. These include: UV absorbance near the laser wavelength; crystallization; and, the presence of relevant chemical functionalities which act as a proton source. So far, all the organic molecules used as MALDI matrices absorb strongly near 337 nm (emission wavelength of a nitrogen laser), undergo

extensive crystallization, and are generally substituted phenols, carboxylic acids and/or amines such as 2,5-dihydroxybenzoic acid, α -cyano-4-hydroxycinnamic acid, 4-nitroaniline, etc.

1.2 The Role of Matrix in UV MALDI

Ionization mechanisms in MALDI are believed to involve chemical and/or thermal ionization such as: gas-phase photoionization, ion-molecule reactions, disproportionation, excited-state proton transfer, energy pooling, thermal ionization and desorption of preformed ions.³ However, the exact source of ions in MALDI is still under investigation.

Despite the above claims, more recent research suggests that the co-crystallization of matrix and analyte, and/or the need for exchangeable protons are not as relevant as previously thought. Researchers have demonstrated that there is no correlation between the physical appearance of the matrix crystals and the analyte domains.⁴ Although unnecessary,⁵ analyte incorporation in a matrix crystal network may be helpful for the generation of large analyte ions.⁶ In addition, analytes do not seem to have to be incorporated into matrix network for a good performance; rather, surface contact is sufficient for needed energy transfer.⁷ The larger the surface-to-volume ratio of the MALDI matrix used, the larger the likelihood for an analyte molecule to be in contact with such a surface. These claims are supported by the recent, successful use of a highly porous surface of high UV absorbance as a matrix, whereby analyte was applied after the surface was formed.^{8,9}

In the case of standard acidic matrices, gas phase proton transfer reactions between matrix ions and analyte are regarded as the main ionization pathway.¹⁰ A standard free matrix is involved in gas-phase reactions and its ability to perform is

strongly dependent on the factors that influence this mechanism (such as excitation by UV light, sublimation point, and chemical functionality). MALDI spectrum is generally populated with singly charged protonated, sodiated or potassiated ions, as well as numerous matrix-related signals in the low mass region. Despite the belief that a carboxylic acid group, where present, determines the matrix performance, several studies have been published that demonstrate that the source of protons is a phenol rather than an acid.^{11,12,13,14} It is certain that the acidic properties of aromatic derivatives are strongly enhanced when molecules are laser excited, and in the gas phase phenols are known to be more acidic than carboxylic acids.¹⁵ A matrix that undergoes an intramolecular hydrogen proton transfer reaction (such as sinapinic acid) is said to undergo an excited-state proton transfer reaction from matrix to analyte.¹⁶ However, some analogous matrices, such as 2,5-dihydroxybenzoic acid (2,5-DHB), do not undergo excited-state proton transfer (ESPT) reaction, but rather experience gas-phase photoionization and/or energy pooling.¹⁷ Whether a process occurs via protonation by an excited-state proton transfer or by other mechanism, such as energy pooling or photoionization, is greatly dependent on the matrix used. Derivatization of the hydroxyl groups was found by some authors to strongly degrade MALDI efficiency of the matrix, whereas others came to the opposite conclusion.¹⁸ It was further demonstrated that exchangeable protons are not needed with some free matrices for ionization to take place after all. These results suggested that alternative mechanisms may be at play in MALDI process.

The question on what makes a material function as a matrix remains ambiguous and undecided. Further evidence exists that analyte ionization takes place in the expanding plume as well as in the surface (where preformed ions are generated).¹⁹

Moreover, thermal ionization was proposed to be the mechanism responsible for observing analyte ions when alternative methods (free of acidic organic matrix) were used. In these cases, the factors such as high photoabsorption, low heat capacity, large surface area and rapid heating were termed responsible for efficient desorption and ionization.

Thus, further investigation is necessary in order to determine the effects of factors such as surface area, matrix localization and chemical nature of free matrix, which are deemed to be relevant in MALDI performance.

1.3 MALDI Limitations and Solutions

The limitations which are intrinsic to the MALDI methodology are poor shot-to-shot and sample-to-sample reproducibility and a “sweet” spot phenomenon (certain areas of the deposited analyte/matrix spot give better signal intensity than others), which stem from inhomogeneous sample preparation. In addition, the standard MALDI method utilizing organic matrices could only be used for the analysis of high molecular weight compounds (>1000 Da), since the low mass region is generally complicated by the matrix-related peaks, the extent of which strongly depends on the nature of the matrix. The ideal matrix for low molecular weight materials would provide efficient ionization, minimal or at least controllable fragmentation, and would exhibit a lack of mass interference, so that it can be used for analysis of low molecular weight compounds (LMW), while still preserving the advantages associated with MALDI methodology. It is due to these reasons that extensive work has been done recently in order to develop methodology that would allow for the study of smaller molecules and that would allow for more reproducible data and more controlled sample preparation.

Though a number of approaches have been investigated for analysis of LMW species, such as the use of a higher molecular weight matrix, or of liquid matrices, numerous issues remained unsolved.^{20,21,22} While high molecular weight matrices resolve the issue of matrix interference in the low mass region, their respective ions still dominate the overall mass spectrum. Liquid matrices lead to low mass resolution, high chemical background, potential instrumentation contamination and poor ionization efficiency.

Since it has been demonstrated that a traditional organic matrix was not necessary for MALDI performance, several other materials have been developed and investigated as MALDI alternatives. All of these newly developed methods utilize materials of high photoabsorption, low heat capacity and large surface area (see next section).

1.3.1 Inorganic Matrix Approach

Matrix free approaches to MALDI have been developed. One such approach involves the use of simple surface supported MALDI, as in the desorption/ionization on porous silicon (DIOS), for the analysis of LMW species.^{23,24} The DIOS acts to trap the analyte and assist in evaporation and ionization, which produces minimal molecular fragmentation and allows for great sensitivity. DIOS surfaces, however, are easily oxidizable, which limits their usage to immediate application, and once used, these supports are limited to several laser shots.

An alternative to silicon exploits inorganic metal oxides, the use of which is referred to as surface-assisted desorption/ionization (SALDI).²⁵ When applied, the method produces minimal molecular fragmentation of analytes and allows for great sensitivity. For example, inorganic matrices, such as fine metal particles or two-phase matrices such as ultra fine cobalt (or graphite) particle in glycerol or metal oxides (TiO₂

and ZnO) suspended in liquid paraffin or glycerol, have also been employed. It was found that SALDI mass spectra exhibit relatively low chemical background making it suitable for characterization of LMW compounds such as polar and non-polar organic molecules and peptides of lower molecular weight (<12000Da).^{26,27,28} Despite these advantages, a higher laser fluence was needed for ionization of high molecular weight analytes, which caused increased analyte fragmentation. In addition, the “sweet spot” effect was still observed with these suspension-type matrices. In addition, these matrices do not allow for simultaneous study of a whole range of analytes of both low and high molecular weight.

1.3.2 Surface-based Approach

In order to develop materials of large surface area that are photon absorbing, a number of systems have been developed that combine sol gel methodology with commonly used organic matrices. Among these, higher surface area silicas have been prepared using the sol gel approach where the matrix-related interferences are reduced by incorporating the matrix into the sol-gel.²⁹ The incorporation of matrix into sol-gel structures, termed sol-gel assisted laser desorption/ionization (SGALDI), has led to relatively matrix interference-free backgrounds in the mass spectra. Only 2,5-DHB was entrapped in silica gel to reduce the low mass interference in the spectrum, due to its widespread use as matrix.³⁰ The methodology involved use of non-covalent interactions by simple premixing of the organic matrix, at various concentrations, with Si(OEt)₄ (TEOS) as sol gel precursor. In addition 2,5-DHB and α -cyano-4-hydroxy cinnamic acid (CHCA) were also covalently bound to silica surface.³¹ In an alternative approach, a chemically modified silica gel, developed by use of isocyanate spacer as a linker between

the organic matrix and preformed sol gel, was successfully used as a MALDI support.³¹ Use of such silica as a MALDI support led to a successful ionization and desorption of analytes; however, average signal intensity was greatly compromised (several hundreds, see Chapter 2). There is a great need to develop a suitable material which allows for higher signal-to-background ratio, and yet results in overall signal intensity comparable to that of free matrix. Despite the advances made using sol gel technology, it has been shown that binding a matrix molecule to the surface of silica gel has led to the loss of matrix's ability to transport the analyte into the gas phase.³⁰ Moreover, no studies have been performed on the effects of inherent silica mesoporosity and/or macroporosity, and on the advantages these parameters might have on the matrix behaviour and protonated analyte ion yields.

A sol gel hybrid containing an organic matrix with amino functionality was successfully used in the MALDI analysis of oligonucleotides, where amine groups acted as a sodium ion filters in the desalting process.³² Similarly, sol gels doped with crown ethers were used as MALDI supports for oligonucleotide analysis.³³ The beneficial ability of such materials to greatly reduce alkaline cation adduction of oligonucleotides, which dominates the mass spectrum, is compromised by the necessary time consuming and extensive sample preparation. Sol gel hybrids have also been used as supports for tryptic digestion and subsequent MALDI analysis.³⁴ Recently, Chen et al.^{9,35} showed that not only silica but also TiO₂-sol gel films are suitable for MALDI analysis. Such surface-supported matrix is capable of not only desorption and ionization but also of selective binding of the analytes from the solution. In general, the recent success of some MALDI-

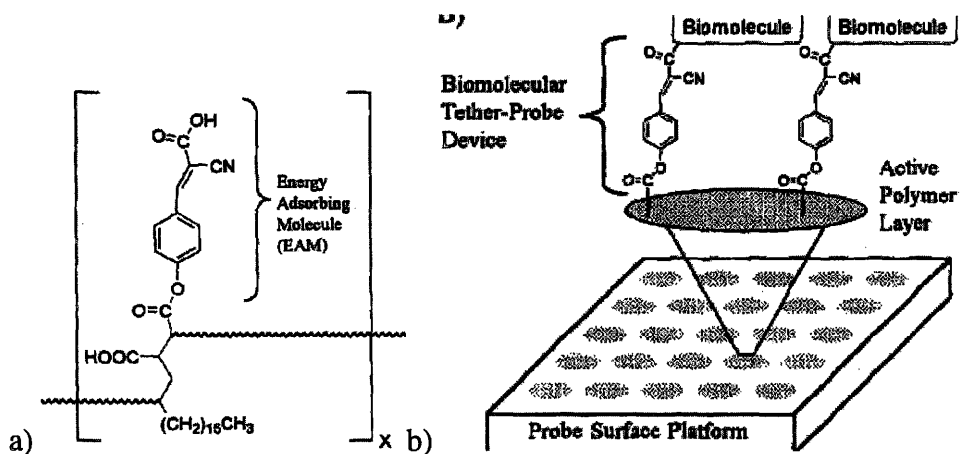
sol gel supports under certain conditions suggests that higher surface area materials can be effectively used in MALDI analysis.

When porous polymeric monoliths (methacrylate-derived block-copolymer) were used in surface-enhanced laser desorption/ionization (SELDI) for analysis of small molecules, it was demonstrated that enhanced ion generation is the result of high porosity and surface area, optical absorption and thermal conductivity.⁸ However, the use of these organically derived polymeric monoliths resulted in wide degradation and fragmentation as well.

Despite the advances made in matrix-signal suppression the average signal intensity was greatly compromised when compared to free matrix. Analyte signal intensity comparable to those with free matrix was observed only with reappearance of the matrix-related peaks. Hence, the reduction of matrix-related peaks is accompanied by an unavoidable reduction in analyte signal intensity.

More recently, it was demonstrated that covalent binding of the compound can lead to analyte ionization as well. Surface-enhanced neat desorption (SEND) is another matrix-free method for small molecule analysis which involves chemically attaching an energy-absorbing compound to the probe surface by chemical modification or physisorption.^{36,37} A covalently bound CHCA was reported to work as a matrix in study of peptide of higher molecular weight (>2000 Da).^{38,39} The ability to ionize analytes in the form of molecular ions or as matrix adducts (monomer and dimer) was dependent on the use of photolabile ester and amide linkages (Scheme 1-1.).

Scheme 1-1. Polymers with a) UV absorbing molecules and b) covalently tethered biomolecules.



The degree to which only covalently linked matrix remained permanently tethered on these surfaces was uncertain in these studies, due to the incomplete washings of unbound CHCA. Hence, the CHCA molecules absorbed on the surface, rather than covalently linked, could be a reason for successful analyte ionization observed. Ching et al.⁴⁰ have further extended the approach to the photoinduced uncoupling /desorption of biomolecules covalently tethered to photoactive azobenzene derivatives as the UV absorbing compounds. Despite the successful desorption and ionization of peptides, irreproducibility in absolute signal intensity and in S/B ratios was observed. Various ions were observed in the mass spectrum, since the laser irradiation induced numerous photolytic cleavage products. More alarmingly, irreproducible analyte desorption was observed from the same probe surface (i.e., appearance and disappearance of signals on the same surface). While these approaches led to signals, and in some cases improved S/B, very low signal intensities were observed (60-600) and the approaches were not applied to the study of low molecular weight species. In addition, all of the previous surface-based approaches have involved the use of photoactive bonds. It is not

unreasonable to assume that the UV absorbing surface could be developed which would allow for the study of low molecular weight species and which would provide excellent S/B values, while being permanently surface-bound via non-photolabile linkages.

1.4 Research Goals

Since the MALDI method is not limited to the use of standard solid organic matrices, and in light of a recent use of alternative approaches to MALDI, we have decided to explore the use of highly porous and/or chemically tethered matrix supports in order to develop an optimal MALDI material. An ideal support would minimize a matrix interference and maximize an analyte signal intensity, as well it would provide for enhanced sensitivity and reproducibility due to its homogeneous nature. Intuitively, a matrix-related signal could be removed by matrix entrapment within the solid support, or by covalently linking the matrix to the solid support, in order to avoid matrix desorption into the gas-phase. The objectives were therefore twofold: to understand in detail the relation between silica constituents and morphology in the MALDI experiment, and to exploit that understanding to develop better photoactive supports.

Herein, we describe our MALDI study of the use of highly macroporous and mesoporous silica surfaces in order to reduce matrix-related interferences, where porosity formed is a result of phase separation due to the presence of poly(ethylene oxide). It is reasonable to hypothesize that the porosity and higher surface area will lead to an enhancement of signal-to-background in mass spectrum. It would be advantageous as well to develop a porous surface that would exhibit analyte selectivity and/or selective analyte signal intensity enhancement.

We further decided to examine the potential benefits, including reduced matrix-based signals, of tethering the matrix to the porous surface. Ideally, such surfaces would have higher surface areas, UV absorptivity, and/or selectivity and would allow for extremely large S/B ratios, which would supersede those observed for standard matrix.

1.5 Outline of the Thesis

This thesis consists of four chapters. The second chapter is concerned with interactions between MALDI matrix with nonporous, mesoporous and macroporous silicas. Such sol gel systems were investigated in terms of nature of additives, porosity, morphology, and MALDI performance. Advantages associated with the mesoporous silica and its ability to minimize the matrix signal interference while allowing for higher signal-to-background ratio and higher selectivity aroused our interest to focus further investigations on the covalently tethered compounds. Chapter 3 includes the preparation of chemically modified standard MALDI matrices and their characterization in terms of UV absorbance and crystallization behaviour. Such derivatives were further modified in order to introduce triethoxysilyl ($-\text{Si}(\text{OEt})_3$) functionality, which allowed for covalent binding to the surface and permanent, non-photolabile tethering of the UV absorbing matrix. In addition, a case study was provided, in Chapter 4, where surface-bound highly selective matrix was studied in detail in terms of sol gel processing methodology.

1.6 References

¹ Karas, M. and Hillenkamp, F., *Anal. Chem.*, 60, 1988, 2299-23001.

² Marvin, L.F, Roberts, M.A. and Fay, L.B., *Clin. Chim. Acta*, 337, 2003, 11-21.

- ³ Zenobi, R. and Knochenmuss, R., *Mass Spectrom. Rev.*, 17, 1998, 337-366.
- ⁴ Dai, Y., Whittall, R.M. and Li, L., *Anal. Chem.*, 68, 1996, 2494-2500.
- ⁵ Vorm, O., Roepstorff, P. and Mann, M., *Anal. Chem.*, 66, 1994, 3281-3287.
- ⁶ Strupat, K., Karas, M. and Hillenkamp, F., *Int. J. Mass Spectrom.*, 111, 1991, 89-102.
- ⁷ Horneffer, V., Forsmann, A., Strupat, K., Hillenkamp, F. and Kubitscheck, U., *Anal. Chem.*, 73, 2001, 1016-1022.
- ⁸ Peterson, S.D., Luo, Q., Hilder, E.F., Svec, F. and Frechet, J.M.J, *Rapid Comm. Mass Spec.* 18, 2004, 1504-1512.
- ⁹ Chen, T.-C. and Chen, Y.-C., *Rapid Comm. Mass Spectrom.*, 18, 2004, 1956-1964.
- ¹⁰ Breuker, K., Knochenmuss, R. and Zenobi, R., *Int. J. Mass Spectrom.*, 184, 1999, 25-38.
- ¹¹ Bashir, S., Mutter, R. and Derrick, P.J., *Analyst*, 128, 2003, 1452-1457.
- ¹² Baer, T., Ng, C.Y. and Powis, I., Ed. *Large Ions: Their Vaporization, Detection, and Structural Analysis. Chapter 2: Steps towards a more refined picture of the matrix function in UV MALDI* by Karas M., Bahr U., Zeng, J.-R., New York: Wiley, 1996.
- ¹³ Gimon, M.E., Preston, L.M., Solouki, T.M., White, A. and Russell, D.H., *Org. Mass Spectrom.*, 27, 1992, 827-827.
- ¹⁴ Preston, L.M., Kinsel, G.M. and Russell, D.H., *J. Am. Soc. Mass Spectrom.*, 5, 1994, 800-805.
- ¹⁵ a) Hassin, F.Y. and Marynick, D., *J. Mol. Struct.*, 629, 2003, 223-235; b) Krause, J., Stoeckli, M. and Schlunegger, P.U., *Rapid Comm. Mass Spectrom.*, 10, 1996, 1927-1933; c) Notario, R., *J. Mol. Struct.*, 556, 2000, 245-252.

- ¹⁶ a) Krause, J., Stoeckli, M. and Schlunegger, P.U., *Rapid. Comm. Mass Spectrom.*, 10, 1996, 1927-1933; b) Chiarelli, M.P., Sharkley, A.G. and Hercules, D.M., *Anal. Chem.*, 65, 1993, 307-311; c) Kovi, P.J., Miller, C.L. and Schulman, S.G., *Anal. Chem. Acta*, 61, 1972, 7-13; d) Paul, L.W., *Anal. Chem. Acta*, 69, 1974, 195-199; e) Lahmani, E. and Zehnacker, R.A., *J. Phys. Chem. A*, 101, 1997, 6141-6147; f) Acuna, A.U., Toribio, F., Amat, G.F. and Catalan, J., *J. Photochem.*, 30, 1985, 339-352.
- ¹⁷ a) Ehring, H., Karas, M. and Hillenkamp, F., *Org. Mass Spectrom.*, 27, 1992, 427-431; b) Karbach, V. and Knochenmuss, R., *Rapid Comm. Mass Spectrom.*, 12, 1998, 968-974.
- ¹⁸ Grigorean, G., Carey, R.I. and Amster, I.J., *Eur. Mass Spectrom.*, 2, 1996, 139-143.
- ¹⁹ Calba, P.J., Muller, J.F. and Inouye, M., *Rapid Comm. Mass Spectrom.*, 12, 1998, 1727-1731.
- ²⁰ Ayorinde, F.O., Garvin, K. and Saeed, K., *Rapid Comm. Mass Spectrom.*, 14, 2000, 608-615.
- ²¹ Chen, Y-T. and Ling, Y-C., *J. Mass Spectrom.*, 7, 2002, 716-730.
- ²² Salsbury, R.L. and Hercules, D.M., *Rapid Comm. Mass Spectrom.*, 16, 2002, 1575-1581.
- ²³ Go, E.P., Prenni, J.E., Wei, J., Jones, A., Hall, S.C., Witkowska, H.E., Shen, Z. and Siuzdak, G., *Anal. Chem.*, 75, 2003, 2504-2505.
- ²⁴ Wei, J., Buriak, J.M. and Siuzdak, G., *Nature*, 399, 1999, 243-246.
- ²⁵ Sunner, J., Dratz, E. and Chen, Y., *Anal. Chem.*, 1995, 67, 4335-4342.
- ²⁶ Kinumi, T., Saisu, T., Takayama, M. and Niwa, H., *J. Mass Spectrom.*, 35, 2000, 417-422.

- ²⁷ Zhang, Q., Zou, H., Guo, Z., Zhang, Q., Chen, X. and Ni, J., *Rapid Comm. Mass Spectrom.*, 15, 2001, 217-223.
- ²⁸ Crecelius, A., Clench, M.R., Richrads, D. S. and Parr, V., *J. Chromat. A*, 958, 2002, 249-260.
- ²⁹ Cohen, J.L. and Cox, J.A., *J. Sol-gel Sci. Tech.*, 28, 2003, 15-18.
- ³⁰ Lin, Y-S. and Chen, Y-C., *Anal. Chem.*, 74, 2002, 5793-5798.
- ³¹ Zhang, Q., Zou, H., Guo, Z., Zhang, Q., Chen, X. and Ni, J., *Rapid Comm. Mass Spectrom.*, 15, 2001, 217-223.
- ³² Chen, W-Y and Chen, Y-C., *Anal. Chem.*, 75, 2003, 4223-4228.
- ³³ Weng, M-F. and Chen, Y-C., *Rapid Comm. Mass Spectrom.*, 18, 2004, 1421-1428.
- ³⁴ Lin, Y-S, Yang, C-H. and Chen, Y-C., *Rapid Comm. Mass Spectrom.*, 18, 2004, 313-318.
- ³⁵ Chen, C-T. and Chen, Y-C., *Anal. Chem.*, 76, 2004, 1453-1457.
- ³⁶ Hutchens, T.W. and Yip, T.-T., U.S. Patent 5,894,063, 1999.
- ³⁷ Mouradian, S., Nelson, C.M and Smith, L.M., *J. Am. Chem. Soc.*, 118, 1996, 8639-8645.
- ³⁸ Voivodov, K.I., Ching, J. and Hutchens, T.W., *Tetrahedron Lett.*, 32, 1996, 5669-5672.
- ³⁹ Hutchens, T.W. and yip, T.-T., *Rapid Comm. Mass Spectrom.*, 7, 1993, 576-580.
- ⁴⁰ Ching, J., Voivodov, K.I. and Hutchens, T.W., *J. Org. Chem.*, 61, 1996, 3582-3583.

2 CHAPTER 2. HIGH SURFACE AREA MALDI-TOF SUPPORTS*

2.1 Introduction

Matrix-Assisted Laser Desorption/Ionization-Time of Flight (MALDI-TOF) allows effective vaporization and ionization of non-volatile, high molecular weight biological samples from the solid-state phase directly into the gas phase, where they can be detected by mass spectrometry. In conventional MALDI, the matrix in the free state not only absorbs and transfers energy from the laser, but can be vaporized into the gas phase. Matrix interferences generally appear in the low-mass range, making it very difficult to analyze molecules with molecular weight below 1000 Da.

A number of different approaches have been developed to minimize the extent to which matrix-related interferences are present in the low molecular mass region of the spectrum. For example, several materials that do not contain an organic matrix have been used as MALDI supports, including porous silicon (DIOS),¹ and fine metal or metal oxide inorganic particles, such as TiO₂ and ZnO.² Porous DIOS is an example of surface-assisted laser desorption/ionization (SALDI) where the researchers successfully took advantage of the higher surface area and effective electron transfer process in order to develop a matrix-free MALDI support. These newly developed methods use materials of high photoabsorptivity, low heat capacity and large surface area. The methods produce minimal molecular fragmentation of analytes and can allow for great sensitivity. However, these methods are generally applied only to lower molecular weight analytes

* This Chapter has been submitted as a manuscript to Analytical Chemistry. Some of the introductory material is duplicated from the introduction.

(<10000 Da). In addition, they exhibit limited capacity in terms of number of shots per spot. An ideal MALDI method would contain minimal matrix interference signals, and acceptable analyte signal intensity over a much larger mass range.

The methodology which exploited non-covalent interactions by simply premixing the organic matrix, at various concentrations, with the silica precursor Si(OEt)₄ (TEOS), in the sol, was referred to as sol-gel-assisted laser desorption/ionization (SGALDI).^{3,4,5} In an alternative approach, a chemically modified silica gel, developed using an isocyanate spacer as a linker between the organic matrix and preformed sol gel, was successfully used as a MALDI support.⁶ The use of such silicas as MALDI supports can lead to the successful ionization and desorption of analytes; however, average signal intensity is greatly compromised. There is thus a motivation to better understand the factors that attenuate signal intensity in silica-based systems.

Recently, Chen et al.^{7,8} showed that TiO₂-sol gel films are also suitable for MALDI analysis. These represent an alternative MALDI matrix that is capable of not only desorption and ionization, but also of selective binding of the analytes from the solution. More recently, Wiesner et al.⁹ have developed SELDI protein chip arrays where the protein interaction with chromatographic support allows for further sample clean-up and the complex digests analysis.¹⁰ In addition, Hutchens et al. have developed surface-enhanced for neat desorption (SEND) in which energy absorbing CHCA was covalently attached to the polymer by a photolabile ester linkage, and was able to ionize covalently bound biomolecules as CHCA adducts.¹¹

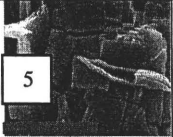


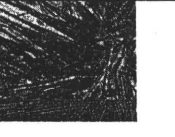
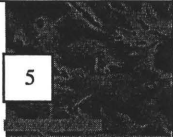

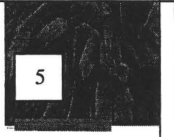


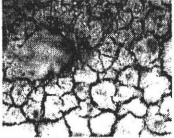
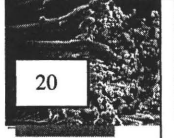


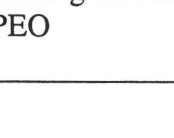
Despite these advances using higher surface area sol gel supports for matrix-signal suppression in MALDI analysis, factors such as sample stability, reproducibility and surface morphology have not been addressed in detail. It has been suggested that the signal intensity increases with pore size and surface area. However, little information has been provided on the effect of sample morphology on the optical properties, matrix crystallization and overall reproducibility of the matrices. In particular, there is a paucity of data describing the degree of signal suppression when non-standard matrices are exploited.



Our group has developed methods to make highly porous biocompatible silicas,¹² based on Nakanishi's precedent.¹³ The use of a porogen such as poly(ethylene oxide)(PEO) in combination with sugarsilanes results in the formation of spongy porous structures that provide higher surface area materials which can be used as monolithic columns for frontal affinity chromatography.¹² We were interested in exploring if such porous materials are suitable as MALDI supports. Therefore, silica monoliths of different compositions, and containing additives such as 2,5-DHB and/or PEO, were studied using optical and scanning electron microscopy, FTIR and UV spectroscopy. Our objectives were to correlate chemical and morphological characteristics, including the role of PEO, silica porosity, network morphology, degree of DHB crystallization and the nature of interactions between matrix, silica and polymer with MALDI performance as measured both by total signal, and signal to background when comparing analyte to signals derived from matrix. Two kinds of silicas were used: those with embedded matrix and those in which the matrix was placed on the silica support surface.

2.2 Results

Amorphous silica is readily prepared using a sol gel process.¹⁴ The acid-catalyzed hydrolysis at ambient temperature of an alkoxy silane, in this case $\text{Si}(\text{OEt})_4$ (TEOS), was followed by condensation that leads to mesoporous silica (mesopores typically of dimensions 1.3 nm,¹⁵ Figure 2-1a). The sol was placed on a gold coated MALDI substrate and, in the absence of additives to prevent shrinkage,¹³ formed an adherent, cracked film upon condensation. The additional incorporation of the matrix 2,5-dihydroxybenzoic acid in the sol led to crystalline domains of DHB dispersed in the silica (Figure 2-1.a).

Figure 2-1. Micrographs of silicas, optionally containing DHB.

	No DHB		With DHB	
	SEM ^a	Optical ^b	SEM ^a	Optical ^b
a:Mesoporous silica TEOS:DHB:PEO 1:0.042:0 molar ratio				
b:Macroporous silica TEOS:DHB:PEO 1:0.081:2.2x10 ⁻⁴ , untreated ^c (PEO IN)				
c:Macroporous silica, treated ^d (DHB on top)				
d:Macroporous silica with 10k PEO TEOS:DHB:PEO 1:0.081:20x10 ⁻⁴				0.25 g/ml 10k PEO 
e:Macroporous silica with 10k PEO				0.025 g/ml 10k PEO 

TEOS:DHB:PEO 1:0.081:2x10 ⁻⁴				
f: Macroporous silica with 100k PEO TEOS:DHB:PEO 1:0.081: 2x10 ⁻⁴				0.025 g/ml 100k PEO 

^a Scale bar = μm .

^b 20 x magnification.

^d Macroporous silicas are also mesoporous. These were made using a recipe of TEOS:DHB:PEO 1:0:2x10⁻⁴ molar ratio. In addition these have been further thermally treated or washed with water.

^c Macroporous silicas are also mesoporous. These were made using a recipe of TEOS:DHB:PEO 1:0.081:2x10⁻⁴ molar ratio.

The incorporation of high molecular weight poly(ethylene oxide)(PEO) in the sol changes the cure chemistry such that phase separation occurs before gelation and a highly bimodal macroporous and mesoporous structure results (Figure 2-1 b).^{16,17} In this case, much of the PEO remains entrained in the resulting monolith. However, if the silica is washed exhaustively with water which removes most of the PEO, or better, thermally treated at high temperatures (~500 °C) to remove all the PEO, meso and macroporous silica, with macropores ranging from 5-10 μm were obtained (Figure 2-1c). As with the mesoporous silicas, DHB may be incorporated into the sol that forms the macroporous gel (Figure 2-1b). The degree of crystallinity of DHB domains in these silica monoliths was inversely proportional to the quantity of PEO present, as shall be further discussed below. Thus, it is possible to prepare a variety of structural morphologies and to optionally incorporate MALDI matrix, 2,5-DHB, into the sol so that it will be retained in the gel.

A systematic study of silica films, formed by varying the porosity and the optional incorporation of DHB, was undertaken by depositing sol solutions (for compositions, see Table 2-1. and Table 2-2) onto gold coated MALDI plates or depositing sol solutions (for compositions, see Table 2-3 and Table 2-4) onto stainless steel plate, and allowing them to air dry.

Table 2-1. The conditions of TEOS:DHB sol gels.

TEOS (mmol/ μ L) ^b Molar percentage (%)	DHB (mmol/ μ L) ^a Molar percentage (%)	Molar ratio ^c TEOS:DHB:PEO
2.2 (96.0)	9.2 (4.0)	1:0.042:0
2.2 (82.3)	17.7 (7.7)	1:0.080:0
0.22 (56.4)	17.0 (43.6)	1:0.773:0
2.2 (98.7)	2.9 (1.3)	1:0.013:0
11.9 (98.6)	17.0 (1.4)	1:0.014:0
22.0 (99.2)	17.0 (0.8)	1:0.008:0

^a Concentration (mmol/ μ L) * 10⁻⁵. ^b Concentration (mmol/ μ L) * 10⁻³; ^c TEOS normalized.

Table 2-2. The conditions of TEOS:DHB:PEO macroporous sol gels.

MW PEO	PEO ^a (mmol/ μ L) Molar %	TEOS ^b (mmol/ μ L) Molar %	DHB ^a (mmol/ μ L) Molar %	Molar ratio TEOS:DHB:PEO ^c
400	6.3 (5.7)	1.1 (88.8)	8.9 (5.5)	1:0.081:570
10000	0.024 (0.02)	1.1 (92.58)	8.9 (7.4)	1:0.081:2.2
	0.024 (0.02)	1.1 (97.48)	2.9 (2.5)	1:0.026:2.2
100000	0.022 (0.02)	1.1 (92.58)	8.9 (7.4)	1:0.081:2
	0.022 (0.02)	1.1 (97.48)	2.9 (2.5)	1:0.026:2

^a Concentration (mmol/ μ L) * 10⁻⁵. ^b Concentration (mmol/ μ L) * 10⁻³; ^c mol PEO in x10⁻⁴

Table 2-3. The conditions of TEOS-PEO sol gels (heated).

TEOS Molar percentage (%)	10 000 MW PEO <u>Molar ratio</u> <u>TEOS:DHB:PEO^a</u> Molar percentage (%) (%w/v)	100 000 MW PEO <u>Molar ratio</u> <u>TEOS:DHB:PEO^a</u> Molar percentage (%) (%w/v)
99.3	<u>1:0:70.5</u> 0.7 (17.5)	
99.8	<u>1:0:20</u> 0.15 (5)	
98.6	<u>1:0:140</u> 1.4 (35)	
99.97		<u>1:0:3</u> 0.03 (5)
99.98		<u>1:0:2</u> 0.02 (3.3)

^a mol PEO in $\times 10^{-4}$

Table 2-4. The conditions of TEOS-PEO macroporous sol gels (washed).

TEOS Molar percentage (%)	10 000 MW PEO Molar ratio TEOS:DHB:PEO ^a (Molar percentage (%))	100 000 MW PEO Molar ratio TEOS:DHB:PEO ^a (Molar percentage (%))
99.9984	1:0:0.16 (0.0016)	
99.966	1:0:0.34 (0.0034)	
99.9871	1:0:1.29 (0.0129)	
99.973	1:0:2.7 (0.027)	
99.891	1:0:10.9 (0.109)	
99.77	1:0:23.1 (0.230)	
99.9986		1:0:0.14 (0.0014)
99.9969		1:0:0.31 (0.0031)

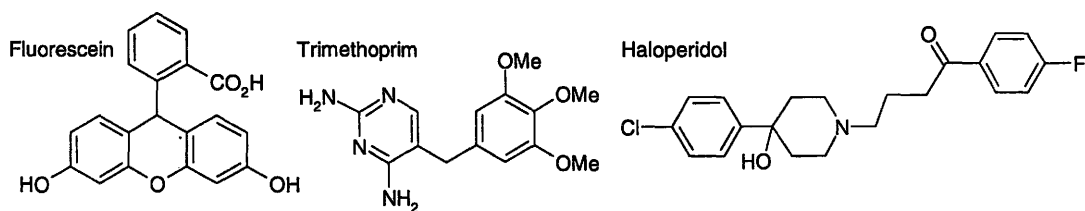
^a moles of PEO x 10⁻⁴

The behavior of these supports in the MALDI experiment was then correlated with surface morphology. The mass spectrometric study described below is partitioned into the examination of silica films of four distinct structural types: DHB/analyte mixtures placed on pre-cured mesoporous or meso/macroporous silica gel, and DHB entrained in mesoporous or meso/macroporous silica gel.

2.2.1 Standard MALDI Protocol

The analytes chosen for the study, haloperidol, trimethoprim (TMP), fluorescein, and the oligopeptide glu¹-fibrinopeptide (glu-fib) (EGVNDNEEGFFSAR), provide variety both with respect to molecular weight and structure (Scheme 2-1).¹⁸

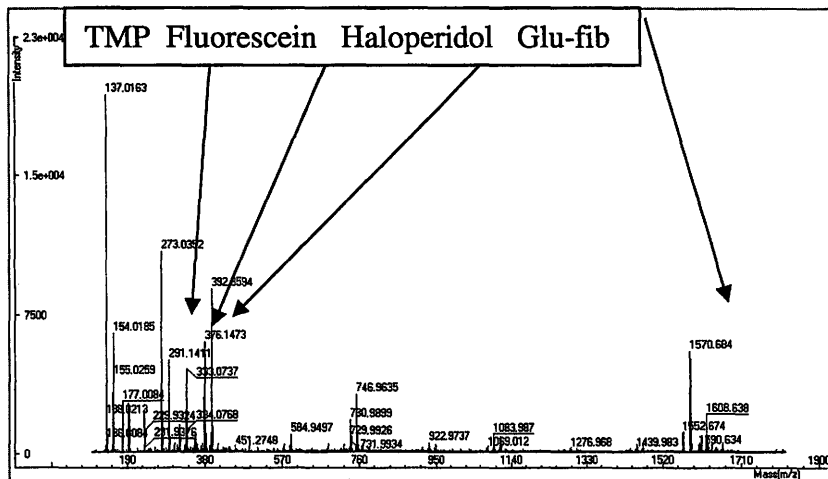
Scheme 2-1. Structure of fluorescein, trimethoprim and haloperidol.



Trimethoprim (MW 290) is an aromatic amine that will be protonated at neutral pHs, while haloperidol (MW 375) is a neutral, aromatic halide also possessing an aliphatic tertiary hydroxyl group. Glu-fib (MW 1570) and fluorescein (MW 332) both have a number of phenolic and carboxylic acid groups that can be involved in hydrogen bonding: the compounds are anionic at neutral pHs. Glu-fib is a much larger molecule than the other analytes and was chosen both for its size and its structural relevance to peptidic drugs.

A representative MALDI mass spectrum of analytes using free 2,5-dihydroxybenzoic acid (DHB) as matrix on a stainless steel MALDI plate is given below.

Figure 2-2. MALDI MS of glu-fibrinopeptide, haloperidol, trimethoprim and fluorescein with DHB (@ 0.129 M).



All four analytes were simultaneously ionized as the proton adducts $[M+H]^+$, where intact molecular ion peaks at m/z 291, 333, 375 and 1571 were associated with TMP, fluorescein, haloperidol and glu-fib, respectively. In addition, numerous ions derived directly from 2,5-DHB appeared at m/z 137 $[M-17]^+$, 155 $[M+H]^+$ and 177 $[M+Na]^+$; the matrix adducts dominated the low mass region of the mass spectrum. The extensive matrix-related signal interference observed in a low mass region renders the analysis of small molecules using the standard MALDI procedure difficult. A comparison of the intensity of m/z 137 $[M-17]^+$ for the matrix with the molecular ion peaks for the analytes noted above is used below in the discussions of experimental signal to background below.

2.2.2 Matrix in Silica Films

2.2.2.1 DHB in Meso/macroporous Silica

High surface area meso/macroporous silicas were investigated with DHB entrained within the silica. These materials were prepared using a silica sol gel process in which high molecular weight PEO was incorporated as a co-constituent of the sol that also contained DHB matrix at a variety of concentrations. The resulting monolithic silica optionally contained excess free PEO with entrained DHB (Table 2-2). To establish the role of PEO in a material that is not macroporous, a sample of mesoporous silica prepared using 400 MW PEO was also examined.

Figure 2-1d-e shows the optical micrographs of a representative porous silica hybrid (TEOS:DHB:PEO 1:0.081: 2×10^{-4} (20×10^{-4}) molar ratio) containing free 10000 MW PEO. Figure 2-1f shows the optical micrographs of porous silica hybrids (TEOS:DHB:PEO 1:0.081: 2×10^{-4}) with 100000 MW PEO. Increases in PEO concentration were associated with a decrease in matrix crystallinity (Figure 2-1d and e). In general, increases in PEO molecular weight also repress crystallization, although these changes are rather subtle (Figure 2-1e and f).

The introduction of PEO into silica provided overall lower absolute analyte signal intensities as well as lower S/B ratios in the MALDI experiment (Table 2-5, column 1-2 and 5-6): note that the PEO suppresses matrix signal more than analyte.

Table 2-5. Average signal intensities and signal-to-background ratios as a function of meso/macroporous sol gel compositions with entrained DHB and residual PEO.

Column #	TEOS:DHB:PEO molar ratio (signal/background) ^a					
	1:0.026: A ([DHB]=0.03M)		1:0.081:A ([DHB]=0.089M)			
	1	2	3 ^b	4 ^c	5 ^d	6
Molar % PEO	0.02%	0.02%		5.7%	0.02%	0.02%
A	2.2×10^{-4}	2×10^{-4}	0	5.7×10^{-2}	2.2×10^{-4}	2×10^{-4}
Peaks	10k PEO (0.24mM)	100k PEO (0.22mM)	24 (1.0) ^f	400PEO (63mM) ^d	10k PEO (0.24mM)	100k PEO (0.22mM)
DHB 137 m/z ^e	191 (1.0)	0	0	26411 (1.0)	4122 (1.0)	1445 (1.0)
Trimethoprim 291 m/z	0	0	0	7398 (0.28)	497 (0.12)	228 (0.16)
Haloperidol 375 m/z	0	0	0	9772 (0.37)	567 (0.14)	37 (0.03)
Fluorescein 333 m/z	184 (0.96)	0	0	8624 (0.33)	488 (0.12)	116 (0.08)
Glu-fib 1571 m/z	113 (0.59)	0		18506 (0.70)	770 (0.19)	182 (0.17)

^a Relative intensity of signal compared to DHB (at 137 m/z) + analyte on same support, i.e., within a vertical column

^b PEO free samples with the same amount of DHB for comparison; this column is reproduced in Table 2-6.

^c Samples prepared from PEO MW 400 are not macroporous.

^d **Figure 2-1.b + DHB**

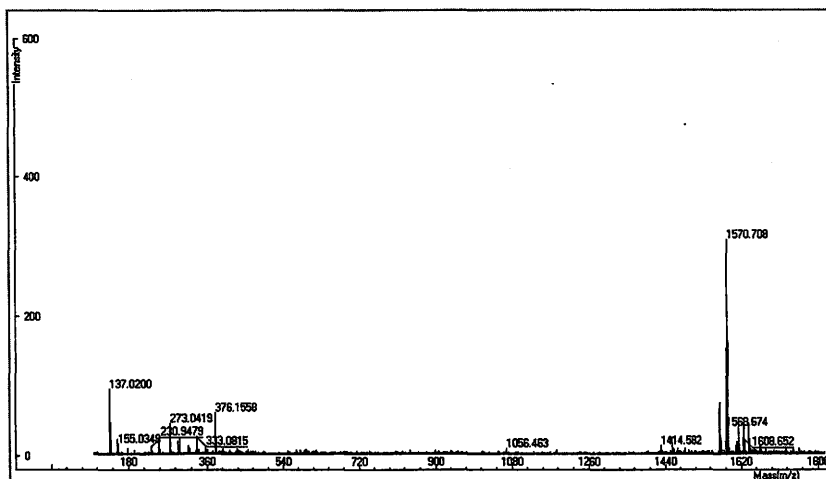
^e Total signal intensity can be established comparing the intensity of this peak; compare across the row.

^f Highly cracked and unstable film.

Several complementary factors led to analyte signal intensity suppression: excess PEO present within sol gel led to increased dissolution of DHB, and consequently, a reduction in the degree of matrix crystallization; the direct interaction between DHB and PEO noted above also reduces the efficacy of the matrix, the magnitude of which is directly related to molecular weight and concentration of polymer (Figure 2-1d,e,f).

The result with 400 MW PEO is anomalous in this regard (Table 2-5, column 4). High overall signal intensities were accompanied by good S/B ratios that exceeded those of the MALDI or MALDI on silica experiments (Figure 2-3).

Figure 2-3 . MALDI MS of glu-fib, TMP, haloperidol, fluorescein using mesoporous silica TEOS:DHB:400 PEO 1:0.081:0.057 molar ratio.



The weight% and, therefore, $[\text{CH}_2\text{CH}_2\text{O}]_n$ monomer concentrations of PEO in the monoliths shown in Table 2-5 are comparable. The molar concentrations, are quite different. The effect of the different molecular weight PEO polymers on DHB signal intensity is profound: high DHB signal intensity was observed in the presence of 400 MW PEO, but signal suppression increased with PEO MW.

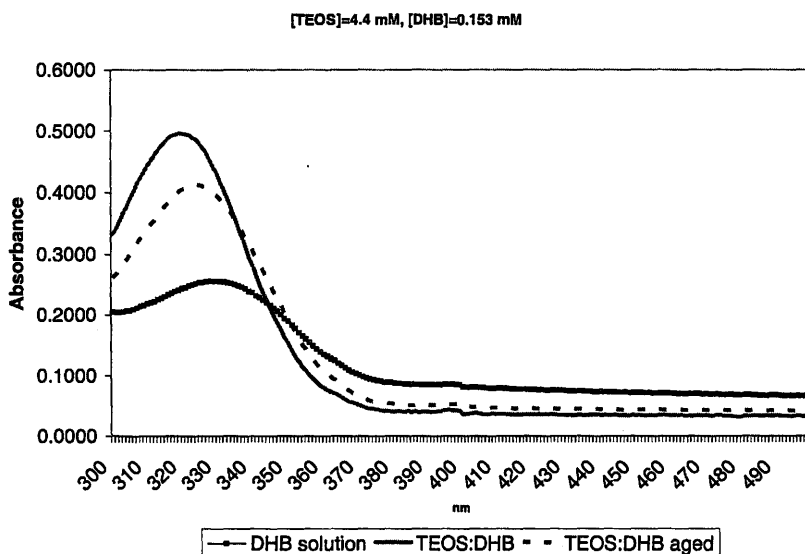
2.2.2.2 DHB in PEO Free Mesoporous Silica

DHB was also directly incorporated in TEOS sols at a variety of concentrations to give mesoporous structures. The TEOS concentration in the sol was varied in order to maximize film adhesion and consistency.¹⁹ In order to determine the effect of TEOS concentration on matrix crystallinity, an experiment was developed in which the analyte/matrix molar ratio in the sol was kept constant ($[\text{Analyte}] = 2.5 \text{ ng}/\mu\text{L}$,

[DHB]=26000 nmol/ μ L , molar ratio~ Analyte:DHB ~ 10400) and the TEOS concentration varied. Amongst the TEOS:DHB:PEO molar ratios studied (Table 2-1.), 1:0.773:0 and 1:0.042:0 gave rise to the most stable, adhering compositions and to the most matrix crystals.

While matrix concentration was kept constant, an increase in TEOS concentration led to a decrease in the number of DHB crystal domains, which is consistent with the dilution of the matrix by silica. Other TEOS:DHB:PEO sol gel hybrids were also studied as MALDI supports, in which the DHB concentration was varied while the TEOS concentration was kept constant. Here too, the degree of DHB crystallization correlated directly with its concentration in the sol. As with the experiments containing PEO described above, the λ_{max} of the matrix increased from that of DHB alone during cure to 326 nm (Figure 2-4), closer to the wavelength of the laser used (337 nm).²⁰

Figure 2-4. UV study of TEOS:DHB sol solutions.



In terms of MALDI performance (Table 2-6), the mesoporous TEOS:DHB:PEO (1:0.773:0 and 1:0.042:0 molar ratios) sol gel hybrids gave rise to reasonable protonated signal intensities for all four analytes studied and offered overall performances comparable to that obtained with free matrix in the absence of silica (Figure 2-5, Figure 2-6): it should be noted that the final concentration of DHB in 1:0.77:0 hybrid was comparable to its concentration when applied as free matrix.

Table 2-6. Average signal intensities and signal-to-background ratios as a function of mesoporous sol gel composition with entrained DHB.

Column #	DHB ^b (S/B) ^a	TEOS:DHB:PEO molar ratio ^a					
		1	2	3	4	5	6
Peaks		1:0:0 (no DHB in sol) ^b	1:0.77:0	1:0.0 8:0	1:0.014:0, 1:0.008:0	1:0.042:0 (DHB=0.0 9M) ^d	1:0.013: 0 (DHB= 0.03M)
DHB 137 m/z ^c	75226 (1.0)	19573 (1.0)	17363 (1.0)	24 (1.0)	0	3804 (1.0)	0
Trimethoprim 291 m/z	15050 (0.20)	4213 (0.22)	11730 (0.68)	0	0	2070 (0.54)	0
Haloperidol 375 m/z	16383 (0.22)	5498 (0.28)	16410 (0.95)	0	0	880 (0.23)	0
Fluorescein 333 m/z	13824 (0.18)	6864 (0.35)	5284 (0.30)	0	0	2559 (0.68)	0
Glu-fib 1571 m/z	26667 (0.35)	11776 (0.60)	10500 (0.61)	0	0	8029 (2.11)	0

^a Relative intensity of signal compared to DHB (at 137 m/z) + analyte on same support, i.e., within a vertical column

^b DHB was placed on this material to permit comparison with PEO containing samples.

^c Total signal intensity can be established comparing the intensity of this peak; compare across the row.

^d For micrograph, see **Figure 2-1a**, with DHB.

Figure 2-5. MALDI MS of glu-fibrinopeptide, haloperidol, trimethoprim and fluorescein with mesoporous silica TEOS:DHB:PEO 1:0.042:0 molar ratio.

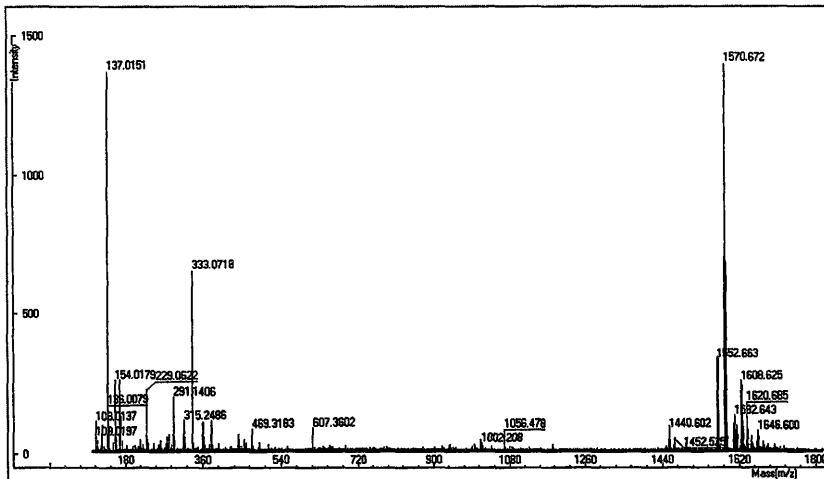
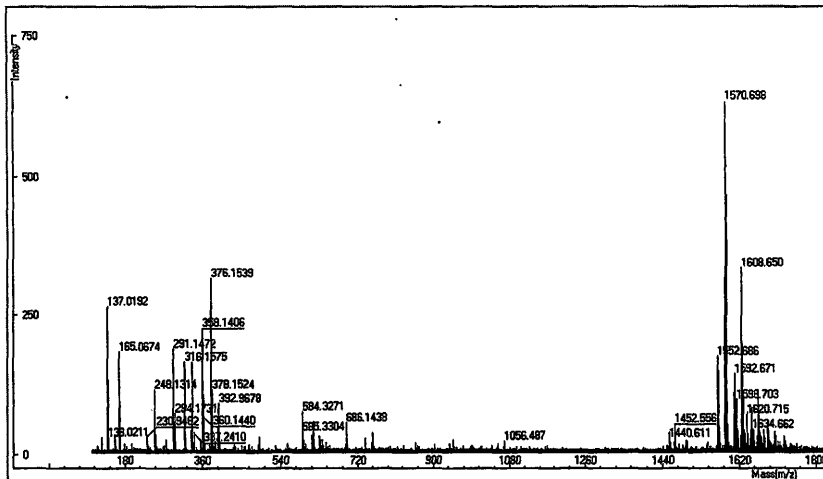


Figure 2-6. MALDI MS of glu-fib, haloperidol, TMP, fluorescein with mesoporous silica TEOS:DHB:PEO 1:0.77:0.



There was a selective enhancement of 350-450% in S/B for the cationic and neutral analytes trimethoprim and haloperidol in the silica with a TEOS: DHB: PEO ratio of 1:0.773:0 (Table 2-6, column 2). By contrast, in the absence of silica, both the number and intensity of the undesired peaks due to DHB exceeded those of the

silica/matrix hybrid (Table 2-6, column DHB). That is, the signal-to-background ratio, a ratio of analyte signal intensity over the matrix-related signal intensity (137 m/z [M-17+H]⁺), for the 1:0.773:0 silica/matrix system was 1.5-4.5 times better than when compared to the free matrix. Similarly, 1:0.042:0 silica/matrix gave rise to S/B ratios that were between 1-6 times higher (Table 2-6, column 5) than those obtained with free DHB. In terms of spot-to-spot reproducibility, these silica/matrix hybrids are comparable to free DHB, although with an attenuated signal (Table 2-7).

Table 2-7. Spot-to-spot reproducibility in MALDI of DHB versus TEOS:DHB:PEO 1:0.042:0 hybrid.

Analyte	DHB		TEOS:DHB:PEO 1:0.042:0	
	Absolute Average Signal	Standard Deviation	Absolute Average Signal	Standard Deviation
Trimethoprim	15050	9710 (65%)	2070	1542 (74%)
Haloperidol	16383	8638 (53%)	880	663 (75%)
Fluorescein	13824	9377 (67%)	2758	2001 (73%)
Glu-fib	26667	17521 (66%)	8029	4682 (58%)

2.2.3 Matrix on Silica Films

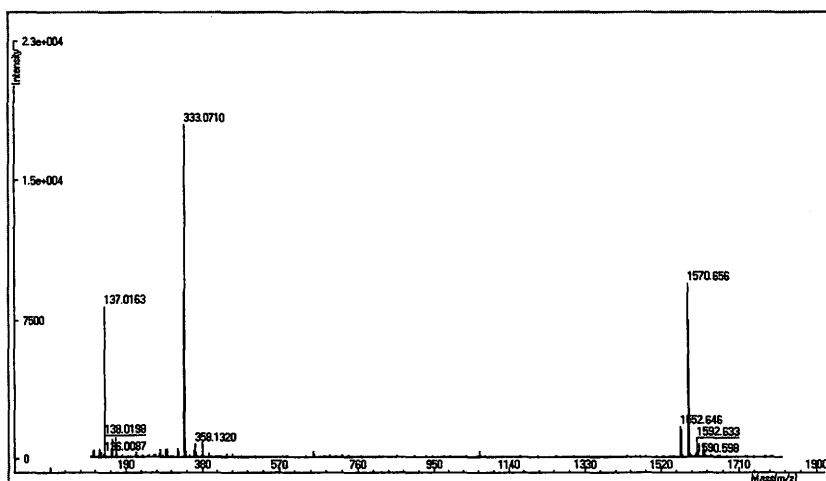
2.2.3.1 Porous Silica (treated and untreated)

It has been reported that a high surface area is beneficial for MALDI performance (e.g., with the techniques SGALDI⁵ and using porous silicon DIOS as a support) for two reasons: it provides an improved opportunity to host guest molecules (i.e., matrix), and leads to a higher probability of energy transfer between matrix and the analyte to be analyzed. Matrix free films of highly macroporous silica were prepared by incorporating

10000 and 100000 MW PEO in a TEOS sol (for sol gel compositions, see Table 2-3 and Table 2-4).

The resulting films were optionally treated with aqueous washing or heated to *ca.* 500 °C to remove residual PEO from the silica. After appropriate aging of the gels (with or without treatment), matrix/analyte solutions were applied to the surface prior to MALDI analysis. SEM and optical images of porous thermally treated silica supports are presented in Figure 2-1c. It can be seen that in the absence of matrix, the silica surface is highly macroporous (the mesoporosity cannot be seen at this magnification): this is not affected by the presence of the matrix, which segregates into crystalline domains. A representative MALDI mass spectrum obtained using such high porous supports is presented in Figure 2-7.

Figure 2-7. MALDI MS of Glu-fib, TMP, haloperidol and fluorescein using heat treated porous silica TEOS:DHB:100kPEO 1:0:2x10⁻⁴ (DHB on top).



It can be seen from Table 2-8 that the presence of both 10k and 100k MW PEO at higher concentrations negatively affect the absolute signal intensity of the matrix and

of the analytes: although signal intensity was reduced in all samples compared to the DHB control, PEO almost completely suppressed signals.

Table 2-8. Average signal intensity for silica with (untreated) and without (heat treated)^a residual PEO (DHB on top).

	Silica:DHB:PEO 1:0:20 ^c (0.15% mole 10k PEO)		Silica:DHB:PEO 1:0:2 ^c (0.02% mole 100k PEO)	
	Untreated	Treated (500 °C) ^a	Untreated	Treated (500 °C) ^{b,c}
DHB 137 m/z	0	3419	124	1578
Trimethoprim	0	2735	0	739
Haloperidol	0	868	0	0
Fluorescein	0	1908	137	2571
Glu-fib	0	2609	87	2655

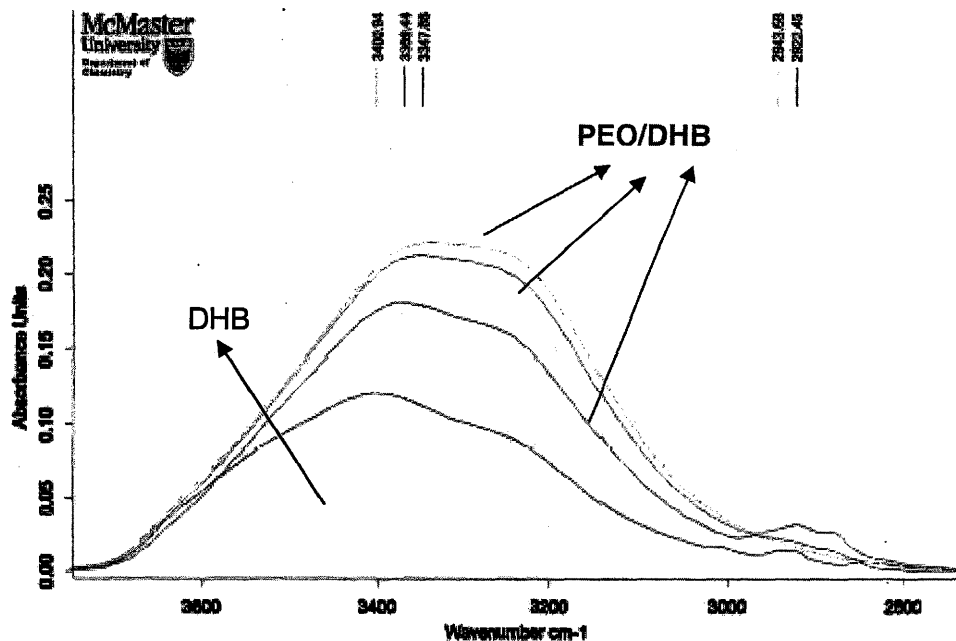
^a This removes all the PEO from the silica. Porosity in the silica monolith was generated using PEO, which was then removed using combustion.

^b Figure 2-1c with DHB.

^c mole PEO x10⁻⁴

In order to study possible interactions between PEO and DHB, IR and UV studies were performed. An FTIR study demonstrated that extensive hydrogen bonding existed between the matrix and PEO polymer. Overall, the introduction of polymer led to shifting of carboxylic acid stretching band (3500-3200 cm⁻¹) to lower wavenumbers (3400-3000 cm⁻¹) and to the overall broadening of the absorbance peak (Figure 2-8): this effect was greatly increased by presence of HMW PEO.

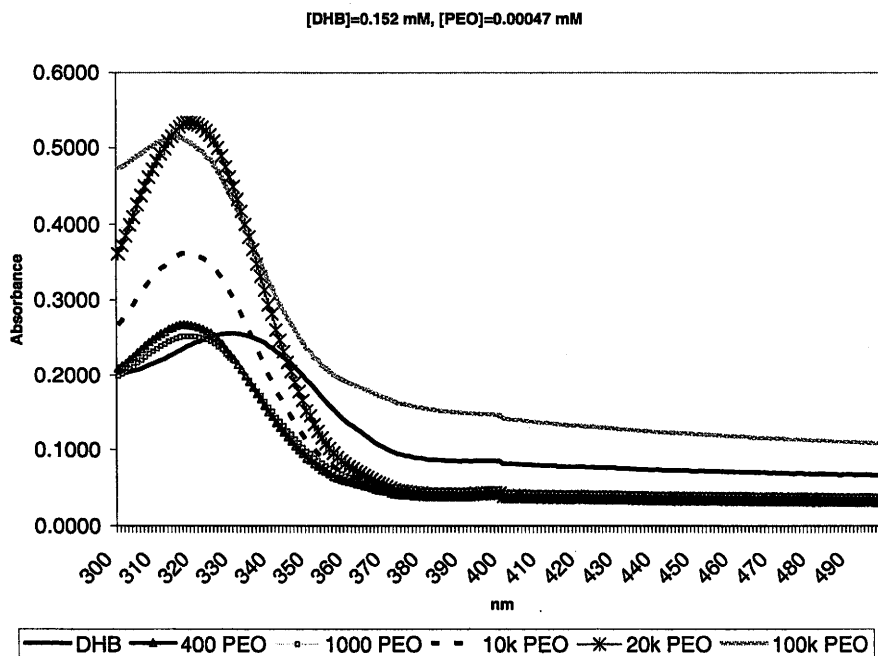
Figure 2-8. IR study of various PEO/DHB sol solutions.



Analogous to work done by Wu et al.,²¹ who have used phenolic compounds to increase number of crosslinking within the gel, phenols present in our system can act as excellent hydrogen-donors within the gel. Thus, extensive hydrogen bonding of DHB with both unreacted Si-OH groups and PEO chains exist and give rise to a peak shifting, absorbance increase and broadening effect observed in IR spectra.

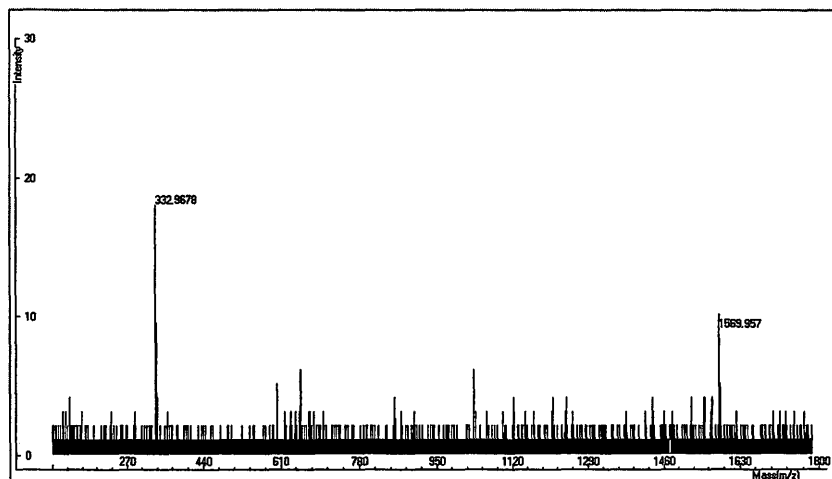
The 2,5-DHB UV absorbance was studied as a function of exposure to PEO molecular weight at specific concentrations. The introduction of PEO shifted the maximum DHB absorption band to lower wavelength (Figure 2-9).

Figure 2-9. UV studies of PEO/DHB solutions as a function of PEO molecular weight.



The extinction coefficients (at 337 nm) observed for matrix/PEO were higher than those obtained for free DHB. It had been anticipated that these changes in photoresponsiveness would improve the MALDI performance but, as noted, both matrix and analyte signals were significantly suppressed when PEO was able to intervene in the normal photoevents. The very low signal intensities with residual 100k MW PEO present were accompanied by higher selectivity for 2 of the analytes (Figure 2-10). However, the overall signal intensity was so low that we do not consider these materials further.

Figure 2-10. MALDI MS of glu-fib, TMP, haloperidol and fluorescein using untreated porous TEOS:DHB:PEO 1:0:2x10⁻⁴ molar ratio (DHB on top).



There are many interlinked variables associated with the performance of the silica supports in the MALDI experiment including meso/macroporosity, the location of the matrix on or within the silica and the presence of residual PEO. Mesoporous silica leads to enhanced signal intensity compared to macroporous silica, when DHB is placed on the surface (Table 2-8 vs Table 2-9, column 2). In general, better signal intensity arose when DHB was placed on, rather than in, the silica monolith, particularly in the absence of PEO (Table 2-6 column 1 vs column 5).

Table 2-9. Average signal intensities and signal-to-background ratios as a function of mesoporosity (washed silica, DHB on top)^a.

	No silica	TEOS	TEOS: DHB: PEO ^e (signal/background) ^b		
Column #	1	2	3	4	5
Molar ratio		1:0:0	1:0:0.018	1:0:0.16	1:0:0.14
Peaks		No PEO	400 PEO ^d	10k PEO	100k PEO
Molar%		0	1.8%	0.0016%	0.0014%
Wt%		0	1.25%	0.025%	0.25%
DHB 137 m/z ^c	75226 (1.0)	19573 (1.0)	4022 (1.0)	14188 (1.0)	15158 (1.0)
Trimethopri m	15050 (0.20)	4213 (0.22)	840 (0.21)	3297 (0.23)	3597 (0.24)
Haloperidol	16383 (0.22)	5498 (0.28)	937 (0.23)	3306 (0.23)	4177 (0.28)
Fluorescein	13824 (0.18)	6864 (0.35)	13863 (3.45)	6463 (0.46)	4040 (0.27)
Glu-fib	26667 (0.35)	11776 (0.60)	12728 (3.16)	12953 (0.91)	9035 (0.59)

^a Most of the PEO is removed from the matrix by extensive washing with water.

^b Relative intensity of signal compared to DHB (at 137 m/z) + analyte on same support, i.e., within a vertical column

^c Total signal intensity can be established comparing the intensity of this peak; compare across the row.

^d Silica containing LMW PEO was untreated.

^e mol PEO x10⁻⁴

The role of PEO is multifactorial. Increased contact between PEO and matrix/analyte reduces signal intensity. Placing the matrix/analyte upon a silica surface containing PEO leads to a reduction in signal intensity, when compared to a PEO-free monolith, but the residual signal is still very strong both for analyte and matrix (in the tens of thousands, Table 2-9). The PEO-associated reduction in overall signal intensity occurs to a smaller extent than when the DHB is also entrained within the silica.

However, reductions in signal intensity can be advantageous, with respect to analyte sensitivity. For example, when washed silica materials that still contain 10k MW PEO were used as MALDI supports, significantly greater S/B ratio was observed for fluorescein and glu-fib compared to the PEO-free analogous material (Table 2-9 column 4 vs. Table 2-9 columns 2): TMP and haloperidol did not respond as effectively. The silica containing 100k MW PEO showed similar effect (Table 2-9 column 5).

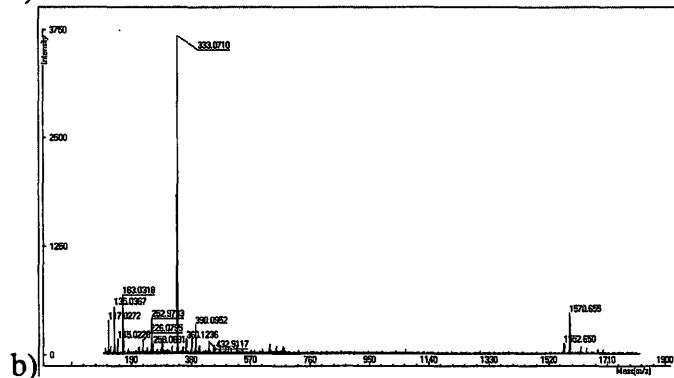
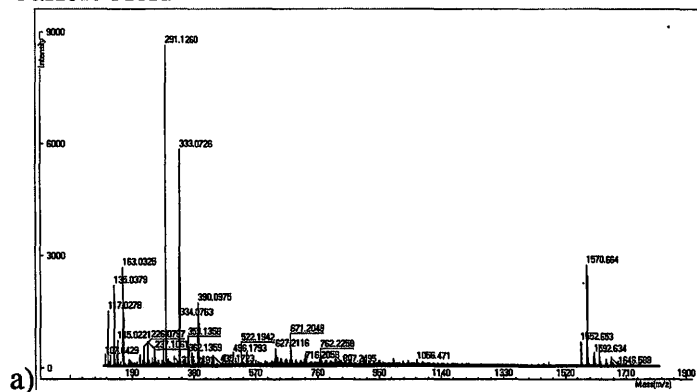
The effect of PEO on anionic analytes was further amplified when 400 MW PEO was present in the mesoporous silica (Table 2-9 column 3). In this case, the S/B is increased by > 300% because of selective suppression of matrix, haloperidol and trimethoprim signals.

2.2.3.2 Other Matrices on Meso/macroporous Silica

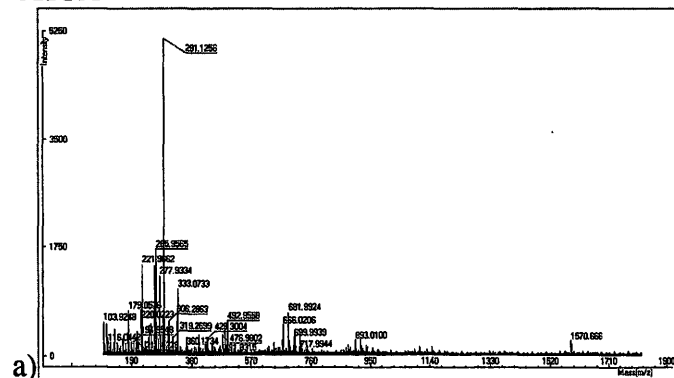
In order to study the applicability of our untreated supports with matrices other than DHB, the mesoporous supports were tested with α -cyano-4-hydroxycinnamic acid (CHCA) and 3,4-dihydroxycinnamic acid (CA), other commonly used MALDI matrices. Significant interference for the analytes glu-fib and fluorescein was observed in the low mass region for CHCA on porous silica (Figure 2-11b). However, when porous silica was used with CA as the matrix, a dramatic reduction in low mass interference was observed (Figure 2-11a).

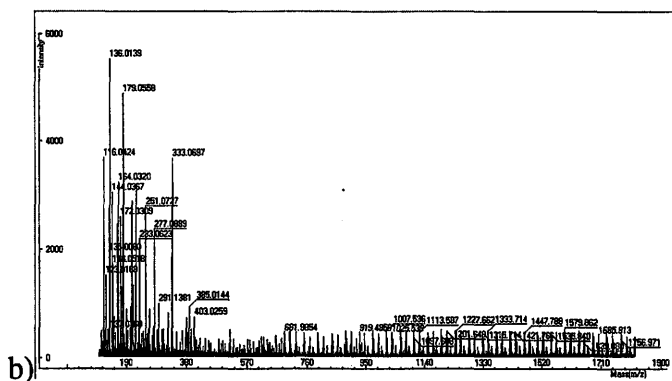
Figure 2-11. MALDI spectra using optimal macroporous silica with residual PEO present with matrix on top: caffeic acid ((a) free and b) over porous silica); CHCA ((a) free and b) over porous silica).

Caffeic Acid



CHCA





These results clarify that matrix-PEO interactions are restricted to and dependent upon the type of matrix used. The similarity in chemical structure between DHB and CA could be responsible for their common behavior under these experimental conditions.

2.2.4 Location of the Analyte

A comparison was made between the total signal intensity when the analyte was mixed with the matrix in the silica monolith (Table 2-10) or placed on top (Table 2-9 columns 4,5). With 10k PEO, there are few differences, with the exception of the analyte glu-fib, which has a much higher S/B when placed in the sol. With 100k PEO, by contrast, incorporating the analyte in the monolith leads to complete signal suppression.

Table 2-10. Analyte entrained in silica:DHB:PEO sol.

	Premixed analyte TEOS:DHB:PEO ^a 1:0.074:2.2 (10k PEO)	Premixed analyte TEOS:DHB:PEO ^a 1:0.074:2 (100k PEO)
DHB 137 m/z	3065	34
Trimethoprim	660	0
Fluorescein	2828	19.6
Haloperidol	363	0
Glu-fib	5087	29.4

^a mole PEO x10⁻⁴

2.2.5 Spot-to-Spot Reproducibility

The preceding discussion needs to be tempered by a comment on the morphology of the spot. When DHB is directly spotted on a MALDI plate, there is a “ring” of crystals which forms at the exterior of the original deposited solution. Decent signals are only obtained when the laser is shot at the crystalline ring. When analyte is spotted on the silica disks, it is readily obvious by eye. There are no apparent distortions across the spot either by eye, or by optical microscopy. However, this apparent homogeneity belies the actual distribution of analyte and matrix across the spot. In general, it is necessary to do several laser shots to obtain the optimal signal and S/B. The “sweet spot” may be associated with an appropriate mix of crystalline matrix domain and concentrated analyte, but this has not yet been ascertained.

Applying matrix to the preformed and aged sol gels reduces contact between DHB and PEO polymer. The reduced contact between silica and PEO allows for matrix crystals to form, and also permits sufficient energy to be transferred to the analytes. However, matrix-related signals are attenuated by residual interactions with PEO. The localization of the matrix/analyte co-crystals within the spot was studied by UV imaging, which revealed that analyte/matrix co-crystallization is dependent on PEO concentration and molecular weight. For the 10000 PEO/silica supports, the matrix/analyte co-crystals were distributed non-homogeneously and were located preferentially at the periphery of the spot, while for 100000 PEO/silica support (a much more viscous polymer), the matrix/analyte aggregates were localized homogeneously across the spot.

2.3 Discussion

The utility of the MALDI experiment hinges both on the ability to detect the signals of analytes of various structural types (charge, molecular weight, etc.) and the ability to discriminate between analyte signals and those derived from the matrix used to promote the formation of gas phase ions (signal to background ratio). As described above, we have examined the effects on absolute and relative intensities of signals from analytes and matrix (DHB): of the presence of silica on a standard MALDI plate; of the effect of matrix placement in or on the silica layer; of the effect of porosity of the silica; of the effect of the contaminant poly(ethylene oxide) used to create porosity; of the degree of crystallinity of the matrix; and on the effect of the PEO molecular weight. In particular we have attempted to optimize the experimental conditions around systems that have relatively high signal intensities (> 1000), which will be of more general use. For purposes of comparison, some data showing high selectivity but low sensitivity is provided. The results of these experiments provide guidance to design of new MALDI supports.

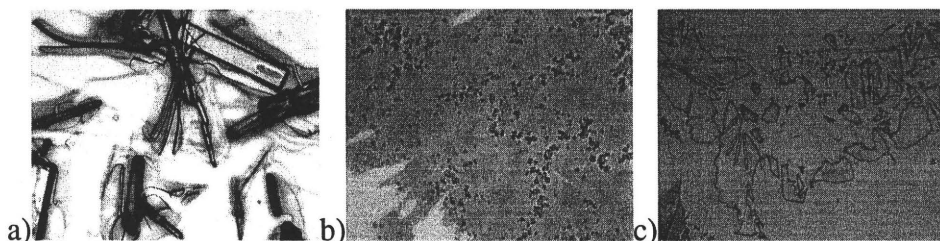
2.3.1 Matrix Crystallinity

2,5-DHB readily forms crystals when deposited either on MALDI plates or silica surfaces from aqueous solutions (e.g., Figure 2-1 a,b,c,e,f). The ability to prepare crystalline domains is an important criterion for effective signal intensity: the lower the degree of crystallinity, the lower the intensity both of matrix and analyte signals. As shall be described below, the intensity of matrix and analyte signals are affected differently by their environment.

2.3.2 Effect of Incorporating DHB in Mesoporous Silica

A series of adherent silica films, on MALDI plates, were systematically prepared varying silica:DHB ratios. The correlation between increased silica fraction and decreased signal intensity with dramatic changes of silica: DHB: PEO from *ca.* 1:0.773:0 (mole ratios) to 1:0.008:0 led to complete attenuation of all signals (Table 2-6, columns 2,3 and 4). Note that the same quantity of DHB was placed in each of the sols. Accompanying this change is a decrease in the degree of crystallinity of matrix (Figure 2-12). In general, the formation of crystals within the silica was more difficult than their formation when spotted on top of a preformed silica film. This is due both to the constraints on crystallization space placed on the DHB within the monolith and to the presence of PEO.

Figure 2-12. Optical images of variable TEOS:DHB:PEO hybrids with varying TEOS concentration: a) 1.66×10^{-4} mol/mL; b) 9×10^{-3} mol/mL; c) 1.66×10^{-4} mol/mL, (20x magnification).



The addition of PEO to the silica, in order to engender increased porosity, is typically disadvantageous to the overall signal intensity. PEO of all molecular weights acts as a solvent for DHB, suppressing crystallization: dramatically higher signal intensity was observed when crystalline DHB domains were observed. Thus, samples with DHB incorporated in the PEO/silica support, in which crystalline domains were absent, were

very poor MALDI targets. However, there are additional mechanisms through which PEO suppresses matrix and analyte signals.

The magnitude of matrix signal suppression is directly related to the molecular weight of the PEO, a factor which is much more important than either the molar concentration of polymer or the total concentration of available monomer $[(\text{CH}_2\text{CH}_2\text{O})_n]$ in the different MW PEO polymers. Low molecular weight (400) PEO only slightly affects the matrix signal (cf. Table 2-5 columns 4 vs 5 and 6) even when present in very high concentrations, while significant suppression is observed with 100,000 MW polymer at much lower PEO concentrations. PEO undergoes extensive hydrogen bonding with DHB as was demonstrated by IR and UV (Figure 2-8, Figure 2-9). It is well-known that the electronic transitions and proton transfer reactions of chromophores, necessary for formation and ejection of analyte ions, are affected when introduced into silica sol gels.²²

A key observation is that the low molecular weight polymer, 400MW PEO, led to lower DHB absorbance, whereas the HMW polymers resulted in higher absorbance. The very large difference in low MW matrix signals observed between silica containing LMW and HMW PEO could be explained by number of factors. First, since DHB has two phenolic groups present, the longer chain PEO can more effectively fold over around the DHB molecule and bind the two available phenol groups, and/or such chains could form clusters which are crosslinked via single DHB molecule. The increased viscosity of the high molecular weight polymer also confounds matrix desorption. The interactions above between PEO and matrix, should also apply to PEO and analyte. However,

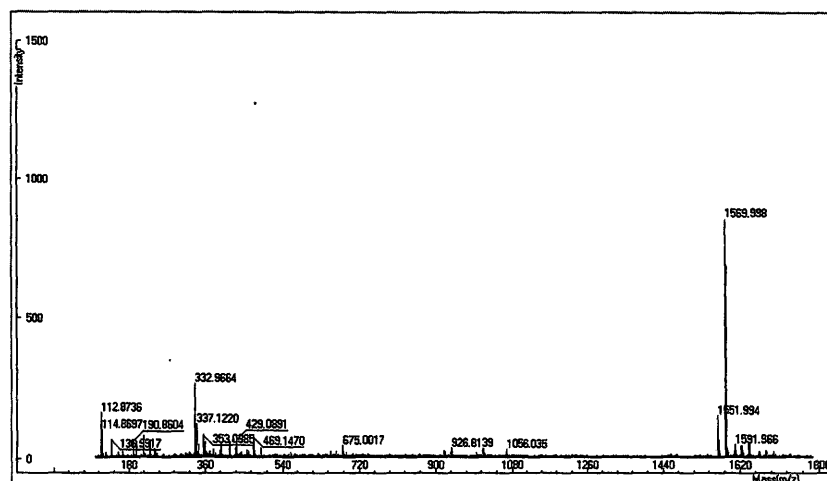
although both analyte and matrix interact with the PEO, preferential suppression of matrix signals occurs and the overall S/B increases.

2.3.3 Effect of Silica on Signal Intensity (DHB and analyte placed on the top)

A comparison of the response from a normal MALDI experiment to one in which DHB was spotted with analyte onto a silica film prepared from TEOS alone is shown in Table 2-9. The presence of silica on the plate per se has a small effect on the overall intensity of the MALDI signals (90% of signal, columns 1, 2). Macro/mesoporous silicas behaved differently than mesoporous silicas. High porosity silicas lead to a further attenuation of signal (columns 4, 5). It had been anticipated that the higher surface area²³ would lead to more effective distribution of crystalline matrix, more contact between matrix and crystal, and higher signal intensities. However, the macroporous channels partly responsible for the higher surface area also permit the matrix/analyte to penetrate the silica monolith below the region accessible to the laser, and the net effect is lower absolute signal intensity.

The clear exception to this trend is the silica prepared with 400 MW PEO. This material is mesoporous, with a higher accessible surface area than silica derived from TEOS. The signals due to matrix, trimethoprim and haloperidol were attenuated (Table 2-9, column 3). By contrast, the anionic analytes fluorescein and glu-fib showed dramatic enhancement in both absolute signal and signal to background ratio (Figure 2-13).

Figure 2-13. MALDI MS of glu-fib, TMP, haloperidol, fluorescein using untreated mesoporous silica TEOS:DHB:400PEO 1:0:0.018 (DHB on top).



The origin of the selectivity for anionic substrates is not currently understood, but may be related to the surface chemistry of silica, which is also anionic in nature. That is, the reduced affinity of anionic materials for an anionic surface may facilitate ejection into the gas phase. That is, the low MW PEO selectively interacts with matrix, trimethoprim and haloperidol, but does not similarly interact with anionic compounds.

Optimizing the formulation for silica-based MALDI supports depends greatly on the objectives of the experiment. Providing sufficient DHB is available, the presence of silica generally leads to some suppression of the DHB signal, but much less suppression of the analyte signals, irrespective of the placement of the matrix within or on top of the silica. If specific, known analytes are to be detected, formulations can be developed that select for specific analytes, but only at very low signal intensities (e.g., Figure 2-10, Table 2-8). In the absence of PEO, protonated and neutral analytes can be enhanced, with respect to matrix, by incorporating DHB within the silica layer and balancing its concentration so that crystals readily form. The signal to background of anionic analytes,

by contrast, can be dramatically enhanced by incorporation of low MW PEO in the silica and placement of the matrix on top of the silica layer.

2.4 Conclusions

Silica supports derived from a sol gel synthesis exhibited MALDI analyte signal intensities that greatly depended on the extent of matrix crystallinity, and on the interactions between constituents of the silica support, particularly PEO and the matrix. In terms of sensitivity, sol gel derived materials provided better signal-to-background ratios when compared with free matrix, although the absolute intensity of both matrix and analyte signals were lower in the presence of silica. Balancing the DHB:silica ratio permits selective enhancement of the neutral and cationic analytes: although LMW weight signals from matrix were still present, they were greatly reduced. It was observed that PEO of different molecular weights, at the concentrations used, affected the crystallization behaviour of DHB. Extensive hydrogen binding and other electrostatic interactions between high MW PEO, DHB and/or analytes can reduce the efficacy of MALDI performance. However, low MW PEO can be advantageously used to enhance the signal from anionic analytes.

2.5 Experimental Procedure

2.5.1 Chemicals

Tetraethyl orthosilicate (TEOS, 99.999%), poly(ethylene oxide) (PEO) MW 400, 1000 and 100000 PEO were obtained from Aldrich Chemical Company Inc (Milwaukee, WI, USA) while 10000 PEO, 20000 PEO, 2,5-dihydroxybenzoic acid and 0.1N HCl were obtained from Fluka Chemika (Steinheim, Switzerland). Methanol was purchased from

Caledon Laboratories; trifluoroacetic acid (TFA), trimethoprim, haloperidol and fluorescein were purchased from SIGMA Chemical Company. Glu¹-fibrinopeptide B (C₆₆H₉₅N₁₉O₂₆), custom cut stainless steel plates and the gold coated MALDI slides (manufactured by ArrayIt Microarray Technology (SuperGold Substrates)) were a generous donation from MDS Sciex (Vaughan, Ontario, Canada).

2.5.2 Sol Gel Preparation

- a) **Silica sol.** The silica sol solution was prepared by mixing TEOS (1 mL, 4.4 mmol) and HCl (2 mL, 0.1 M). The mixture was sonicated (approximately an hour) in an ice bath, until it became a single uniform phase. Gelation was induced by drying at room temperature with exposure to air.
- b) **Silica/DHB.** DHB was entrained in the silica monolith by simple mixing into the sol. Various amounts of DHB were added to previously hydrolyzed TEOS (600 μ L) sol solution. The various sol gel compositions obtained are presented in Table 2-1. Gelation was allowed to occur as in a).
- c) **Silica/DHB/PEO.** The following PEO solutions were prepared: 400 MW PEO (0.5g in 10 ml of water), 100000 MW PEO (0.5g in 10 ml of water) and 10000 MW PEO (0.05g in 10 ml of water). The final PEO solutions used, which were obtained by direct dilution of these concentrates with water, are given in Table 2-2. The sol gel/DHB hybrid materials were prepared by mixing DHB (2.7 mg and 8.3 mg, respectively) with previously hydrolyzed TEOS (300 μ L) and solutions of 400, 10000 or 100000 molecular weight PEO (300 μ L), respectively. The final silica compositions were TEOS/400 PEO (2.5% w/v), TEOS/10k PEO

(0.25% w/v) and TEOS/100k PEO (2.5% w/v). Gelation was allowed to occur as in a).

- d) **Silica/PEO (washed).** To previously hydrolyzed TEOS (95 μL) following solutions were added: 0.005 g/ml 10k PEO (5 μL), 0.05 g/ml 10k PEO (5 μL), 0.5 g/ml 10k PEO (5 μL), 0.05 g/ml 100k PEO (5 μL). To previously hydrolyzed TEOS (90 μL) following solutions were added: 0.005 g/ml 10k PEO (10 μL), 0.05 g/ml 10k PEO (10 μL), 0.5 g/ml 10k PEO (10 μL), 0.05 g/ml 100k PEO (10 μL) (Table 2-4). The final silica compositions were TEOS/10k PEO (0.025, 0.05, 0.25, 0.5, 2.5, 5.0 %w/v) and TEOS/100k PEO (0.25 and 0.5 %w/v). The film was aged for over 4 days and subsequently was soaked in water over a period of 3 days, with frequent water change (every 6 hours).
- e) **Silica/PEO (heated).** To previously synthesized TEOS either 10k PEO or 100k PEO was added. The final composition of solution was silica/10k PEO (5, 17.5 and 35% w/v) and silica/100k PEO (3.3 and 5 %w/v). After 1 day gelation at room temperature, the plates were exposed to the following heat cycle: 100 °C (30 min), 200 °C (15 min), 450 °C (2 h) (Table 2-3).
- f) **Silica/PEO (untreated).** To hydrolyzed TEOS either 10k or 100k PEO was added. The final composition of solution was silica/10k PEO (0.14, 0.7, 1.4 %molar PEO) and silica/100k PEO (0.019 and 0.029 %molar PEO). Gelation was allowed to occur as in a). The solutions of either DHB/analyte, caffeic acid/analyte, or CHCA/analyte were subsequently spotted on the top of aged gels prior to MALDI analysis.

- g) **Silica/400 PEO.** To previously hydrolyzed TEOS (500 μL), 0.05 g/ml 400 PEO (166 μL) was added and the solution was mixed and subsequently spotted on the plate. The final composition of the solution was 1.25 %w/v of 400 PEO. Gelation was allowed to occur as in a).
- h) **Silica/DHB/PEO/analyte.** To previously hydrolyzed TEOS (150 μL), DHB (4.1 mg) and 25 μL analyte mixture (containing 1:1:1:1 %v/v of all four analytes whose final concentration was 130 ng/ μL) were added and the solution was mixed in with either 10k PEO (150 μL , 0.005 g/ml) or 100k PEO (150 μL , 0.05 g/ml). The final solution was mixed and subsequently spotted on the plate. The final composition of the solution was silica/10k PEO (0.25 %w/v) and silica/100k PEO (2.5 %w/v). Gelation was allowed to occur as in a).

2.5.3 Formation of the MALDI Support Film.

Two types of MALDI plates were used: stainless steel and gold coated slides.

- a) Stainless steel plates were used to study the macroporous silicas that were free of DHB and that were either exposed to washing or heating treatment in order to remove the excess PEO present. A 1 μL sample of well mixed sol solutions (see above) was manually applied to the MALDI plate, stainless steel plate of 5x5x0.3 cm dimensions. After sol deposition and drying, the MALDI gel spots were 2-3 mm in diameter; about 40 spots were applied per plate. The plates were then either heated or washed following the procedure given above. After the silica supports on the plates were treated, 1 μL of matrix/analyte solution was deposited on top of each spot and MALDI was performed. The stainless steel

plates had on average 40 spots (~2mm wide; ~300-500 μm thick; spaced 3 mm apart).

- b) Gold coated slides were used for all of the porous and nonporous silicas that contained entrained DHB as well as an excess PEO. A 1 μL sample of well mixed sol solutions (see above) was manually applied to the MALDI plate, a glass slide coated with gold film (~ 100 Å) of 2x2x0.2 cm dimensions. After sol deposition and drying, the MALDI gel spots were 2-3 mm in diameter. The gold coated slides each had, on average, 30-40 spots ~300-500 μm thick, spaced about 2 mm apart. The gels were aged for 24-48 h in air and at room temperature. For each plate, 3-5 MALDI reference spots were used, free of sol gel, with DHB as the matrix. For each series of sol gel hybrid composition, 10 representative spots were tested.

2.5.4 MALDI Sample Preparation

Four types of molecules were used for MALDI analysis in order to test the applicability of our system for various analytes, including small peptide and small organic molecules (Scheme 2-1): Glu¹-fibrinopeptide B (Glu-fib) (MW 1570), trimethoprim (TMP) (MW 290), haloperidol (MW 375), and fluorescein (MW 332). The final molarity of each analyte in water or in 0.1% TFA/acetonitrile was calculated to be glu-fib (6.36 pmol/ μL), TMP (34.48 pmol/ μL), haloperidol (26.66 pmol/ μL) and fluorescein (30.12 pmol/ μL). The standard analyte solution was prepared at a 1:1:1:1 ratio by volume of Glu-fib, TMP, haloperidol, fluorescein (final concentration of each analyte =2.5 ng/ μL).

Three different approaches were used to introduce the analyte onto the MALDI plate, depending on the location of the matrix and analyte:

- a) *Silica support with embedded matrix.* Droplets containing 1 μL of 2.5 $\text{ng}/\mu\text{L}$ solution of each analyte within the standard mixture were deposited on the preformed and aged sol gels on gold coated MALDI plates and air dried. The matrix:analyte ratio used was about 4000:1 (10000:2.5 $\text{ng}/\mu\text{L}$).
- b) *Silica support without matrix.* DHB (20 mg/mL) was premixed with standard analyte mixture (2.5 $\text{ng}/\mu\text{L}$) in 1:1 ratio by volume. Droplets containing 1 μL of matrix:analyte solution were deposited on the preformed and aged silica spots on gold coated MALDI plates and air dried. The matrix:analyte ratio used was about 8000:1 (20000:2.5 $\text{ng}/\mu\text{L}$).
- c) *Analyte and matrix with silica support.* As previously reported TEOS, PEO, DHB and analyte solutions were premixed and spotted on the MALDI plate. The matrix:analyte ratio used was about 30000:1 (12600:0.43 2.5 $\text{ng}/\mu\text{L}$).

The resulting dried droplet spots were ca. 2 mm wide For each series of sol gel hybrid composition, 10 representative spots were tested. As shall the discussed below, the analytes were not evenly distributed across the spotted area.

Reproducibility study presented in Table 2-7 was obtained by guiding the laser from spot-to-spot within the same plate and given values represent the average of minimum 5 measurements.

2.5.5 MALDI Instrumentation

MALDI analysis was done using a prOTOFTM 2000 MALDI O-TOF Mass Spectrometer (PerkinElmerSCIEX) equipped with a 337-nm N₂ laser and a 20-kV acceleration voltage. Mass spectra were generated from the average of 300 laser shots, at 10 Hz laser rate, 210 mL/m focusing gas flow, 90 mL/m cooling gas flow and 70% laser energy.

2.5.6 Characterization Studies

Scanning electron microscopy (SEM) images were obtained on a Philips SEM 515 field emission microscope using an acceleration voltage of 20 kV to examine the morphology of the dried gels. To avoid charging effects the sample plates were sputter coated with approximately 100-150 Å of gold. Optical microscopy images were collected using Olympus BX41 (at 5x and 20x magnifications) in order to study the sol gel morphology at the macroscopic scale.

Absorption measurements of solutions were made using Tecan SAFIRE spectrophotometer. The wavelength resolution was 1 nm, the scan number was 401 at the ambient temperature.

FT-IR studies were recorded on a Bruker Equinox 55 spectrometer by running 50 background scans and 100 sample scans.

2.6 References

- ¹ Go, E.P., Prenni, J.E., Wei, J., Jones, A., Hall, S.C., Witkowska, E., Shen, Z. and Siuzdak, G., *Anal. Chem.*, 75, 2003, 2504-2506.
- ² Kinumi, T., Saisu, T., Takayama, M. and Niwa, H., *J. Mass. Spectrom.*, 35, 2000, 417-422.
- ³ Cohen, J.L. and Cox, J.A., *J. Sol-gel Sci. Tech.*, 28, 2003, 15-18.
- ⁴ Lin, Y-S, Yang, C-H. and Chen, Y-C., *Rapid Comm. Mass Spectrom.*, 18, 2004, 313-318.
- ⁵ Lin, Y-S. and Chen, Y-C., *Anal. Chem.*, 74, 2002, 5793-5798.
- ⁶ Zhang, Q. , Zou, H., Guo, Z., Zhang, Q., Chen, X. and Ni, J., *Rapid Comm. Mass Spectrom.*, 15, 2001, 217-223.
- ⁷ a) Chen, C-T. and Chen, Y-C., *Anal. Chem.*, 76, 2004, 1453-1457. b) Chen, W-Y and Chen, Y-C., *Anal. Chem.*, 75, 2003, 4223-4228.
- ⁸ Chen, C.-T. and Chen, Y.-C., *Rapid Comm. Mass Spectrom.*, 18, 2004, 1956-1964.
- ⁹ Vorderwulbecke, S., Cleverley, S., Weinberger, S.R. and Wiesner, A., *Nature Methods*, 2, 2005, 393-395.
- ¹⁰ Peterson, S.D., Luo, Q., Hilder, E.F., Svec, F. and Frechet, J.M.J., *Rapid Comm. Mass Spectrom.*, 18, 2004, 1-9.
- ¹¹ Voivodov, K.I., Ching, J. and Hutchens, T.W., *Tetrahedron Lett.*, 37, 1996, 5669-5672.
- ¹² Zheng, Z., Chen, Y., Hodgson, R., Brook, M.A. and Brennan, J.D., *Macromol. Symp.*, 226, 2005, 253-262.

- ¹³ Ishizuka, N., Kobayashi, H., Minahuchi, H., Nakanishi, K., Hirao, K., Hosoya, K., Ikegami, T. and Tanaka, N., *J. Chrom. A*, 960, 2002, 85-96.
- ¹⁴ Brinker, J.C. and Scherer, G.W., *Sol-Gel Science*, Academic Press Inc., NY: New York, 1990.
- ¹⁵ Brook, M. A., Chen, Y., Guo, K., Zhang, Z. and Brennan, J. D., *J. Mater. Chem.*, 14, 2004, 1469-1479.
- ¹⁶ a) Nakamura, N., Takahashi, R., Sato, S., Sodesawa, T. and Yoshida, S., *Phys. Chem. Chem. Phys.*, 2, 2000, 4983-4990. b) Ishizuka, N., Minakuchi, H., Nakanishi, K., Hirao, K., and Tanaka, N., *Colloids and Surfaces, A: Phys. Eng. Asp.*, 187-188, 2001, 273-279.
- ¹⁷ Chen, Y., Zhang, Z., Sui, X., Brennan, J. D. and Brook, M. A., *J. Mater. Chem.*, 15, 2005, 3132-3141.
- ¹⁸ Loboda, A.V., Ackloo, S. and Chernushevich I. V., *Rapid Comm. Mass Spectrom.*, 17, 2003, 2508-2516.
- ¹⁹ As noted above, matrix free metal oxide films can act as MALDI supports. Several different structural silica morphologies were examined for their ability to participate in the MALDI experiments. However, it was demonstrated that, in the absence of DHB matrix (either entrained in or deposited on the silica surface), sol gel silicas were incapable of promoting analyte ionization.
- ²⁰ a) Ludemann H.-C., Hillenkamp, F. and Redmond, R.W., *J. Phys. Chem. A*, 104, 2000, 3884-3893. b) Dreisewerd, K., *Chem. Rev.*, 103, 2003, 395-426. c) Zenobi, R. and Knochenmuss, R., *Mass Spectrom. Rev.*, 17, 1998, 337-366.

²¹ Wu, J., Chiu, S-C., Eli, M.P. and Kwei, T.K., J. Pol. Chem. A: Pol. Chem., 39, 2001, 224-231.

²² Pines E. and Huppert D., J. Phys. Chem., 87, 1983, 4471-4478.

²³ Mesoporous silicas: pore size 1.29 nm (radius), BET surface area 830 m²/g; Macroporous silica (heated): pore size 0.25-1.45 μm (radius) and 2-5 nm (radius of mesopores), BET surface area 500-600 m²/g.

3 CHAPTER 3. HIGHLY SELECTIVE TETHERED MALDI MATRIX

3.1 Introduction

As noted in Chapter 2, the laser photoexcitation from a variety of supports can lead to ion desorption and, ultimately, characterization of the ions utilizing mass spectrometry. The most common protocols currently employed use photoactive compounds – matrices - that typically possess weakly acidic groups.

It has been suggested that the functions of the matrix include: incorporation of the analyte into matrix crystals (without which signal intensity is dramatically attenuated, as noted in Chapter 2), a collective photon absorption and ablation event during which the matrix and accompanying analyte are ejected into the gas phase, and an active role by the matrix in ionizing the analyte. It was believed that matrix crystallinity, purity and the nature of functional groups on the matrix molecules are relevant for obtaining good analyte signals in the MALDI experiment. However, numerous studies have demonstrated that free phenols and acids are not MALDI prerequisites. Some studies have additionally suggested that while crystalline matrices are required for high signal intensity, co-crystallization of analyte and matrix is not important. The latter issue has been addressed in the previous chapter, which demonstrates that premixing the analyte and matrix within the sol does not improve the desorption and ionization processes over placing the analyte on top of the preformed porous silica:DHB films. However, the results presented in Chapter 2 strongly suggest that matrix crystallization is important for successful analyte desorption and ionization when DHB was used; this observation could be extended to

classic acidic matrices (e.g., DHB, CHCA), which undergo chemical ionization that leads to gas phase ion formation. That is, a key constituent of the MALDI process involves the transfer from matrix acidic groups, including phenolic and carboxylic acid groups, of protons to analytes in MALDI. Classically, the most effective organic matrices have some of the following functional groups: OH, COOH, NO₂, NH₂, and/or CONH. In fact, despite the extensive research done to correlate matrix functionality with MALDI performance, conflicting results and views exist. For example, a number of studies have shown, using chemical derivatization to mask phenols or carboxylic acids, that significant MALDI performance can occur in the absence of these acidic protons.¹ Similarly, the utility of matrix-free methods show that protons are not necessarily required. However, the mechanism of activation in such cases is unknown.

When matrices are used, it is well known that the typical MALDI mass spectrum is mostly composed of matrix-related signals in the low mass region (<700 m/z), accompanied by ion peaks arising from the analytes. Such interferences tend to disable the study of low molecular weight compounds, since their molecular ions are overlapped by extensive, intensive matrix peaks. Several approaches have been developed to entrain the matrix within the surface in order to minimize its desorption; a similar study was described using DHB in variety of nonporous, mesoporous and macroporous silica gels (Chapter 2). As shown in Chapter 2, we successfully reduced matrix-related signals and improved S/B values by entrapping DHB within the mesoporous silica, or applying it to a mesoporous silica surface. While it was possible to nearly completely suppress matrix

signals, doing so led to low overall absolute intensities for analyte signals, that were far inferior to the standard MALDI experiment.

It has been demonstrated that covalent binding of the matrix compound can lead to analyte ionization, and to reduce the intensity of low mass interference signals. Small molecules have also been immobilized on to a DIOS surface (porous silicon) via Diels-Alder attachment and were successfully desorbed upon laser irradiation.² Self-assembled monolayers (SAMs) of aromatic compounds have also been investigated as MALDI supports. When Mouradian et al³ used matrix type monomers bound to gold surface, a desorption and ionization of insulin and cytochrome C was successful. However, analytes could be observed only from SAMs of aromatic acetamide and not from an aromatic carboxylic acid. Moreover, no analyte peaks were observed when aromatic acetamide monomer was used as a conventional matrix. In addition, depletion of the monolayer with time was observed as well which has led to unavoidable reoccurrence of low mass interference signals (monomer ions).⁴ An approach of matrix tethering via photolabile bonds, in order to fully remove matrix-related signals, was explored by Voivodov et al.⁵ and Hutchens et al.⁶ CHCA was chemically bound to the polymeric surface through an ester linkage or to agarose beads to which biomolecules were consequently attached. The agarose bead-CHCA system allowed for ionization of myoglobin without evident CHCA ions, while the polymer-CHCA system allowed for ionization of smaller peptides (>2200 Da) in the form of molecular ions or as matrix adducts (monomers and dimers). It is uncertain whether both chemisorption and physisorption existed in the case of agarose-CHCA system due to the poor washing procedures used, and hence the results shown

cannot be attributed to the bound CHCA alone. The researchers have also demonstrated that certain compounds which do not work as matrices when in free state, perform very well once surface bound. For example, Hutchens et al.⁶ demonstrated that cinnamide was an ineffective matrix when present in excess as a free molecule, however, it performed well once bound to the activated sepharose. Ching et al.⁷ have further extended the approach to the photoinduced desorption of covalently tethered biomolecules. In a three layer system, biomolecules were tethered to photoactive azobenzene derivatives, that were in turn linked to the surface. Despite the successful UV initiated desorption and ionization of peptides, via azobenzene cleavage, irreproducibility of absolute signal intensity and of S/B ratios was observed with this system. Of greater concern was the observation of irreproducible analyte desorption from the same surface (i.e., appearance and disappearance of signals on the same surface). The approaches described above exhibited for relatively low signal intensity (60-600) and were not applied to the study of low molecular weight species. All the previous studies demonstrated that the chemical nature of the tethered matrix, and the nature of binding (monolayer or thin film) are critical in the desorption/ionization process. However, all of the previously reported approaches employed a photoactive linkages, which led to extensive adduct formation upon longer laser irradiation. Hence further investigation is necessary in order to develop MALDI materials that could be applied to the study of LMW compounds, that exhibit tailored selectivity and that are surface-bound via nonphotolabile bonds.

In light of the confusion and ambiguity of the studies in the literature, we have decided to systematically modify MALDI matrices. We have examined the modified

matrices before and after their covalent bonding to a silica surface. We have also investigated the effect of chemical modification on the factors that were previously reported to be the decisive elements in MALDI process, including UV absorbance and crystallization. We have prepared a number of derivatives of typical MALDI matrices in which the functional group patterns were modified either by changing the functional groups themselves, or by capping them (to remove active hydrogens). These derivatives were tested as MALDI matrices as a function of laser intensity, analyte concentrations and solvent composition amongst other factors, in order to find the conditions for their optimal performance in MALDI. We have also investigated the ability of these compounds to undergo crystallization as a function of silica support morphology, solvent effects, and UV absorbance in solution, and have related these to the MALDI performance as measured both in terms of total intensity and relative intensity of the analyte signals with respect to matrix. After the parameters were optimized, analogous compounds were prepared that contain Si(OEt)₃ groups. These were bound to silica supports, which we have described elsewhere,⁸ and their efficacy in grafted form in the MALDI experiment determined.

3.2 Results and Discussion

3.2.1 Synthesis

The compounds we have examined (Table 3-1) are derivatives of 2,5-dihydroxybenzoic acids (DHB) (**5**, **6**, **23**, **25**), 3-methoxy-4-hydroxybenzoic acid (**1**, **21**, **22**), 3,4-dihydroxycinnamic acid (**9**, **11**, **12**, **14**), 3,4-dihydroxybenzaldehyde (**7**, **8**) and α -cyano-4-hydroxycinnamic acid (**8**), respectively. The synthetic sequences used are well

precedented manipulations that utilize protecting group chemistry. Ultimately, the compounds prepared need to be amenable to hydrosilylation (see below) and we have used allyl groups for this purpose.

3.2.2 Synthetic Methods Used

Allyl groups were introduced in two complementary ways: Williamson etherification of phenols, or amidation of carboxylic acids by the carbodiimide-catalyzed reaction of the amine with the carboxylic acid. Protection of the carboxylic acid was needed in some cases during phenol etherification, due to the sensitivity of the subsequent hydrosilylation experiments with triethoxysilanes to acidic hydrogens.

A representative scheme for etherification and subsequent hydrosilylation is presented in Figure 3-1 (a complete listing of compounds is provided (Table 3-1).

A number of other chemical approaches were investigated in order to prepare silicon-containing matrix analogues. For example, a one step synthetic approach was used for the modification of hydroxyphthalamic anhydride with a common silicon linker (3-aminopropyltriethoxysilane) (APTES) as shown in Figure 3-2. In addition, a third approach was adopted which involved yet another silicon-based linker, isocyanatopropyltriethoxysilane (IPTES), which reacted efficiently with coumarin (Figure 3-3).

Figure 3-1. Synthetic scheme proposed for phenolic allylation and subsequent hydrosilylation to give 1.

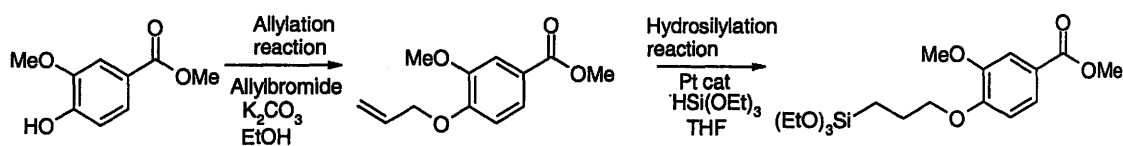


Figure 3-2. Synthetic approach utilizing for 3-hydroxyphthalic anhydride to give 2.

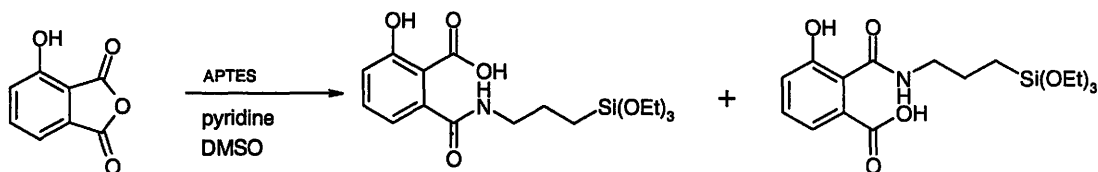
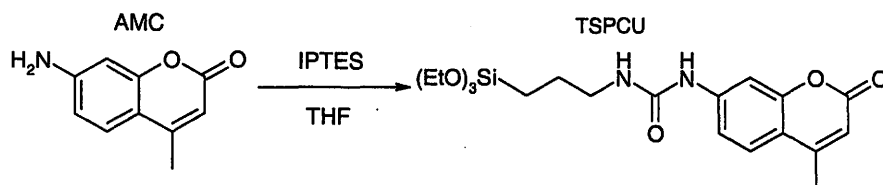


Figure 3-3. Synthesis of triethoxysilylated coumarin to give 3.



The hydrosilylation reaction, an addition of Si-H across the C=C double bond, was utilized to introduce Si(OEt)₃ moieties. In a number of instances we observed the direct reaction of phenols with HSi(OEt)₃, which led to conversion of phenols into O-Si(OEt)₃ groups. However, during sol gel processing these groups underwent deprotection to liberate the phenol during the hydrolysis step.

As will be discussed below, our investigation of the effect of group functionality on MALDI performance has revealed that the phenols were much more relevant for ionization purposes than was the carboxylic acid. Hence, we further investigated a second synthetic approach. A typical synthetic scheme proposed for allylation at the carboxylic acid end and subsequent hydrosilylation is presented in Figure 3-4 with modification of 2,5-dihydroxybenzoic acid **4** given as the example. An experimental procedure for allylation and hydrosilylation are given in detail in the synthetic part below. A number of compounds that were developed using such approach are given in Figure 3-5.

Figure 3-4. Synthetic scheme for carboxylic allylation via amide formation and hydrosilylation to give 5.

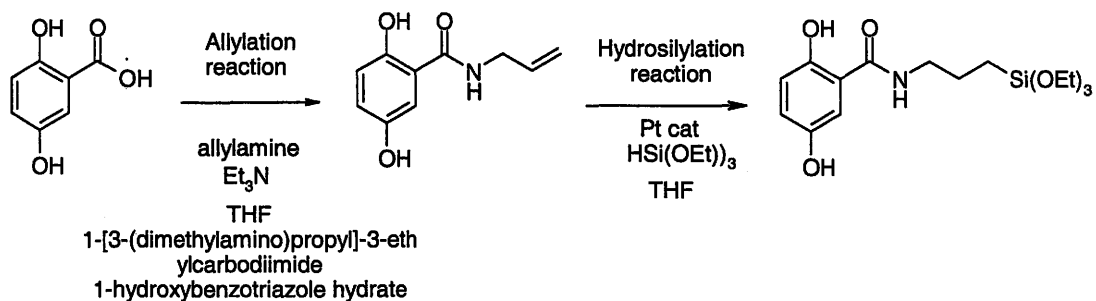
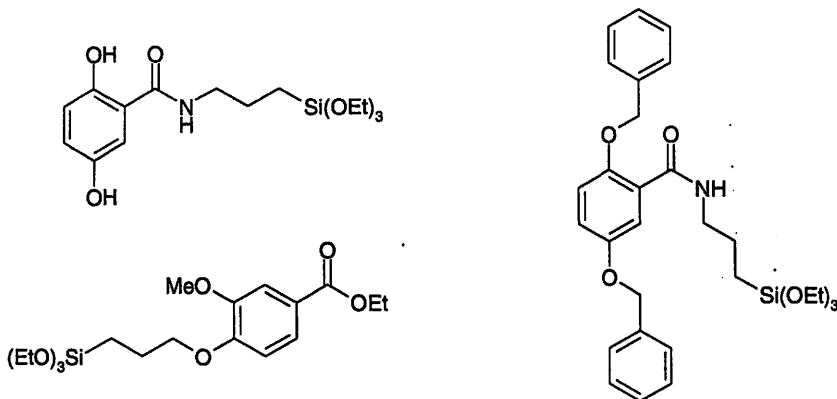
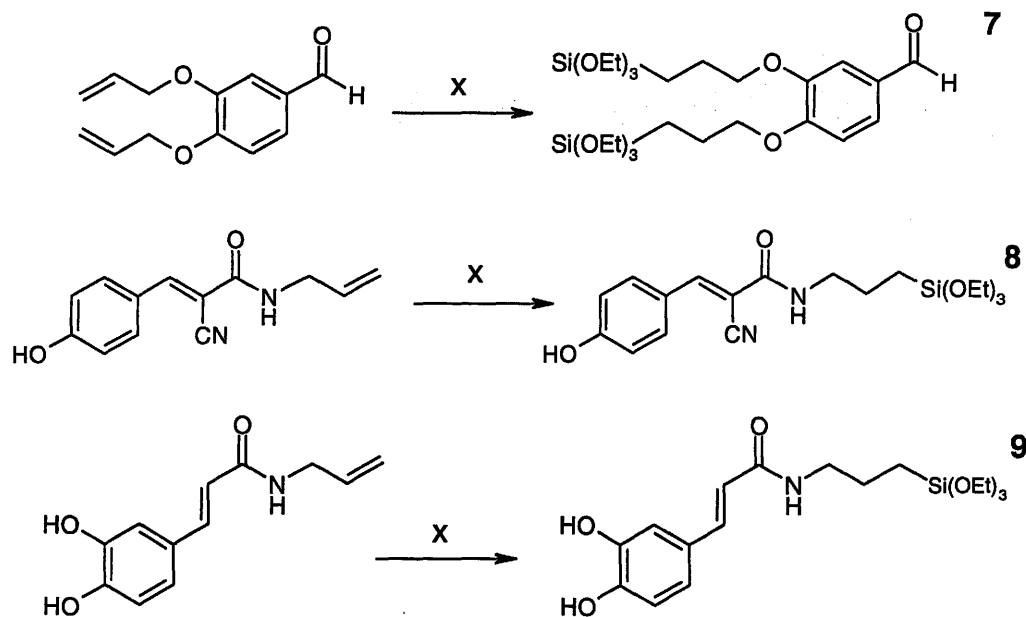


Figure 3-5. The triethoxysilylated compounds 1, 5 and 6.



Despite the reported ease of hydrosilylation,⁹ several compounds were not amenable to this reaction. Judging from the proton NMR, the hydrosilylation at room temperature was incomplete or did not occur for the compounds shown in Figure 3-6. Longer reaction times (2-4 days) and subsequent addition of more catalyst did not improve this outcome. No further temperature treatment was employed to effect the reactions.

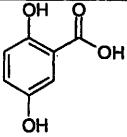
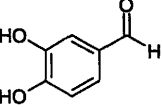
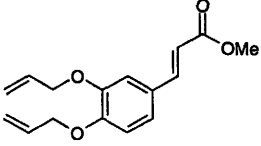
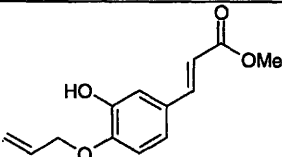
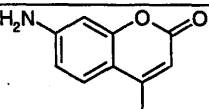
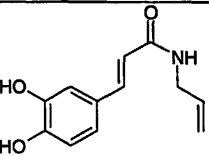
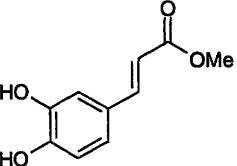
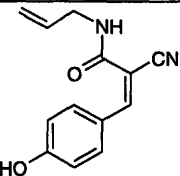
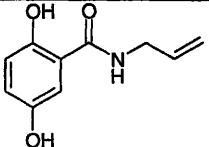
Figure 3-6. Challenges associated with hydrosilylation reactions of 7, 8 and 9.

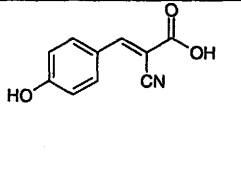
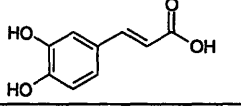
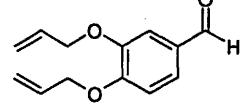
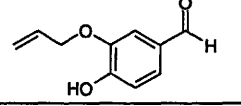
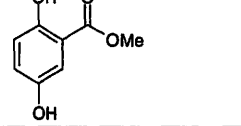
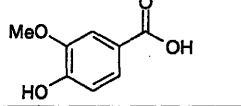
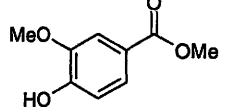
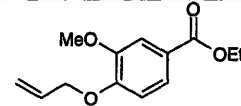
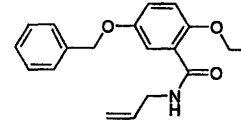


3.2.3 UV Studies

It was suspected that MALDI performance was strongly dependent on UV absorbance of the matrix support, as has been discussed in previous reports.¹⁰ Groups such as phenols and amines exhibited, in many cases, increased acidity in their electronically excited states in gas-phase, and hence were thought to act as the proton source.¹¹ By contrast, carboxylic acids were not generally affected by electronic excitation, which made them less likely to be the proton donors. We were interested to study the effect of chemical modification on UV absorbance and extinction coefficients. The chemical structures of the synthesized model matrix compounds and their λ_{max} and extinction coefficient values (@337nm) are presented in Table 3-1.

Table 3-1. UV values of synthesized organic matrices, 0.120 mM.

Structure	Compound number	λ_{max} (nm)	$\epsilon_{@337\text{nm}}$ L/mol*cm
	4	332	4139
	10	308	2738
	11	300	2373
	12	322	10222
	13	354	14600
	9	318	9083
	14	324	8545
	8	326	8516
	15	324	4691

	16	342	24467
	17	322	16023
	7	304	1500
	18	310	2416
	19	332	4347
	20	292	1066
	21	292	1055
	22	294	1077
	23	313	12312

When the UV absorbances of standard MALDI matrices were compared with the synthetic derivatives described above, several trends were observed. It appears that esterification did not affect maximum UV absorption as dramatically as amide formation and introduction of an allyl group did, both of which led to shifting of λ_{\max} to lower wavelength (compare **4**, **15**, **19** in Figure 3-7 with **9**, **12**, **14**, **17** in Figure 3-8).

Interestingly, the greater the number of allyl functionalities present, the lower the UV absorbance (Figure 3-8)).

Figure 3-7. UV of DHB derivatives, 0.12 mM.

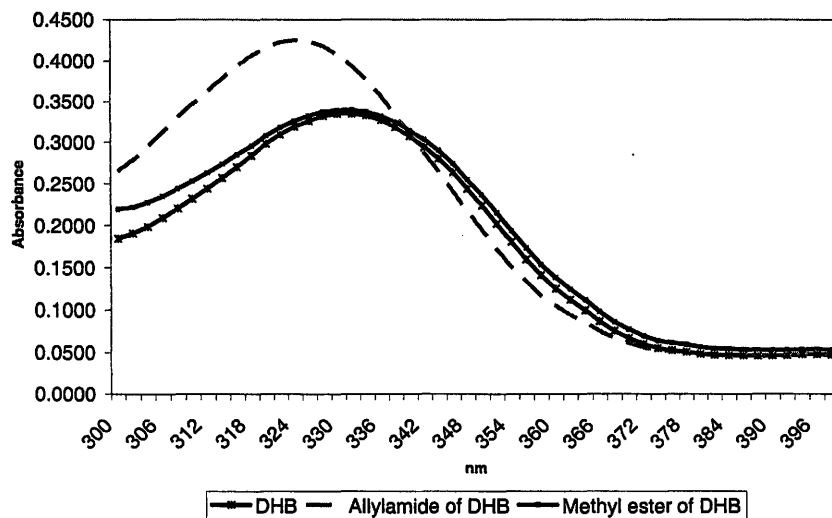
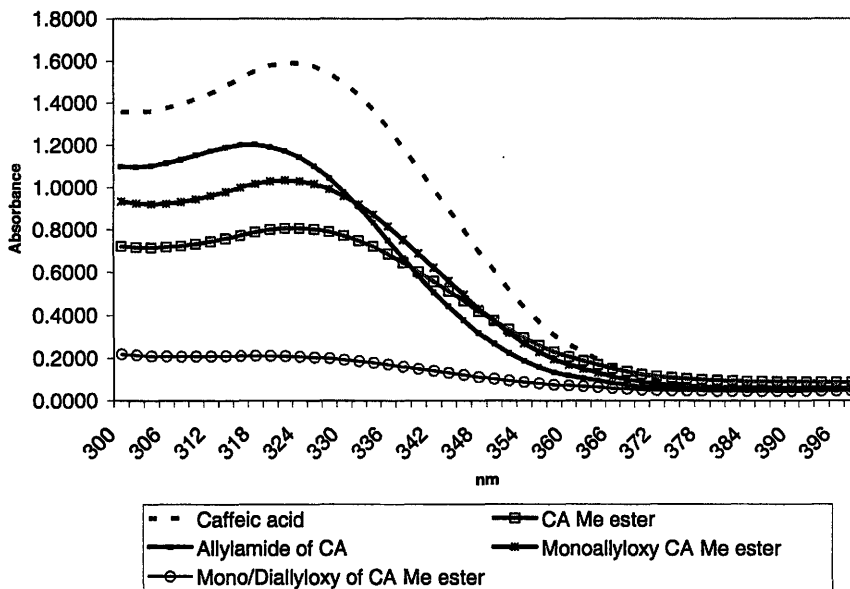
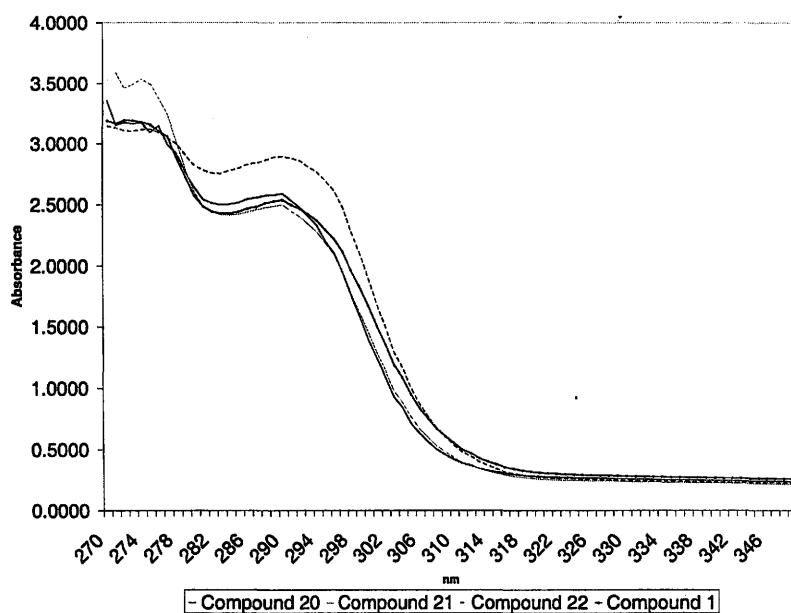


Figure 3-8. UV of CA derivatives, 0.12 mM.



The chemical modification of phenol and carboxylic acid moieties generally led to a lowering of UV absorbance frequencies, for most of the derivatives prepared. However, electronic transitions of 4-hydroxy-3-methoxybenzoic acid (HMBA) and its derivatives greatly deviated from this trend: the allyloxy ester derivative **22** gave rise to the highest UV absorbance (Figure 3-9) of the compounds studied.

Figure 3-9. UV of HMBA derivatives, 0.12 mM.




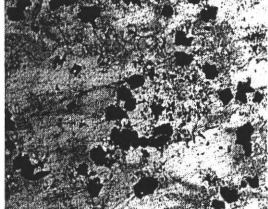


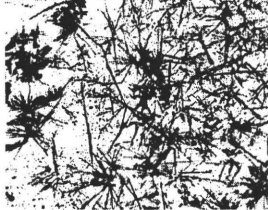

In terms of molar extinction coefficients, the nature of functional groups greatly affected the UV absorptivity values at the wavelength of nitrogen laser. For every standard matrix and its derivatives, $\epsilon_{337\text{nm}}$ values were mostly lower for those molecules with fewer OH groups and/or absent the carboxylic acid. However, such trends were strongly dependent on the matrix used and were not universal. No consistent correlation between the functional groups modified, the specific modification, and the λ_{max} and $\epsilon_{337\text{nm}}$ values.




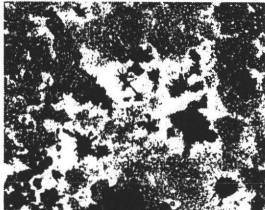


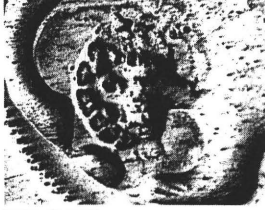
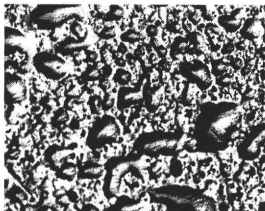




3.2.4 Crystal formation and morphology of synthetic matrices

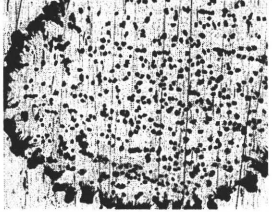
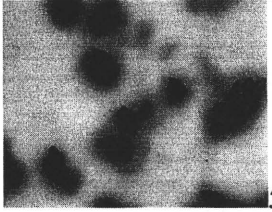
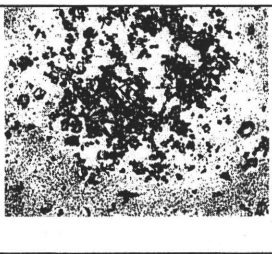
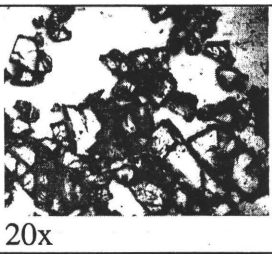
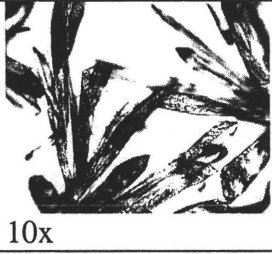

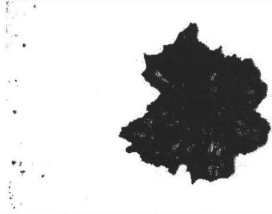

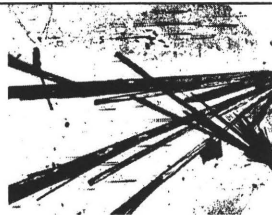
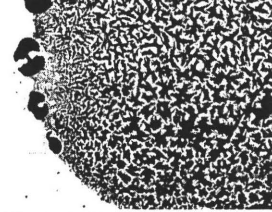
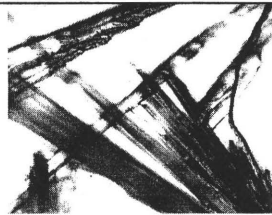
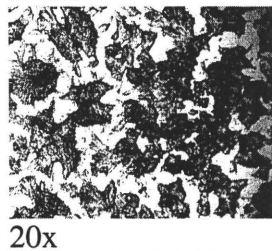
It was concluded in the previous study (Chapter 2) that for the free matrix to work, crystallization must not be impaired. A similar trend was observed by others who claimed that co-crystallization of the matrix and analyte was a necessary factor for good performance.¹² Opposing views were presented by those who have found that the matrices which lack crystal structure still have performed equally well.^{1,13} Since the extent of crystallization is dependent on the nature of the matrix and the specific system studied, we have investigated the ability of the chemically modified materials, presented in Table 3-1, to undergo crystallization. Crystal growth, of course, can be affected by a broad variety of factors such as drying conditions (open air or under vacuum), crystallization temperature (ambient or elevated) and air quality, which all affect the crystallization process in unpredictable ways. The synthetically modified matrix analogues were each (~20 mg) dissolved in 0.1% TFA:acetonitrile (1 mL, 50:50%vv or 75:25%vv) mixture and were deposited on MALDI support such as a stainless steel plate. Optical photographs of these compounds and the standard matrices are given in Table 3-2. In general, chemical modification has led to obvious changes in crystallization behaviour, but retention of the ability to form crystalline domains. For all the matrices investigated, a 50:50%vv solvent composition gave rise to large needle-like crystals, while 75:25%vv solvent mixture led to the large crystal aggregates. The replacement of a carboxylic acid group by an ester led to the formation of crystalline aggregates rather than to elongated needles. Notably, HMBA derivatives led to purely amorphous films with the complete absence of crystals.

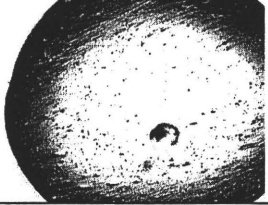
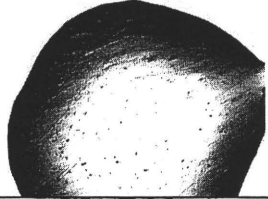
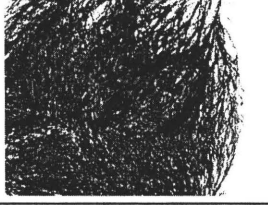
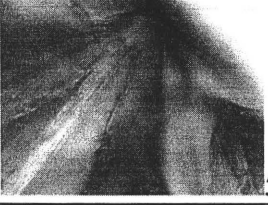
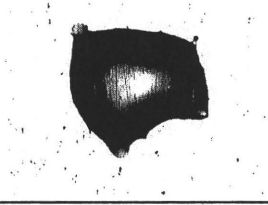
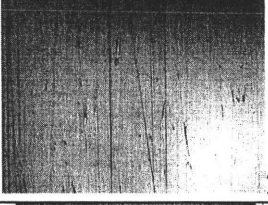
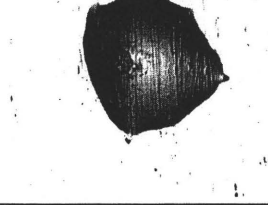
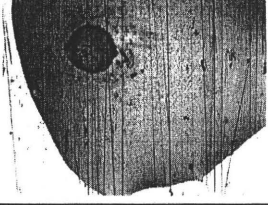

Overall, extensive crystallinity was observed for most of derivatives with slight changes in crystal morphology. We were next interested to see what effect these slight changes, if any, had on the overall MALDI performance of the matrix in question.

Table 3-2. Optical micrographs of standard MALDI matrices and their derivatives.

Compound	Optical micrographs (x magnification) 50 :50% (top) OR 75 :25% vv (bottom) ACN :0.1% TFA	
Caffeic acid 17	 <p>75:25%</p> 	 <p>50x</p>  <p>50x</p>
Monoallyloxy Methyl ester of CA 12	 <p>75:25 ACN:0.1%TFA</p>	 <p>50x</p>

		 <p>50x</p>
<p>Methyl ester of CA 14</p>	 <p>75:25%</p> 	 <p>20x</p> <p>75:25%</p> 
<p>Allylamide of DHB 15</p>	 <p>75:25%</p> 	 <p>20x</p> <p>75:25%</p> 
<p>Allylamide of Caffeic acid 9</p>		 <p>20x</p>

<p>CHCA 16</p>		 <p>50x</p>
<p>Allylamide of CHCA 8</p>		 <p>20x</p>
<p>DHB 4</p>	 <p>10x</p>	 <p>20x</p>
<p>Methyl ester of DHB 19</p>		 <p>50x</p>
<p>DHA 10</p>	 <p>75:25</p> 	 <p>75:25</p>  <p>20x</p>

<p>Monoallyloxy DHA 18</p>		
<p>Diallyloxy DHA 7</p>		
<p>3-methoxy-4-hydroxy benzoic acid 20</p>		 <p>50x</p>
<p>3-methoxy-4-hydroxy methyl benzoate 21</p>		 <p>20x</p>
<p>3-methoxy-4-allyloxy ethyl benzoate 1</p>		 <p>10x</p>
<p>7-amino-3- methylcoumarin (AMC) 13</p>	 <p>10x</p>	

3.2.5 Effect of Functionality on MALDI

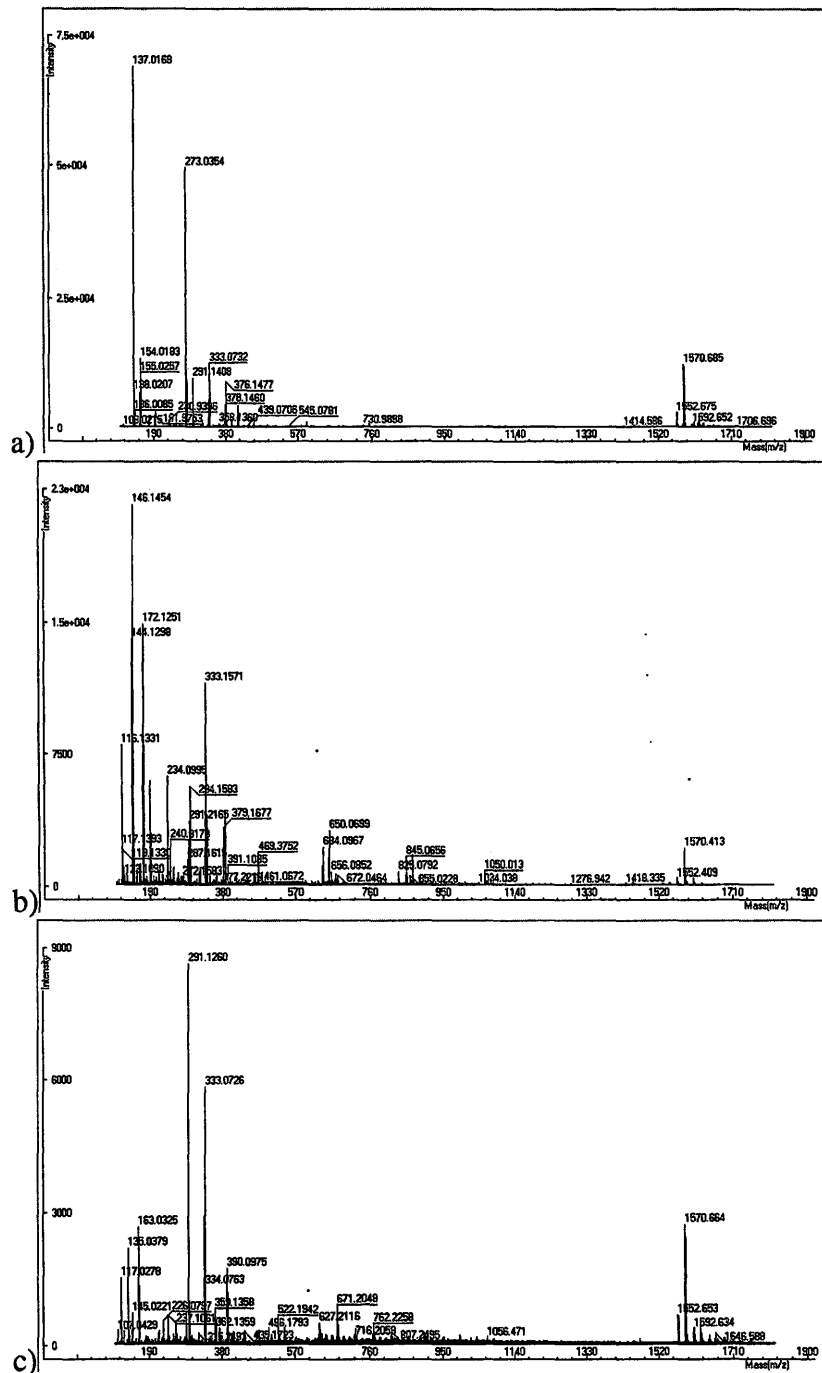
It has been determined that a variety of factors affect matrix performance, such as: chemical structure, degree of crystallization, UV absorbance and physical properties (sublimation point, high vacuum stability). However, the extent of these effects was

greatly matrix dependent. These and other factors were studied and discussed below in turn.

Following the experimentation on the free matrix, reported in Chapter 2, we decided to initially examine the MALDI behaviour of the starting compounds, which possess free phenols and/or acids. The following conditions are optimized: 50:50%v acetonitrile:0.1% trifluoroacetic acid (in water) solvent composition, 16 μ J laser intensity, 20mg/mL matrix concentration and 2.5 nm/ μ L analyte concentration. As in Chapter 2, the following analytes were chosen for the study: haloperidol, trimethoprim (TMP), fluorescein, and the oligopeptide glu-fib (EGVNDNEEGFFSAR). These analytes provide variety with respect to molecular weight and structure. Trimethoprim (MW 290) is an aromatic amine that will be cationic at normal pHs, while haloperidol (MW 375) is a neutral, aromatic halide also possessing an aliphatic tertiary hydroxyl group. Glu-fib (MW 1570) and fluorescein (MW 332) both have a number of phenolic and carboxylic acid groups that can be involved in hydrogen bonding: the compounds are anionic at normal pHs. Glu-fib is a much larger molecule than the other analytes and was chosen both for its size and its structural relevance to peptidic drugs.

When MALDI MS of glu-fibrinopeptide, trimethoprim, haloperidol and fluorescein was performed using the three standard compounds (2,5-DHB, caffeic acid and CHCA) ionization all four analytes were executed successfully (Figure 3-10). These data provide a positive control for the remaining compounds. Since these possess both phenols and an acid, it was unclear which functional group, if either, plays the most important role in facilitating ionization.

Figure 3-10. MALDI MS of glu-fib, TMP, haloperidol and fluorescein using: a) DHB, b) CHCA and c) CA matrix.



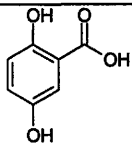
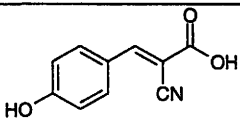
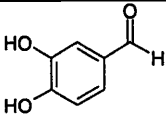
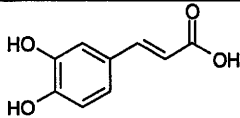
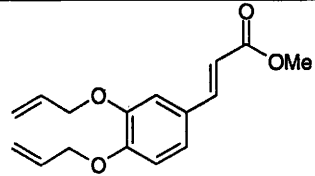
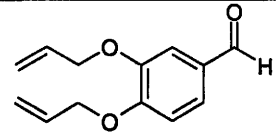
To establish the putative roles of phenol or acids in the MALDI experiment, the acid-free matrix compound 3,4-dihydroxy benzaldehyde **10** was tested as MALDI matrix. The results were positive: this phenolic acid-free matrix led to ionization of all four analytes. Such findings provide a new synthetic handle, the aldehyde, to use to modify possible new matrices.

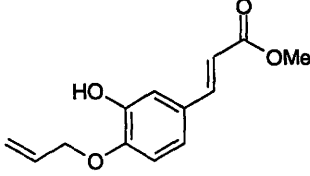
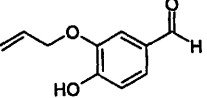
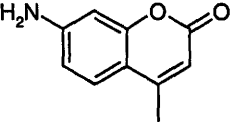
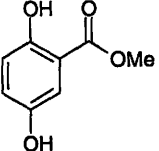
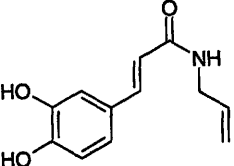
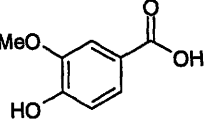
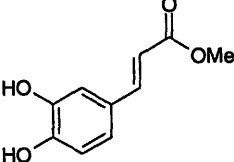
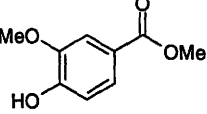
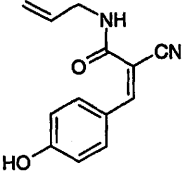
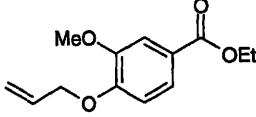
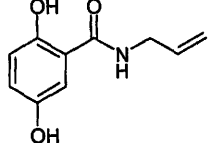
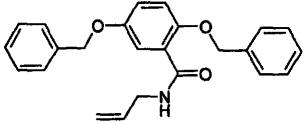
Next, the phenols were capped in these molecules. The derivatization of phenols required acid group protection and subsequent deprotection, which was both time consuming and led to reduced synthetic yields. Amongst all allyloxy derivatives of caffeic acid only 4-allyloxy-3-hydroxy cinnamic acid worked as a MALDI matrix, and was selective for glu-fib and fluorescein. The remaining derivatives had substantial UV absorbance and were crystalline (Table 3-1), however, they worked poorly when compared to the parent matrix (Table 3-3). Monoallyloxy and diallyloxy derivatives of benzaldehyde led to no signals in the MALDI experiment.

The second set of compounds studied was derivatized at the acid group. Esters and allyl amides of 2,5-dihydroxybenzoic, caffeic acid and CHCA behaved differently from their parent compounds. While the methyl ester of caffeic acid was an effective matrix for analytes haloperidol, fluorescein and peptide glu-fib, the ester analogue of DHB **19** failed under identical conditions. Similarly, while *N*-allylamide derivatives of CHCA **8** and caffeic acid **9** were MALDI matrices for fluorescein, haloperidol and glu-fib, the DHB analogue **15** did not work at all. It should be noted that, compared to the other classes of molecules, derivatives of DHB derivatives were generally ineffective in desorption and ionization of analytes.

The above data demonstrates that, among the compounds studies, the best MALDI performance was obtained using derivatized matrices that possessed either one or two phenol groups irrespective of the presence of acid group as it can be seen in Table 3-3: the presence of an acid is not required. As a consequence of high correlation between the presence of phenols and MALDI performance, most of the derivatives examined in detail were modified to allow at least one free phenol.

Table 3-3. MALDI analyte signal intensity observed for series of MALDI matrices.

Structure	Analyte Type (Intensity)	Structure	Analyte Type (Intensity)
 <p>4</p>	TMP (15050) ^a (8) ^b Fluorescein (13824) ^a (31) ^b Haloperidol (16383) ^a (20) ^b Glu-fib (26667) ^a (18) ^b	 <p>15</p>	TMP (17980) ^a Fluorescein (113294) ^a Haloperidol (4580) ^a Glu-fib (89932) ^a
 <p>10</p>	TMP (0.3) Fluorescein (0.12) Haloperidol (0.2) Glu-fib (1.4)	 <p>17</p>	TMP (7) Fluorescein (23) Haloperidol (15) Glu-fib (6.4)
 <p>11</p>	none	 <p>7</p>	none

 <p>12</p>	<p>TMP (8) Fluorescein (4.5) Haloperidol (3.4)</p>	 <p>18</p>	<p>none</p>
 <p>13</p>	<p>TMP^a (3189) Fluorescein^a (55005) Glu-fib^a (63980)</p>	 <p>19</p>	<p>none</p>
 <p>9</p>	<p>Fluorescein (0.18) Haloperidol (0.05) Glu-fib (0.06)</p>	 <p>20</p>	<p>TMP (100)^a Fluorescein (25)^a</p>
 <p>14</p>	<p>Fluorescein (13.5) Haloperidol (2.7) Glu-fib (0.16)</p>	 <p>21</p>	<p>TMP (580)^a Fluorescein (87)^a</p>
 <p>8</p>	<p>Fluorescein (13) Haloperidol (10) Glu-fib (0.43)</p>	 <p>22</p>	<p>none</p>
 <p>15</p>	<p>none</p>	 <p>23</p>	<p>none</p>

^a proTOF™ 2000 MALDI O-TOF Mass spectrometer (PerkinElmerSCIEX, commercially available).

^b Breadboard MADLI-TOF Mass spectrometer (Research)

Although it has been proposed that crystallization may be a key factor for effective MALDI matrices, this contention is not supported by the characteristics of the compounds prepared. No clear trend existed between the presence of matrix crystals and the ability of a compound to ionize the analytes, since highly crystalline derivatives such as methyl 2,5-dihydroxybenzoate failed to work as a matrix. More interestingly, highly amorphous matrices such as that derived from 3-methoxy-4-hydroxybenzoic acid were effective at promoting analyte desorption and ionization, despite the absence of obvious crystals. Hence, crystals are not decisive factors for MALDI performance. In addition, capping of phenol or acid led to an increase in crystal size.

Though it was believed that the absorption coefficient at the laser wavelength used was a very important parameter for MALDI, it does not appear that the absorbance at the laser wavelength and the protonated ion yields are directly correlated. From the extensive UV studies undertaken, it is clear that UV absorption alone is not a sufficient criterion for selecting a useful matrix: two similarly absorbing molecules may perform completely differently. Similarly, it was demonstrated by Bashir et al. that though modified DHB matrices (ester with variable length of alkyl R group) had higher absorbance at 337 nm than did DHB, they were not all able to ionize substance P.¹³

There was no clear trend between λ_{\max} and the chemical derivatization. Neither does a relationship exist between the matrix absorbance at 337 nm and the protonated ion yield observed. Those derivatives with the $\epsilon_{337\text{nm}}$ values higher than DHB did not work better than DHB. Notably, some derivatives with high $\epsilon_{337\text{nm}}$ and free phenol (s) failed to

work as matrices, further suggesting that the UV absorbance alone was not a sufficient criterion for selecting a proper matrix.

It was expected that compounds with a high extinction coefficient at 337 nm, the laser wavelength, would be highly effective matrices. Many were not. Therefore, an assessment of other parameters which could affect performance were investigated, including their physical state and sublimation point. An obvious trend was observed: all those derivatives with melting points $< 76\text{ }^{\circ}\text{C}$ failed to work as matrices despite the high absorbance and presence of the relevant functional groups (such as methyl 2,5-dihydroxybenzoate). By contrast, those compounds that easily sublimed were also more likely to be effective matrices. Thus sublimation point is an important parameter in MALDI environment.¹⁴ Even compounds with free phenols and high UV absorbance could not act as matrices if they were in the liquid state and/or had a low boiling point. Hence, for some of these compounds the most likely mechanism of ionization involves laser induced sublimation of the matrix, followed by proton transfer: molten compounds are not as effectively transferred into the gas phase.

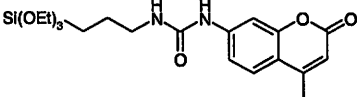
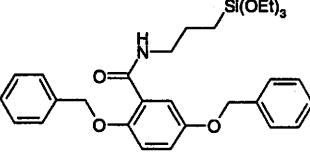
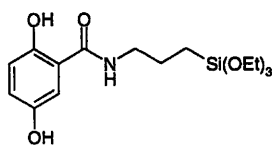
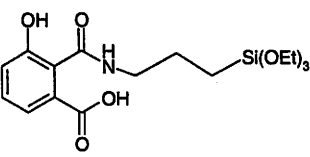
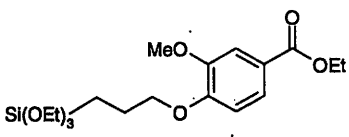
Does this mean the best MALDI matrix material should readily sublime, absorb UV light and be a phenolic molecule? Such requirements only apply to acidic standard matrices. To test this hypothesis, a series of compounds were prepared that can be covalently linked to a support.

3.2.6 Silicon-containing MALDI-TOF matrices

In conventional MALDI, the matrix in the free state not only absorbs and transfers energy from the laser, but can be vaporized into gas phase as a carrier of the analyte, which leads to excessive interference in the low mass region of the mass spectrum.

We have previously investigated immobilizing the matrix within the sol gel (see Chapter 2), and have concluded that in such a system matrix crystallization was most important factor to be considered for matrix efficiency: there was no need for co-crystallization of the matrix and analyte. A second approach for removal of low mass signals from MALDI spectra, which are typically correlated to the matrix, is to chemically tether the matrix to a support. Either the system would not be effective, low molecular weight matrix signals would not be generated, or the matrix would undergo covalent bond cleavage to enter the gas phase. The approach was tested by chemically introducing silicon containing groups onto the matrix molecules. In a second step, these silanes could undergo permanent surface binding using sol gel processes. Thus, high surface area MALDI sol-gel silica support materials have been surface modified with silicon-based matrices and tested for their ability to facilitate desorption and ionization of analytes (Table 3-4). The signal-to-background ratios and/or selectivity for specific analytes were compared with traditional matrices.

Table 3-4. Covalently linked matrices as TQ resins in terms of their MALDI performance.

Silicon matrix	Analyte Type Observed (Signal Intensity)	Silicon matrix	Analyte Type Observed (Signal Intensity)
 <p>3</p>	none	 <p>6</p>	TMP (32, 93, 0, 52)
 <p>5</p>	TMP (242, 19) Haloperidol (13,0)	 <p>2.</p>	none
 <p>1</p>	TMP (8,15,18) Haloperidol (12) Fluorescein (96, 10, 27, 18, 28, 10,75,82, 194, 12, 58, 24, 57, 200, 54, 58, 98)		

3.2.7 Nature of Binding to the MALDI Surface

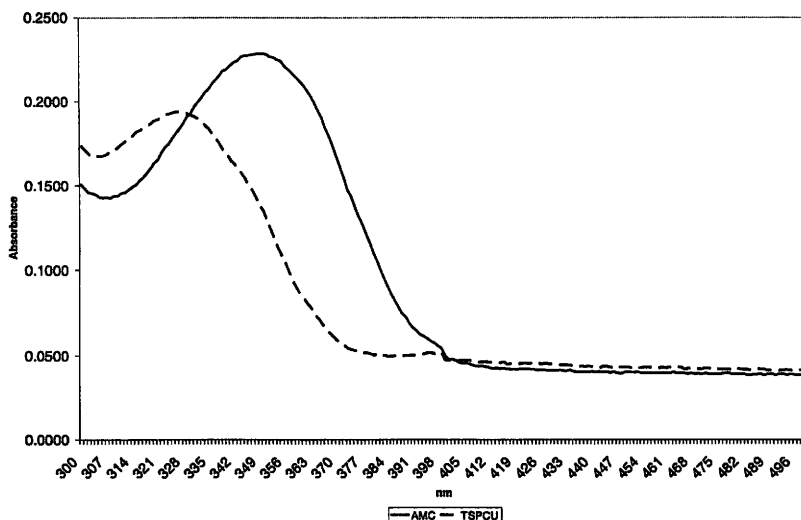
We have decided to develop number of different MALDI supports in order to investigate the effect of introduction of silicon and covalent immobilization on MALDI performance. Alkoxysilane compounds undergo hydrolysis and condensation reactions ($R_3SiOR' + R'OSiR_3 \rightarrow R_3SiOSiR_3 + 2R'OH$) in the presence of water. This provides an opportunity to form complex structures on the MALDI plate comprised exclusively from the silicon-modified matrices (i.e., R_3SiXR' , $R' = \text{matrix}$, $X = O, N$, this is a

silsesquioxane or T resin) or to disperse these materials in silica by cohydrolysis of the matrix with TEOS (to give TQ resins). Selected examples of the silicon-modified matrices were examined for MALDI performance both as T resins and TQ resins.

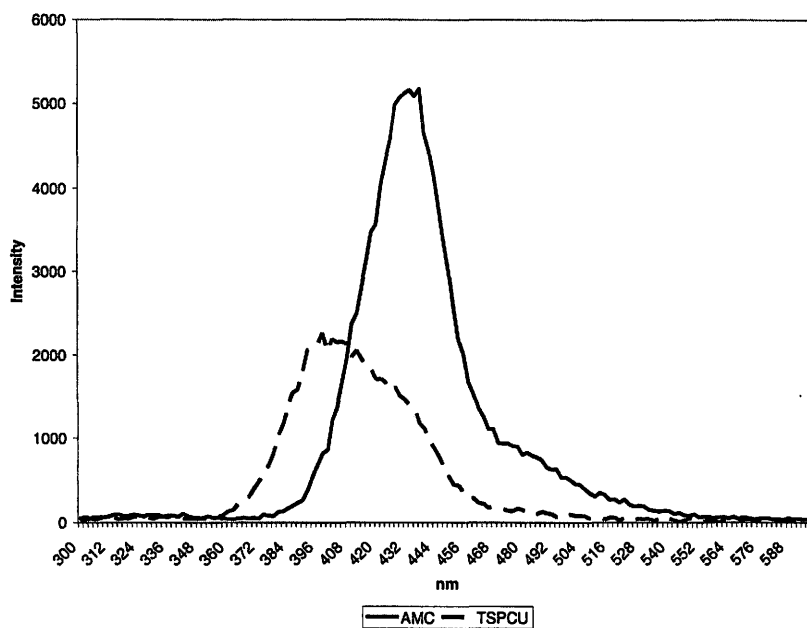
Initially we were interested in the effect of introduction of silicon moiety on UV absorbance of the molecule, since it was desirable to have a strongly absorbing surface. In the case study of triethoxysilylated coumarin (TSPCU) **3**, we observed that the introduction of Si(OEt)₃ resulted in a downshift of λ_{max} from 360 nm to 330 nm, and the fluorescence emission from 440 nm to 390 nm (Figure 3-11).

Figure 3-11. Spectroscopic study of AMC 13 and TSPCU 3: a) UV absorbance, b) Fluorescence emission.

a)

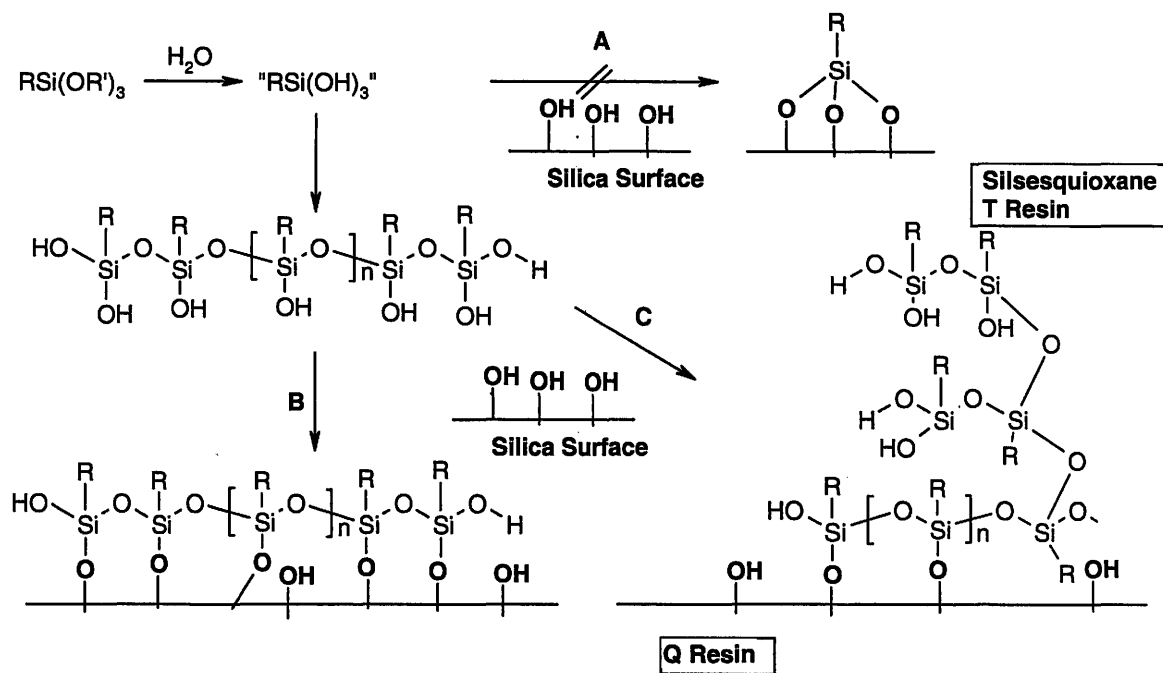


b)



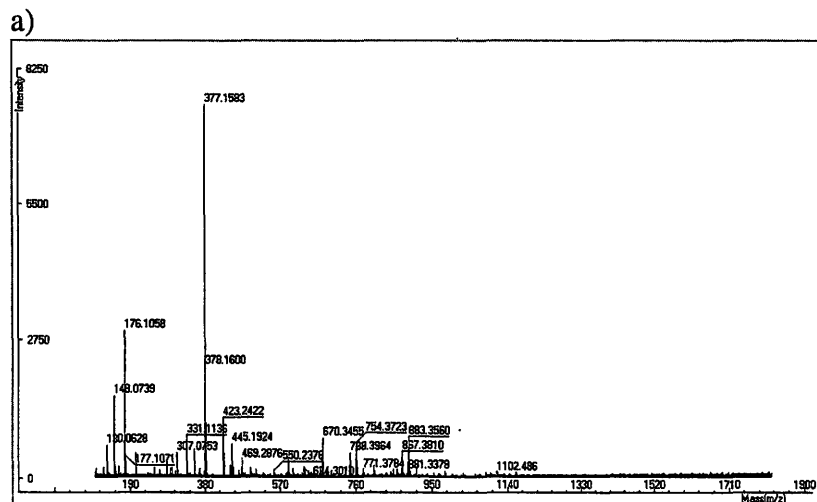
This silicon-based derivative failed to work as a matrix as a monolayer directly on a steel MALDI substrate, as a condensed silsesquioxane (directly hydrolysis/condensation product), or as a TQ resin formed by co-hydrolysis/condensation with TEOS (Scheme 3-1).

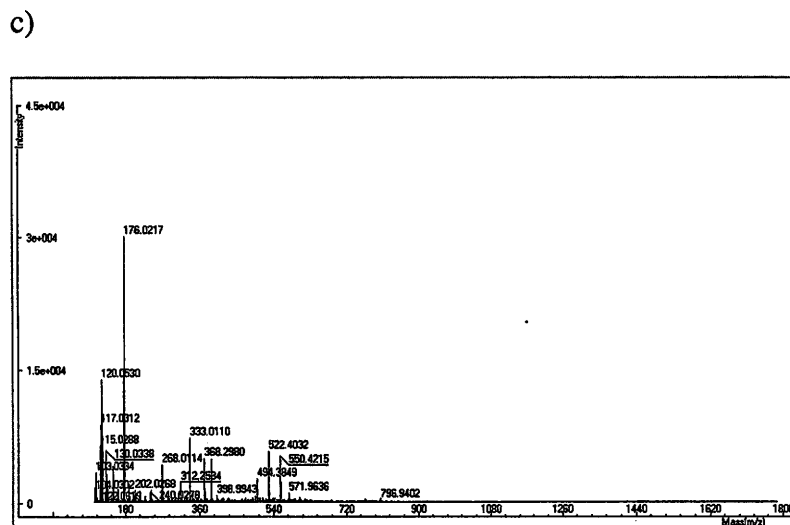
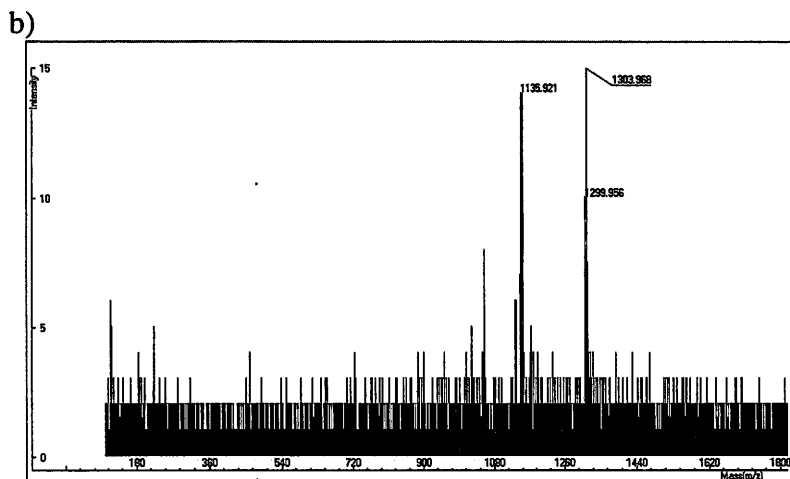
Scheme 3-1. Formation of TQ resins.



By contrast, the performance of a silicon-free analogue AMC was comparable to that of standard matrix such as DHB (Figure 3-12c).

Figure 3-12. MALDI MS of TSPCU sol gel under various conditions: a) TSPCU as T resin (basic conditions), b) TSPCU as T resin (acidic conditions) (pH=1-2), c) AMC.





Since the UV absorbance does not appear to be a factor in these MALDI studies, the poorer performance may be related to the blocking of the primary amine, to the presence of the alkoxy silane or to the absence of phenolic moieties. To pursue this, other case studies were performed where surface-bound phenolic compounds were investigated as matrices.

We have developed two separate UV absorbing supports that possess free phenolic groups which deemed to be necessary for the ionization of protonated analyte ions. With compound 2 (with possesses both a free acid and phenol), the actual

preparation of the MALDI support was an issue, due to compound's exclusive solubility in DMSO or DMF (Figure 3-13). Presence of residual solvent was believed to result in reduced or totally eliminated intensity of analyte-ion signals.¹⁵ Compound **2**. and **5** failed to work as matrices when used as T resins. We observed, however, ionization of trimethoprim and haloperidol ions when the compound **5** was converted into a TQ type surface (Figure 3-14). This performance could be attributed to the presence of phenolic moieties or to the matrix dispersion within silica. In addition, extremely low signal intensities were observed with excessive matrix-related signals in low mass region of the spectrum. The benzyl ether analogue (compound **6**) without free phenols was prepared and tested. Similarly, TMP ionization was observed when TQ resin was used. We were interested in further studying silicon-based compounds (with masked phenolic and acidic groups) as T or TQ resins in order to establish the role of TEOS in MALDI process. Therefore, the role of T vs TQ resins with a derivative of 3-methoxy-4-allyloxy-ethylbenzoate **1** is discussed in the next chapter.

Figure 3-13. MALDI MS using monolayer of triethoxysilyl phthalamic acid (compound 2.) as T resin.

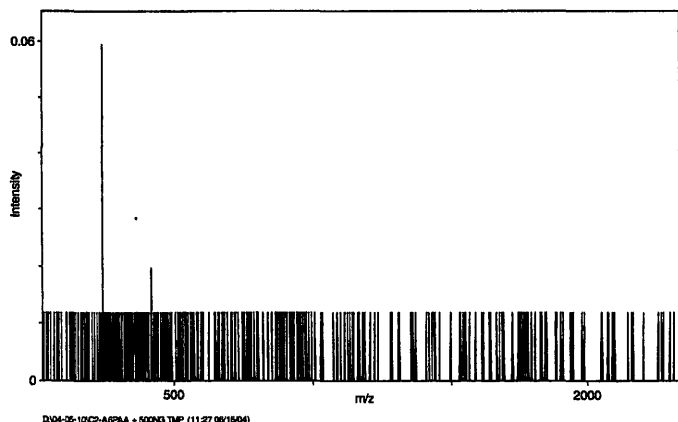
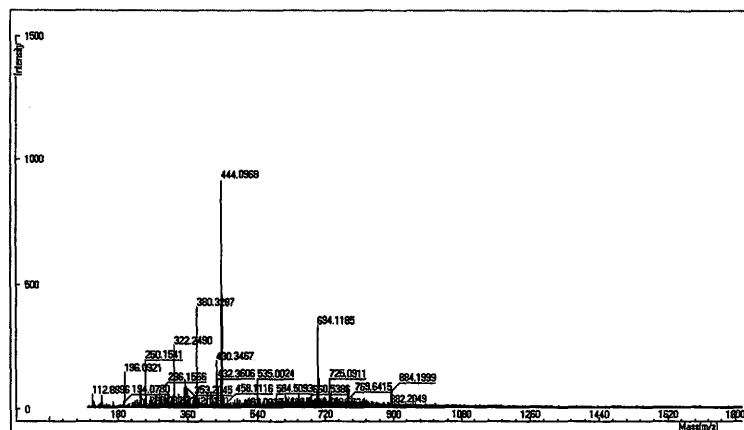


Figure 3-14. MALDI MS using compound 5 as TQ resin.



3.3 Summary

It is believed that the general matrix characteristics for MALDI performance include significant UV absorbance near laser wavelength, presence of phenolic and/or carboxylic groups and low sublimation temperature.¹⁶

It was demonstrated that blocking the carboxylic acid group does not affect the MALDI performance significantly, further suggesting that acidic moiety is relatively unimportant. Blocking the phenolic groups, on the other hand, resulted in a drastic reduction in analyte signal intensity.

When the matrix was modified by adding silicon groups, no change in performance was observed: the modified matrices typically did not perform effectively on their own or after hydrolysis/condensation into a T resin. However, a dispersion of silicon-based matrix into TEOS (to give a TQ resin) led to selective desorption and ionization of analytes. Notably, while no change in functionality was performed by incorporating silylated matrix in silica, dispersing the UV active species throughout a silica monolith, diluting them in effect, led to enhanced MALDI performance. This study

suggested that while some matrices did not work in their free (unbound) state they performed well when surface bound to silica. In addition, none of the surface bound matrices performed as the standard free DHB matrix in terms of overall signal intensity.

3.4 Conclusions

Variable chemical modification did not greatly affect UV absorbance or crystallization behaviour of the matrices. Moreover, no clear trends were evident and the changes observed were highly matrix dependent. It was demonstrated that crystallization was not an issue in terms of MALDI performance for surface bound matrices, moreover, numerous silicon-based supports were developed which were proven to work as highly selective MALDI supports when dispersed in silica.

3.5 Experimental section

3.5.1 Chemicals

Tetraethyl orthosilicate (TEOS, 99.999%), 3-aminopropyltriethoxysilane (APTS), 3,5-dihydroxybenzaldehyde, allylbromide, triethylamine, allylamine, 1-hydroxybenzole hydrate, 1-[3-(dimethylamino)propyl]-3-ethylcarbodiimide, 3-methoxy-4-hydroxybenzoic acid, benzylbromide, 3-hydroxyphthalic anhydride, platinum (0)-1,3-divinyl-1,1,3,3-tetramethyldisiloxane in xylene ($\text{Pt}_2[\text{CH}_2=\text{CHSiMe}_2\text{OSiMe}_2\text{CH}=\text{CH}_2]_4$ 2-3% Pt in xylene (Karstedt's catalyst)), 3-isocyanatopropyltriethoxysilane and trifluoroacetic acid (99.8%) were obtained from Aldrich Chemical Company Inc (Milwaukee, WI, USA). 2,5-dihydroxybenzoic acid, α -cyano-4-hydroxycinnamic acid, triethoxysilane, sulfuric acid (98%), and 0.1N HCl were obtained from Fluka Chemika (Steinheim, Switzerland). Methanol, diethyl ether, ethyl acetate, dimethylformamide, dimethylsulfoxide,

tetrahydrofuran, ethanol, potassium carbonate, dichloromethane, hexane, potassium hydroxide, sodium hydroxide, sodium chloride, magnesium sulfate, thionyl chloride, pyridine were purchased from Caledon Laboratories, LTD (Georgetown, ONT). Silica gel and sodium bicarbonate were purchased from EMD Chemicals Inc (Darmstadt, Germany), while sodium carbonate was purchased from EM Science (Gibbstown, NJ). 3,4-dihydroxycinnamic acid was purchased from SIGMA-Aldrich (St-Louis, MO) and 7-amino-4-methylcoumarin was purchased from INDOFINE Chemical Co. (Hillsborough, NJ).

3.5.2 Characterization

^1H and ^{13}C NMR were performed on either a Bruker AC-200 (200.13 MHz) or a Bruker AC-300 (300.13 MHz). Solid state ^{13}C NMR was performed on a Bruker AC-300 solid state (at 300.13 MHz for ^{13}C) spectrometer. Samples were dissolved in chloroform-d (CDCl_3), DMSO- d_6 or methanol- d_4 with chemical shifts (ppm, δ) reported to relative to TMS as reference. Coupling constants J were recorded in Hertz (Hz).

FT-IR studies were recorded on a Bruker Equinox 55 spectrometer. Peaks were reported in wavenumbers (cm^{-1}) and the samples were run pure in their solid or liquid state.

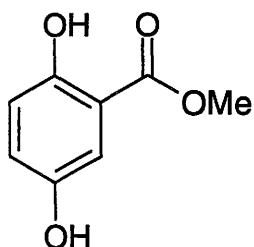
Mass spectrometry was performed using electron ionization (EI), chemical ionization (CI), liquid-chromatography mass spectrometry (LC-MS) or electro-spray ionization (ESI) techniques at McMaster University MS facility.

Optical microscope (Olympus BX41) was used for the morphology study of the corresponding matrices on MALDI plates.

UV absorption measurements of solutions were made using Tecan SAFIRE (monochromator with XFLUOR software) with the wavelength resolution was 1 nm, 401 scans and at the ambient temperature.

3.5.3 Synthesis of protected matrices

3.5.3.1 Methyl 2,5-dihydroxybenzoate, 19

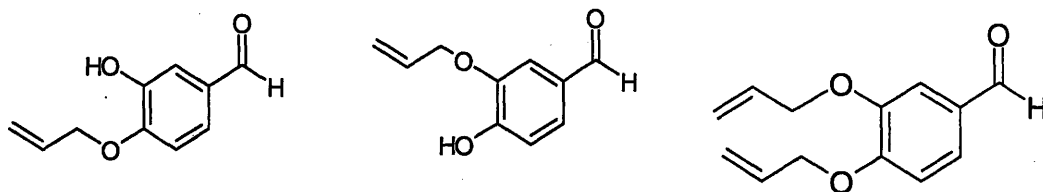


To 2,5-dihydroxybenzoic acid (1.154 g, 7.487 mmol) dissolved in methanol (5.28 mL) was added 98% H₂SO₄ (0.678 mL, 8.970 mmol). After the reaction mixture was refluxed at 65 °C for 29 h, the solution was extracted using diethyl ether. After the evaporation of the organic fractions and recrystallization from water the white solid was obtained, Yield, 0.488 g, 72% (mp 76 °C). The product was characterized using ¹H, ¹³C NMR, EI/CI/ESI MS, UV, LC-MS, IR and fluorescence.

¹H NMR (MeOH-d₄, 200 MHz) δ 4.10 (3H, s), 7.04 (1H, dd, *J*=3.7, 8.9 Hz), 7.18 (1H, d, *J*=3.2, 8.9 Hz), 7.44 (1H, t, *J*=3.4 Hz), 10.5 (1H, s, 2-OH); ¹³C NMR (MeOH-d₄, 200 MHz) δ 52.4, 114.7, 118.5, 121.1, 124.1, 147.8, 154.9, 155.6 ppm; MS CI⁺ *m/z* 136 [M-OH] (100), 168 [M⁺] (73), 108 (21), 80 (8); MS EI⁺ *m/z* 136 [M-OH] (100), 121 (44), 168 [M⁺] (36), 108 (32), 80 (13); ESI MS *m/z* 169 [M+H]⁺ (100), 155 (16), 196 (13), 83 (8);

LC-MS $r_t = 9.45$ min; $\lambda_{\max} = 332$ nm, $\epsilon_{337\text{nm}} = 4347.44$ 1/M*cm, $\lambda_{\text{ex}} = 340$ nm, $\lambda_{\text{em}} = 416$ and 496 nm; IR (neat), ν (cm^{-1}) 3745, 3335, 1686, 1337, 1216.

3.5.3.2 3-Allyloxy-4-hydroxybenzaldehyde; 4-allyloxy-3-hydroxybenzaldehyde, 18 3,4-diallyloxybenzaldehyde, 7



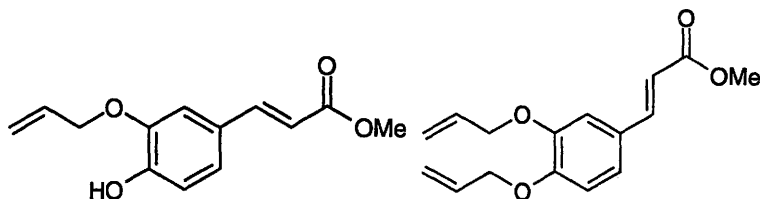
To 3,5-dihydroxybenzaldehyde (4.0234 g, 29.1 mmol) dissolved in 150 mL of absolute methanol, potassium carbonate (4.0273 g, 29.1 mmol), previously oven dried, was added. The mixture was heated up to 50 °C and allyl bromide (3.0405 mL, 1.39 g/mL, 34.9 mmol) was added to the flask drop wise through the septum. The mixture was further heated to 60 °C and then refluxed overnight (16 h). After the solvent was evaporated, the brown liquid was dissolved in ethyl acetate and washed with 1M HCl until an acidic pH was obtained (pH=6.2). After the separation and extraction with ethyl acetate, the organic fractions were washed with brine and dried with anhydrous MgSO_4 . The organic solvent was evaporated and the brown liquid was then separated using silica gel column chromatography with 3% methanol in dichloromethane as the solvent. A three different fractions were recovered: a) monoallyloxy derivative (0.970 g; 24.5 %; brown gel), b) diallyloxy derivative (0.8501 g; 21%; brown liquid) and c) mono/diallyloxy derivative mixture (1.8256 g; 45 %; approximate mono/diallyloxy ratio

in the mixture was 3.1:1 (from LC-MS intensity ratio)). Different eluents were analyzed using ^1H , ^{13}C NMR, LC-MS, UV, IR, CI/ESI MS and fluorescence.

Monoallyl derivative: ^1H NMR (CDCl_3 , 200 MHz) δ 4.68 (2H, d, $J=5.4$ Hz), 5.34 (1H, d, $J=19.5$ Hz), 5.41 (1H, dd, $J=1.0, 17.3$ Hz), 6.04 (1H, m, $J=5.3, 10.6, 18.3$ Hz), 6.94 (1H, d, $J=8.2$ Hz), 7.38 (1H, dd, $J=1.8, 8.1$ Hz), 7.48 (1H, d, $J=1.9$ Hz), 9.80 (1H, s); ^{13}C NMR (CDCl_3 , 200 MHz) δ 69.9, 111.5, 114.4, 119.3, 124.5, 130.7, 131.9, 146.4, 150.9, 191.2; MS CI m/z 178.06 [M^+] (100), 137 (9), 149 (8); MS ESI 177 [M-H^-] (100), 291 [M+TFA^-] (92), 136 (14), 355 [2M-H^-] (11); LC-MS $t_r=15.11$ min; IR (neat), ν (cm^{-1}) 3420, 3090, 2980, 2860, 1681, 1548, 1508, 1271, 1125, 993 cm^{-1} ; $\lambda_{\text{max}}=322$ nm; $\epsilon_{337\text{nm}}=2411.54$ $1/\text{M}\cdot\text{cm}$; $\lambda_{\text{ex}}=340$ nm; $\lambda_{\text{em}}=395$ and 433 nm;

Diallyloxy derivative: ^1H NMR (MeOH-d_4 , 200 MHz) δ 4.58 (2H, d, $J=4.8$ Hz), 4.59 (2H, d, $J=5.13$ Hz), 5.23 (1H, d, $J=1.5, 10.5$ Hz), 5.28 (1H, d, $J=1.5, 10.4$ Hz), 5.38 (1H, d, $J=1.5, 17.3$ Hz), 5.47 (1H, d, $J=1.5, 17.4$ Hz), 6.03 (1H, m, $J=5.2, 10.5$ Hz), 6.04 (1H, m, $J=5.2, 18.3$ Hz), 7.02 (1H, dd, $J=2.5, 8.2$ Hz), 7.38 (1H, d, $J=2.0$ Hz), 7.43 (1H, dd, $J=2.4, 8.2$ Hz), 9.74 (1H, d, $J=2.5$ Hz); ^{13}C NMR (CDCl_3 , 200 MHz) δ 69.8 (2C), 111.6, 112.4, 118.2, 118.4, 126.7, 130.2, 132.4, 132.7, 148.9, 153.9, 190.9; $\lambda_{\text{max}}=304$ nm; $\epsilon_{337\text{nm}}=1500.00$ $1/\text{M}\cdot\text{cm}$; $\lambda_{\text{ex}}=340$ nm; $\lambda_{\text{em}}=394$ and 434 nm; LC-MS $t_r=17.0$ min, IR (neat), ν (cm^{-1}) 3050, 2931, 2750, 1695, 1684, 993. MS CI m/z 218.09 [M^+] (100), 177 (23), 149 (20), 121 (9); ESI m/z 331 [M+TFA^-] (100), 249 (63), 217 [M-H^-] (23), 363 (18), 176 (13).

3.5.3.3 3-Allyloxy-4-hydroxy-methyl cinnamate; 4-allyloxy-3-hydroxy-methyl cinnamate, 12; 3,4-diallyloxy-methyl cinnamate, 11



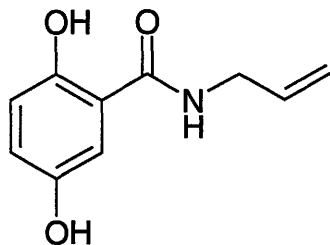
Anhydrous DMF (50 mL) was added to caffeic acid methyl ester (3.772 g, 0.0191 mol), sodium carbonate (3.314 g, 0.0385 mol), sodium iodide (1.005 g, 0.0064 mol) and allyl bromide (3.344 mL, 0.0401 mol). After the reaction was refluxed at 47 °C for 48 h, the solution was washed with aqueous HCl, and extracted with ethyl acetate washings. Combined organic fractions were evaporated to give rise to the brown liquid. The mixture was separated using a 60:40 by volume mixture of hexane: ethyl acetate. The monoallylated ester derivative was obtained as white solid, Yield, 0.6327 g, 17%. The diallyl derivatives was isolated, but contaminated with the monoallyloxy species, 0.4686 g, 12%. Approximate mono/diallyloxy ratio in the mixture was 2.9:1 from LC-MS intensity ratio. The products were recrystallized from hexane. The products were characterized by ^1H NMR, ^{13}C NMR, EI/CI/ESI MS, LC-MS, UV, IR and fluorescence.

Monoallyl derivative: ^1H NMR (CDCl_3 , 200 MHz) δ 3.78 (3H, s), 4.64 (2H, d, $J=5.0$), 5.33 (1H, d, $J=10.6$), 5.40 (1H, d, $J=17.4$), 5.78 (1H, s, 3-OH), 6.01 (1H, m, $J=5.9$, 10.5, 17.7 Hz), 6.28 (1H, d, $J=15.9$ Hz), 6.83 (1H, d, $J=8.3$ Hz), 6.99 (1H, d, $J=8.6$ Hz), 7.10 (1H, s, $J=1.1$ Hz), 7.58 (1H, d, $J=15.9$ Hz); ^{13}C NMR (CDCl_3 , 200 MHz) δ 51.7, 69.9, 111.00, 113.4, 116.0, 118.0, 121.8, 128.3, 132.4, 144.8, 146.2, 147.6, 167.8; MS EI m/z 193 (100), 234.08 [M^+] (45), 133 (41), 165 (14), 203 (10); MS CI m/z 234.08 [M^+] (100),

193 (75), 203 (21), 165 (12), 174 (11); MS ESI m/z 233 [M-H]⁻ (100), 191 (22), 467 [2M-H]⁻(20); LC-MS t_r = 17.03 min; λ_{max} = 322 nm; ϵ_{337nm} =10221.79 1/M*cm; λ_{ex} =340 nm; λ_{em} =435 nm;

Mono and di-allyl mixture: ¹H NMR (CDCl₃) δ 3.78 (3H, s), 4.63 (4H, d, J =5.1 Hz), 5.36 (2H, d, J =12.0 Hz), 5.46, (2H, s), 6.05 (2H, m), 7.43 (1H, d, J =10.1 Hz), 7.29 (1H, d, J =7.5Hz), 7.67 (1H, s), 7.70 (1H, d, J =9.1 Hz), 7.79 (1H, d, J =10.5 Hz); ¹³C NMR (MeOH-d₄, 200 MHz) δ 51.7, 68.3, 69.9, 112.8, 113.5, 115.7, 118.1 (2C), 122.8, 128.9, 131.0, 133.2, 144.9, 146.2, 147.8, 167.9; MS EI m/z 193 (100), 234 [Mono⁺] (48), 133 (41), 165 (13), 203 (12), 274.12 [Di⁺] (10); MS ESI m/z 307 (100), 192 (38), 387 (8) λ_{max} = 304 nm; ϵ_{337nm} =1500.00 1/M*cm; λ_{ex} = 340 nm; λ_{em} = 394 and 434 nm; IR (neat), ν (cm⁻¹) 3420, 2980, 2953, 1715, 1634, 1510, 1437, 1263, 1210, 1053; LC-MS t_r = 15.33, 17.03 min .

3.5.3.4 N-Allyl 2,5-dihydroxy-benzamide, 15

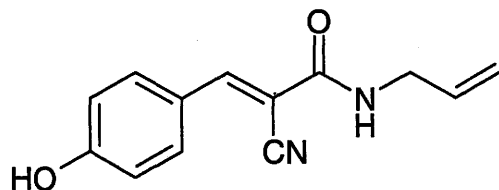


To 2,5-dihydroxybenzoic acid (3.1004 g, 0.0201 mol) dissolved in dry tetrahydrofuran (160 mL), 1-[3-(dimethylamino)propyl]-3-ethylcarbodiimide (EDC) (4.307 g, 0.0221 mol, 1.1 equivalent), (1-hydroxybenzotriazole hydrate) (HOBt) (2.723 g, 0.0201 mol, 1 equivalent), triethylamine (3.08 mL, 0.02211 mol, d =0.726 g/mL, 1.1

equivalent), and DMAP (0.1608 g, 5%) were added. Previously dissolved allylamine (1.513 mL, 0.0201 mol, $d=0.76$ g/mL) in THF was then added to the reaction flask. The mixture was stirred at room temperature overnight. Once the mixture was evaporated to dryness, the solid was dissolved in 0.1 N HCl and washed with ethyl acetate. Organic fractions were washed with NaHCO_3 , H_2O , NaCl, brine and dried over MgSO_4 . Column chromatography was performed with 60:40 %v/v hexane:ethyl acetate in order to remove residual allylamine and isolate the pure product as a white powder (1.0648 g, 34.3 %, mp. 103 °C). The product was characterized by ^1H , ^{13}C NMR, EI/CI/ESI MS, UV, LC-MS, IR and fluorescence.

^1H NMR (MeOH- d_4 , 200 MHz) δ 3.99 (2H, d, $J=5.2$ Hz), 5.17 (1H, dd, $J=1.2, 10.3$ Hz), 5.23 (1H, dd, $J=1.2, 17.2$), 5.92 (1H, m, $J=5.2, 10.3, 19.4$ Hz), 6.74 (1H, d, $J=8.8$ Hz), 6.85 (1H, dd, $J=2.8, 8.8$ Hz), 7.22 (1H, d, $J=2.8$ Hz); ^{13}C NMR (MeOH- d_4 , 200 MHz) δ 42.8, 114.8, 116.2, 117.7, 118.9, 122.3, 135.5, 150.9, 153.5, 170.1; MS CI m/z 193 [M^+] (100), 136 (44), 164 (18), 175 (14), 108 (11); MS ESI m/z 192 [$\text{M}-\text{H}$] (100), 238 [$\text{M}+45$] (97), 306 [$\text{M}+\text{TFA}$] (74), 112 (22), 138 (12) ; MS ESI m/z 194 [$\text{M}+\text{H}$] $^+$ (100), 65 (68), 216 [$\text{M}+\text{Na}$] $^+$ (12); MS CI m/z 193.1 (M^+); FTIR (neat), ν (cm^{-1}) 3399, 3334, 1576, 1546, 1226, 993, 947; $\lambda_{\text{max}}=324$ nm; $\epsilon_{337\text{nm}}=4691.03$ $1/\text{M}\cdot\text{cm}$, $\lambda_{\text{ex}}=340$ nm, $\lambda_{\text{em}}=399, 441, 494$ nm; LC-MS $t_r=8.18$ min.

3.5.3.5 *N*-Allyl-2-cyano-3-(4-hydroxy-phenyl)-acrylamide, 8

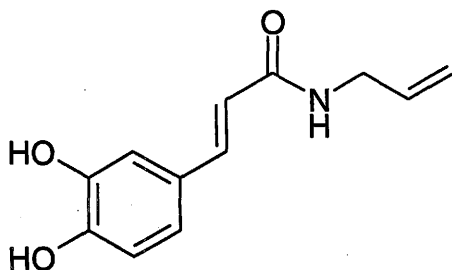


To α -cyano-4-hydroxycinnamic acid (1.995 g, 0.0105 mol) dissolved in dry tetrahydrofuran (160 mL), 1-[3-(dimethylamino)propyl]-3-ethylcarbodiimide (EDC) (2.2238 g, 0.0116 mol, 1.1 equivalent), (1-hydroxybenzotriazole hydrate) (HOBt) (1.418 g, 0.0105 mol, 1 equivalent), triethylamine (1.617 mL, 0.0116 mol, $d=0.726$ g/mL, 1.1 equivalent), and DMAP (0.0997 g, 5%) were added. Previously dissolved allylamine (0.788 mL, 0.0105 mol, $d=0.76$ g/mL) in THF (3 ml) was added to the reaction flask. The mixture was stirred at room temperature overnight. Once the mixture was evaporated to dryness, the solid was dissolved in 0.1 N HCl and washed with ethyl acetate. The organic fractions were washed with NaHCO_3 , H_2O , NaCl, brine and dried over MgSO_4 . Column chromatography was performed with 60:40 %v/v hexane:ethyl acetate in order to remove residual allylamine and isolate the pure product as the yellow powder (1.737 g, 87.06 %, mp. 255 °C). The product was characterized using ^1H and ^{13}C NMR, CI/MS, UV, IR and fluorescence.

^1H NMR (MeOH- d_4 , 200 MHz) δ 3.96 (2H, d, $J=5.3$ Hz), 5.15 (1H, dd, $J=1.2, 10.5$ Hz), 5.22 (1H, dd, $J=1.3, 18.9$ Hz), 5.88 (1H, m, $J=6.9, 10.2, 18.3$ Hz), 6.90 (2H, d, $J=8.7$ Hz), 7.88 (2H, d, $J=8.7$ Hz), 8.10 (1H, s), 9.76 (1H, 4-OH, s); ^{13}C NMR (MeOH- d_4 , 200 MHz) δ 41.7, 99.2, 114.4, 114.9, 115.3 (2C), 122.8, 132.5 (2C), 133.0, 151.3, 161.6, 161.9; MS CI^+ m/z 107 (100), 228.09 [M^+] (94), 172 (48), 221 [$\text{M}-17$] (37), 123 (28), 290

(17); FTIR (neat), ν (cm^{-1}) 3327, 3190, 2970, 2218, 1649, 1568, 1538, 1053; $\lambda_{\text{max}} = 326$ nm, $\epsilon_{337\text{nm}} = 8511.54 \text{ l/M*cm}$; $\lambda_{\text{ex}} = 340$, $\lambda_{\text{em}} = 434$.

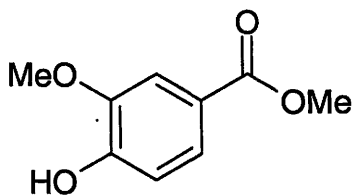
3.5.3.6 *N*-Allyl 3,4-dihydroxycinnamide, 9



To 3,4-dihydroxycinnamic acid (3.8065 g, 0.0211 mol) dissolved in dry tetrahydrofuran (170 mL), 1-[3-(dimethylamino)propyl]-3-ethylcarbodiimide (EDC) (4.4555 g, 0.0232 mol, 1.1 equivalent), (1-hydroxybenzotriazole hydrate) (HOBt) (2.8512 g, 0.0211 mol, 1 equivalent), triethylamine (3.234 mL, 0.0232 mol, $d = 0.726 \text{ g/mL}$, 1.1 equivalent), and DMAP (0.190 g, 5%) were added. Previously dissolved allylamine (1.2048 mL, 0.0211 mol, $d = 0.76 \text{ g/mL}$) in THF (4 mL) was added to the reaction flask. The mixture was stirred at room temperature over 5 days. After evaporating to dryness, the solid was dissolved in 0.1 N HCl and washed with ethyl acetate. Organic fractions were washed with NaHCO_3 , H_2O , NaCl, brine and dried over MgSO_4 . To the oily brown residue ethyl acetate was added and white precipitate was filtered off (2.001 g, 52.57 %, mp. $182 \text{ }^\circ\text{C}$). The product was purified using mixed solvent pair recrystallization, acetone: heptane. The product was characterized using ^1H NMR, ^{13}C NMR, ESI/CI MS, UV, LC-MS, IR and fluorescence.

^1H NMR (MeOH- d_4 , 200 MHz) δ 3.87 (2H, dd, $J=1.3, 3.7$ Hz), 5.08 (1H, dd, $J=1.3, 10.3$ Hz), 5.18 (1H, d, $J=17.4$ Hz), 5.82 (m, 1H, $J=1.4, 10.2, 17.8$ Hz), 6.36 (1H, d, $J=15.7$ Hz), 6.72 (1H, d, $J=8.2$ Hz), 6.88 (1H, dd, $J=1.5, 8.2$ Hz), 7.01 (1H, d, $J=1.6$ Hz), 7.37 (1H, d, $J=15.6$ Hz); ^{13}C NMR (MeOH- d_4 , 200 MHz) δ 42.8, 115.0, 116.3, 116.4, 118.1, 122.1, 128.2, 135.5, 142.5, 146.7, 148.8, 169.1; MS CI m/z 220 [M^+] (100), 163 (82), 136 (35), 153 (16); MS ESI m/z 221 [$\text{M}+\text{H}]^+$ (100), 439 [$2\text{M}+\text{H}]^+$ (62), 261 (6), 163 (5); IR (neat), ν (cm^{-1}) 3340, 3320, 3200, 1649, 1581, 1540, 1234, 1182; $\lambda_{\text{max}}=318$ nm, $\epsilon_{337\text{nm}}=9083.33$ $1/\text{M}^*\text{cm}$; $\lambda_{\text{ex}}=340$, $\lambda_{\text{em}}=438$; LC-MS $t_{\text{r}}=7.78$ min.

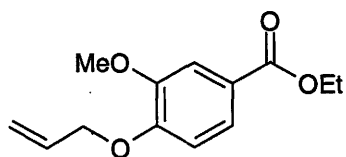
3.5.3.7 Methyl 4-hydroxy-3-methoxybenzoate, 21



After 3-methoxy-4-hydroxy benzoic acid (1.14 g, 6.7 mmol) was dissolved in methanol (50 mL) and cooled to 0 °C, thionyl chloride (2.44 mL, $d=1.683$ g/mL, 33.8 mmol) was added dropwise through the rubber septum. The reaction mixture was stirred at room temperature for 20 h. The solvent was evaporated and the mixture was extracted with diethyl ether, washed with sodium bicarbonate, water, sodium chloride and brine. Organic fractions were evaporated in order to recover an ester (white solid, 0.974 g, 85.4%, mp. 59 °C). The product was characterized by ^1H and ^{13}C NMR, IR, UV, CI MS and fluorescence.

^1H NMR (MeOH- d_4 , 200 MHz) δ 3.84 (OCH₃, 3H), 3.88 (OCH₃, 3H), 6.82 (1H, d, $J=8.7$ Hz), 7.51 (1H, s), 7.54 (1H, s); ^{13}C NMR (MeOH- d_4 , 200 MHz) δ 52.4, 56.4, 113.4, 115.9, 122.5, 124.9, 148.9, 152.8, 168.6; MS CI m/z 151 [M-OMe]⁺ (100), 182 [M]⁺ (85); IR (neat), ν (cm⁻¹) 3537, 3100, 3050, 2940, 1697, 1602, 1512, 1462, 1297, 1217, 1155, 777; $\lambda_{\text{max}}=292$ nm, $\epsilon_{337\text{nm}}=1054.94$ l/M*cm; $\lambda_{\text{ex}}=340$ nm, $\lambda_{\text{em}}=392$ nm, $\lambda_{\text{em}}=432$ nm.

3.5.3.8 Ethyl 4-allyloxy-3-methoxybenzoate, 22

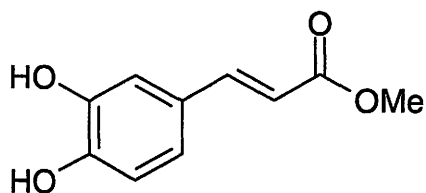


To a solution of 3-methoxy-4-hydroxy-ethyl benzoate (0.974 g, 5.35 mmol) in absolute ethanol (20 mL), previously oven dried potassium carbonate (0.739 g, 5.35 mmol) was added. When the reaction mixture was heated to 50 °C, allyl bromide (0.539 g, 0.377 mL, 4.45mmol) was added dropwise through the septum. The mixture was refluxed over night (16-18 h). After the solvent was evaporated, the brown liquid was dissolved in ethyl acetate and washed with 1M HCl until the acidic pH was obtained (pH=6.2). After separation of the organic fractions and extraction with ethyl acetate, the organic fractions were washed with brine and dried with anhydrous MgSO₄. The organic solvent was evaporated and the brown liquid was then purified using silica gel column chromatography with hexane:ethyl acetate (60:40 vv) mixture as the solvent. The yellow

liquid was recovered in 42.5% yield (0.409 g). The product was characterized by ^1H and ^{13}C NMR, IR, UV, CI MS and fluorescence.

^1H NMR (MeOH- d_4 , 200 MHz) δ 1.38 (3H, t, $J=7.2$ Hz), 3.86 (OCH₃, 3H, s), 4.31 (2H, q, $J=7.2, 14.2$ Hz), 4.62 (2H, d, $J=5.1$ Hz), 5.26 (1H, d, $J=10.5$ Hz), 5.41 (1H, dd, $J=1.4, 17.3$ Hz), 6.05 (1H, m, $J=1.4, 16.7, 10.6$ Hz), 6.96 (1H d, $J=8.4$ Hz), 7.54 (1H, d, $J=1.5$ Hz), 7.60 (1H, q, $J=1.6, 8.4$ Hz); ^{13}C NMR (MeOH- d_4 , 200 MHz) δ 14.6, 56.4, 61.9, 70.6, 113.4, 113.5, 118.1, 124.1, 124.6, 134.3, 150.5, 153.7, 167.9; MS CI m/z 237 [M^+] (100), 195 (28), 151 (9); IR (neat), ν (cm^{-1}) 3084, 2981, 2930, 1708, 1599, 1511, 1267, 1214, 1018, 761; $\lambda_{\text{max}}=294$ nm, $\epsilon_{337\text{nm}}=1076.60$ $1/\text{M}^*\text{cm}$; $\lambda_{\text{ex}}=340$ nm, $\lambda_{\text{em}}=392$, $\lambda_{\text{em}}=433$ nm.

3.5.3.9 Methyl 3,4-dihydroxycinnamate, 14

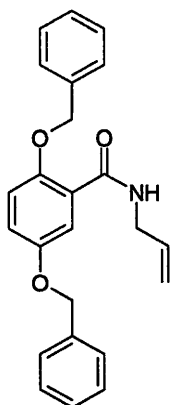


To 3,4-dihydroxycinnamic acid (4.7096 g, 26 mmol) in methanol (150 mL) at 0°C , thionyl chloride (13.5 mL, 0.183 mol) was added dropwise over 30 min. After stirring the mixture for 24 h, the solvent was evaporated and the white solid was isolated. From the acidic medium/diethyl ether workup the organic layers were combined and the solvent evaporated. Further purification using silica column chromatography was performed with chloroform: methanol 9:1% vv solvent composition. The final white solid was obtained in

the 85% yield, 4.001 g, mp 158 °C. The caffeic acid methyl ester was characterized using ^1H , ^{13}C NMR, IR, UV, LC-MS, CI/EI/ESI MS and fluorescence.

^1H NMR (MeOH- d_4 , 200 MHz) δ 3.74 (3H, s), 6.25 (1H, d, $J=15.9$ Hz), 6.77 (1H, d, $J=8.1$ Hz), 6.93 (1H, d, $J=8.1$ Hz), 7.02 (1H, s), 7.53 (1H, d, $J=15.9$ Hz); ^{13}C NMR (MeOH- d_4 , 200 MHz) δ 52.00, 114.8, 115.1, 116.5, 122.9, 127.7, 146.9, 149.6, 156.5, 169.7; MS EI m/z 163 (100), 194.05 [M^+] (93), 134 (25), 145 (23), 117 (21); MS CI m/z 136 (100), 168 (55), 194 [M^+](24), 108 (22), 208 (18); MS ESI $^+$ m/z 221 (100), 194 [$\text{M}+\text{H}]^+$ (55), 406 [$2\text{M}+\text{NH}_4]^+$ (23), 389 [$2\text{M}+\text{H}]^+$ (7); Appearance, white solid. IR (neat), ν (cm^{-1}) 3501, 3450, 3319, 3019, 1704, 1257, 1177. $\lambda_{\text{max}}= 324$ nm, $\epsilon_{337\text{nm}}=8544.87$ 1/M*cm; $\lambda_{\text{ex}}=340$ nm, $\lambda_{\text{em}}=426$ nm; LC-MS $t_r= 15.18$ min.

3.5.3.10 *N*-Allyl 2,5-dibenzyloxybenzamide, 23



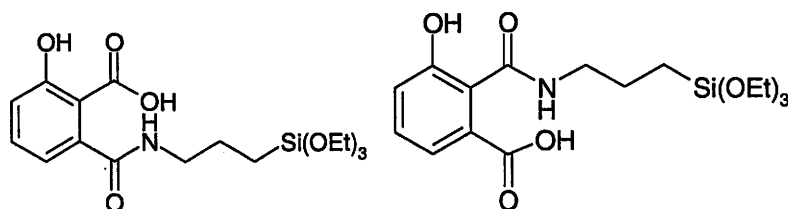
A solution of *N*-allyl-2,5-dihydroxybenzamide (0.29 g, 1.5 mmol) in anhydrous tetrahydrofuran (15 mL) was added to oven dried potassium carbonate (0.70 g, 5.06 mmol) and benzyl bromide (0.236 mL, $d=1.44$ g/mL, 1.98 mmol). After the mixture was refluxed at 70 °C for 7 hours, the solvent was evaporated. After treatment with 0.01 M

HCl (20 mL), the product was extracted with ethyl acetate, and washed with sodium bicarbonate, sodium chloride and brine. Evaporation of all organic fractions yielded a protected product as brown solid without further purification (0.270 g, 93%, mp 131 °C). The product was characterized using ¹H NMR, IR, UV, CI MS and fluorescence.

¹H NMR (MeOH-d₄, 200 MHz) δ 3.91 (2H, d, *J*=1.70 Hz), 5.01 (2H, s), 5.07 (1H, dd, *J*=11.0, 1.3 Hz), 5.12 (2H, s), 5.18 (1H, d, *J*=17.1 Hz), 5.73 (1H, m, *J*=1.7, 4.8, 14.6 Hz), 6.89 (1H, d, *J*=8.6 Hz), 7.13 (1H, dd, *J*=1.6, 7.3 Hz), 7.23-7.51 (benzyl protons, C₆H₅-, 10H, m); 7.54 (1H, s); MS CI *m/z* 91 (100), 282 (65), 374 [M⁺] (15), 242 (10); IR (neat), *v* (cm⁻¹) 3380, 3350, 3090, 2890, 2810, 1670, 1601, 1540, 1502, 1460, 1250, 1210, 1020; λ_{max}= 313 nm, ε_{337nm}=11080.7 l/M*cm; λ_{ex}=340 nm, λ_{em}=392 nm;

3.5.4 Synthesis of Sol Gel Precursors

3.5.4.1 6-Hydroxy-*N*-(3-aminopropyltriethoxysilyl)-phthalamic acid; 3-hydroxy-*N*-(3-aminopropyltriethoxysilyl)-phthalamic acid, 2.

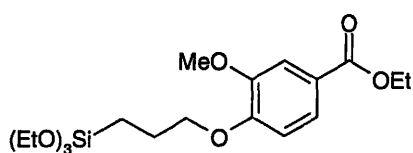


3-Hydroxyphthalic anhydride (0.1588 g, 0.90 mmol) was dissolved in DMSO (3 mL), to which 3-aminopropyltriethoxysilane (0.217 mL, 0.213 g, 0.965 mmol) and anhydrous pyridine (0.217 mL, 0.213 g, 3.13 mmol) were added. After the reaction mixture was stirred for 39 h, the resulting green fluorescent mixture was further evaporated to remove any residual solvent. The yellow-green crystals were recovered as mixture of isomers, Yield, 0.317 g, 98%, mp 116 °C. The ¹H and ¹³C NMR, ²⁹Si NMR,

UV, ESI MS and fluorescence were obtained of product in solution and IR and ^{29}Si CPMAS were performed on the product as isolated solid.

^1H NMR (DMSO- d_6 , 200 MHz) δ 7.17 (1H, q, $J=7.8$, 7.6 Hz), 6.74 (1H, d, $J=7.9$ Hz), 6.53 (1H, d, $J=7.1$ Hz), 3.48 (6H, q, $J=6.9$ Hz), 3.21 (2H, q, $J=6.9$, 2.6 Hz), 1.65 (2H, m, $J=7.3$ Hz), 1.06 (9H, t, $J=6.9$ Hz), 0.61 (2H, m, $J=7.4$ Hz) ppm; ^{13}C NMR (DMSO- d_6 , 200 MHz) δ 18.7, 18.9, 22.8, 56.5, 58.1, 119.6, 120.3, 120.3, 129.3, 131.2, 156.2, 166.5, 167.9 ppm; MS ESI $^-$ m/z 384.4 [$\text{M}-\text{H}$] $^-$ (100), 356 (38), 300 (27), 328 (10); ^{29}Si CPMAS NMR (solid state, 300 MHz) δ -67.53, -61.31, -53.37 ppm; FTIR (neat), ν (cm^{-1}) 3200-2500, 2928, 1687, 1610, 1456, 1402, 1366, 1204, 735; $\lambda_{\text{max}}=347$, $\lambda_{\text{ex}}=340$ nm, $\lambda_{\text{em}}=516$ nm. $^1\text{H}-^1\text{H}$ gradient COSY: showed that methyl and methylene protons in the terminal ethoxy groups are coupled together, as were methylene protons in the propyl chain. For spectrum, see Supplementary Material.

3.5.4.2 Ethyl 3-methoxy-4-(3-propyltriethoxysilyl)benzoate, 1

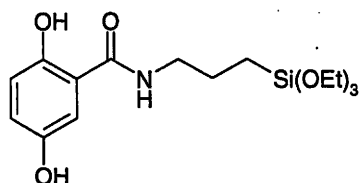


To ethyl 3-methoxy-4-allyloxybenzoate (0.3677 g, 1.65 mmol) in dry THF (10 mL) were added triethoxysilane (0.514 g, 0.604 mL, 3.3 mmol) and Karstedt's catalyst (3 drops). The completion of reaction was ensured using proton NMR. After solvent evaporation, unreacted triethoxysilane was removed under high vacuum and the brown liquid was purified by flash chromatography using hexane:ethyl acetate (30:70 v:v)

mixture as the solvent. The pure brown liquid (84.6%, 0.311 g) was characterized by ^1H NMR, IR, CI/MS, MALDI, UV and fluorescence.

^1H NMR (CDCl_3 , 200 MHz) δ 0.75 (2H, t, $J=8.2$ Hz), 1.21 (9H, t, $J=6.9$ Hz), 1.38 (3H, t, $J=7.1$ Hz), 1.98 (2H, m, $J=7.3, 8.5$ Hz), 3.81 (6H, q, $J=6.9$ Hz), 3.90 (3H, s, OMe), 4.05 (2H, t, $J=6.9$ Hz), 4.34 (2H, q, $J=7.1$ Hz), 6.87 (1H, d, $J=8.4$ Hz), 7.53 (1H, d, $J=1.56$ Hz), 7.65 (1H, q, $J=1.8, 8.4$ Hz); MS CI m/z 197 (100), 358 (62), 249 (39), 205 (35), 163 (32), 373 (20), 239 (18); MALDI-TOF m/z 253, 283, 315, 355 [M-45], 401 [M+H] $^+$; IR (neat), ν (cm^{-1}) 2975, 2950, 2910, 1712, 1600, 1512, 1270, 1073, 881, 790; $\lambda_{\text{max}}=291$ nm. $\lambda_{\text{max}}^{\text{ex}}=340$ nm, $\lambda_{\text{max}}^{\text{em}}=437$ nm.

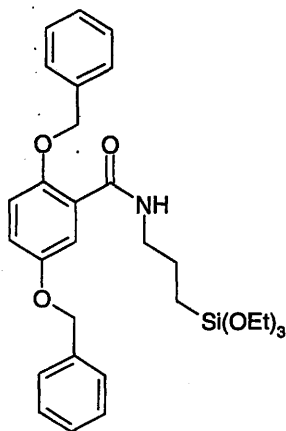
3.5.4.3 *N*-(3-Triethoxypropylsilyl) 2,5-dihydroxybenzamide, 5



To allyl 2,5-dihydroxybenzamide (0.0811 g, 0.419 mmol) dissolved in dry THF (5mL) triethoxysilane (0.38 g, 0.433 mL, 2.52 mmol) and Karstedt's catalyst (3 drops) were added. The reaction mixture was stirred at room temperature for 21 h. The completion of the reaction was followed by proton NMR. After solvent evaporation and removal of excess triethoxysilane under vacuum, the beige solid (0.077, 94.9 %, mp 270 $^{\circ}\text{C}$) obtained was characterized by ^1H NMR, IR, MS CI/ESI, MALDI and UV and fluorescence.

^1H NMR (CDCl_3 , 200 MHz) δ 0.97 (2H, m, $J=7.4$ Hz), 1.22 (9H, m, $J=7.0$ Hz), 1.58 (2H, m, $J=7.7$ Hz), 3.37 (2H, m, $J=6.2$ Hz), 3.83 (6H, q, $J=7.0$ Hz), 6.84 (1H, d, $J=8.9$ Hz), 6.97 (1H, s), 7.06 (1H, d, $J=9.3$ Hz); MS ESI 196 (100), 276 (59), 259 (55), 382 (37), 245[M-3(OCH₂CH₃)+Na] (32), 396 [M+K]⁺ (23), 290.2 [M-2(OCH₂CH₃)+Na] (19), 422 (14), 333 [M-OCH₂CH₃+Na] (12); MS CI m/z 136 (100), 196 (90), 393 (37), 438 (28), 227 (22), 332 (21), 499 (12); MALDI 286, 380.33 m/z [M+Na]⁺, 430, 444, 654, 699, 771;; IR (neat), ν (cm^{-1}) 3420, 2962, 2930, 1547, 1491, 1037, 791; λ_{max} = 396 nm, $\lambda_{\text{max}}^{\text{ex}}$ = 340 nm, $\lambda_{\text{max}}^{\text{em}}$ = 446 and 495 nm.

3.5.4.4 N-(3-Triethoxypropylsilyl) 2,5-dibenzyloxybenzamide, 6

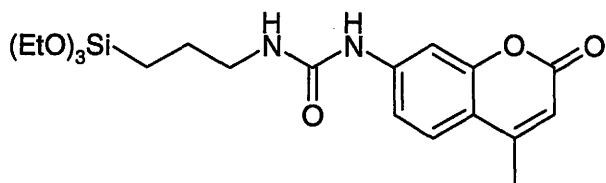


To allyl 2,5-dibenzyloxyamide of benzoic acid (0.0954 g, 0.255 mmol) dissolved in dry THF (5 mL), triethoxysilane (0.118 g, 0.1319 mL, 0.766 mmol) and the platinum(0)-1,3-divinyl-1,1,3,3-tetramethyldisiloxane complex (2 drops) were added. The mixture was stirred at room temperature under nitrogen for 22 h. The completion of the reaction was assured by ^1H NMR. After solvent evaporation, excess triethoxysilane was removed under high vacuum to obtain a product as brown/gold gel. The product was

purified by flash column chromatography using a hexane:ethyl acetate (30:70 v:v) mixture as the solvent, and organic portions were evaporated to obtain clean pale brown gel-like substance (0.0899 g, 94.2 %). The silylated product was characterized by ^1H NMR, IR, UV, MS CI, MALDI and fluorescence.

^1H NMR (MeOH- d_4 , 200 MHz) δ 0.75 (2H, m), 1.29 (9H, t, $J=6.9$ Hz), 1.55 (2H, t, $J=7.8$ Hz), 3.30 (2H, m), 3.85 (6H, q, $J=6.8$ Hz), 6.98 (1H, d, $J=8.9$ Hz), 7.08 (1H, s), 7.33-7.48 (10H benzyl, m), 7.91 (1H, d, $J=9.3$ Hz); MS CI m/z 91 (100), 282 (18), 374 [M-164] (14), 254 (11), 316 (6); MALDI-TOF m/z 236, 308, 342 [M-198], 374 [M-164], 414; IR (neat) , ν (cm^{-1}) 3480, 3360, 2973, 2025, 1638, 1590, 1541, 1449, 1202, 1073; $\lambda_{\text{max}}^{\text{abs}}=320$ nm, $\lambda_{\text{max}}^{\text{ex}}=340$ nm, $\lambda_{\text{max}}^{\text{em}}=399$ and 434 nm.

3.5.4.5 (*N*-(3-Triethoxysilylpropyl)-*N'*-(7-(4-methylcoumarin)) urea (TSPCU), 3



7-Amino-4-methylcoumarin (AMC, 0.092 g, 0.522mmol) was dissolved in dry THF (25 mL). After the mixture was stirred for 35 min at room temperature, (3-isocyanatopropyl)-triethoxysilane (IPTES) (2.575 g, 0.999 g/mL, 10.4 mmol) was added and the mixture was refluxed at 75 °C under nitrogen for 50 h. After the mixture was cooled to room temperature, the solvent was evaporated. The white powder was dissolved in dry dichloromethane (10 mL); hexane (20 mL) was added slowly to precipitate the product. After the mixture was allowed to sit for 3 days, the product was isolated as a

white solid (0.0651 g, 71.1 %, mp 198 °C) with suction filtration and washed with hexane (2 x 5 mL). The product was characterized by ¹H NMR, MS ESI, MALDI, UV, IR and fluorescence spectroscopy.

¹H NMR (MeOH-d₄, 200 MHz) δ 0.67 (2H, m, *J*=7.3 Hz), 1.24 (9H, t, *J*= 7.1 Hz), 1.57 (2H, m), 2.42 (3H, CH₃, s), 3.29 (2H, m), 3.72 (6H, q, *J*=6.8 Hz), 6.18 (1H, s), 7.26 (1H, s), 7.55 (1H, d, *J*=8.1 Hz), 7.61 (1H, d, *J*=7.9 Hz); MS ESI⁺ *m/z* 248 (100), 423 [M+H]⁺ (77), 713 (20), 670 (19); MS ESI⁻ *m/z* 481 [M+59]⁻ (100), 421 [M-H]⁻ (30), 535(29), 903 (12) ; MALDI 377 *m/z* [M-OCH₂CH₃+H]⁺, 423 *m/z* [M+H]⁺, 445 *m/z* [M+Na]⁺, 883 *m/z* [2M+K]⁺; λ_{max}^{abs}=329 nm, λ_{max}^{ex}= 334, λ_{max}^{em}=390 nm, ε=22000 1/M*cm; IR (neat), ν (cm⁻¹) 3480, 3320, 2974, 2940, 1677, 1539, 1073, 954, 773.

3.5.5 Sol Gel Preparation

- a) **Silica Sol.** The silica sol solution was prepared by mixing TEOS (1 mL, 4.4 mmol) and HCl (2 mL, 0.1 M). The mixture was sonicated (approximately an hour) in an ice bath, until it became a single uniform phase. Gelation was induced by drying at room temperature with exposure to air.
- b) **Silica/TSPCU (3) TQ resin.** To TEOS (0.599 mL, 1.99 mmol) in water (0.5 mL) and 0.1M HCl (0.05 mL), compound 3 (0.0740 g, 0.175 mmol) in absolute ethanol (0.1 mL) was added. The solution was sonicated for 1.5 hrs at 0°C. The 1 μL aliquots were then spotted on the stainless steel plate or gold coated plates and gelation was allowed to take place as in a).
- c) **T resin of Compound 2.** Compound 2. (0.019 g) was dissolved in a) a mixture of methanol (0.2 mL) and DMF (0.8 mL) and b) a mixture of

methanol (0.2 mL) and DMSO (0.8 mL). The solution was spotted on the stainless steel plate prior to MALDI analysis.

- d) Silica/Compound 1 TQ resin.** To compound 1 (0.05 mL) in 0.1M HCl (0.2 mL) and THF (0.2mL), TEOS (0.05 mL) was added. The immiscible solution was sonicated at 0°C for 3 hours. A 1 μ L aliquots were then spotted on the stainless steel plate and gelation was allowed to take place as in a).
- e) T resin of Compound 1.**Compound 1 (0.05 mL) was added to 0.1 M HCl (0.2 mL) and THF (0.2 mL) and mixture was sonicated for 3 hrs at 0°C. A 1 μ L aliquots were then spotted on the stainless steel plate and gelation was allowed to take place as in a).
- f) T resin of Compound 5.** To a mixture of methanol (0.05 mL), THF (0.2 mL) and 0.1M HCl (0.2 mL) compound 5 (0.03 g, 0.084 mmol) was added and solution was sonicated at 0°C for 45 minutes. A 1 μ L aliquots were then spotted on the stainless steel plate gelation was allowed to take place as in a).
- g) Silica/Compound 5 TQ resin.** To compound 5 (0.01 g, 0.028 mmol) in THF (0.2 mL) and 0.1 M HCl (0.2 mL) TEOS (0.15 mL) was added. The mixture was sonicated at 0°C for 1.5 hrs. A 1 μ L aliquots were then spotted on the stainless steel plate gelation was allowed to take place as in a).
- h) T resin of Compound 6.** Compound 6 (0.03 g, 0.057 mmol) in mixture of methanol (0.1 mL), 0.1M HCl (0.3 mL) and THF (0.15 mL) was sonicated at 0°C for 45 minutes. A 1 μ L aliquots were then spotted on the stainless steel plate gelation was allowed to take place as in a).

- i) **Silica/Compound 6 TQ resin.** Compound 6 (0.01 g, 0.018 mmol) in THF (0.2 mL) and 0.1 M HCl (0.25 mL), TEOS (0.15 mL) was added and mixture was sonicated at 0°C for 1.5 hrs. A 1 μ L aliquots were then spotted on the stainless steel plate gelation was allowed to take place as in a).
- j) **Silica coated with Compound 1.** Silica sol was prepared as in a). After sol was aged over two days, a 1 μ L aliquot of 5% solution of compound 1 (0.005 mL) in methanol (0.095 mL) was applied as a coating on the top of aged silica. The film was aged over 2 days in open air, prior to MALDI analysis

3.5.6 MALDI Preparation

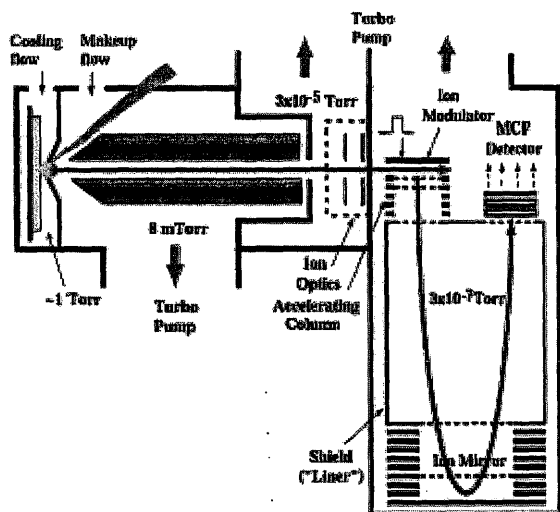
Four types of molecules were used for MALDI analysis in order to test the applicability of our system for various analytes, including small peptide and small organic molecules: Glu¹-fibrinopeptide B¹⁷ (Glu-fib) (MW 1570), trimethoprim (TMP) (MW 290), haloperidol (MW 375), and fluorescein (MW 332). The final molarity of each analyte in water or in 0.1% TFA/acetonitrile was calculated to be glu-fib (6.36 pmol/ μ L), TMP (34.48 pmol/ μ L), haloperidol (26.66 pmol/ μ L) and fluorescein (30.12 pmol/ μ L). The standard analyte solution was prepared at a 1:1:1:1 ratio by volume of Glu-fib, TMP, haloperidol, fluorescein (final concentration of each analyte =2.5 ng/ μ L). 1 μ L of standard analyte mixture was applied to all of the silicon-based films prior to MALDI analysis.

3.5.7 MALDI-TOF Experiments

MALDI analysis was done using proTOFTM 2000 MALDI O-TOF Mass Spectrometer (PerkinElmerSCIEX) equipped with a 337-nm N₂ laser and a 20-kV acceleration voltage.

Mass spectra were generated from the average of 300 laser shots, at 10 Hz laser rate, 210 mL/m focusing gas flow, 90 mL/m cooling gas flow and 70% laser energy. The MALDI-TOF set up used is given in Figure 3-15.

Figure 3-15. Schematic of MALDI Instrument



3.6 References

- ¹ Bashir, S., Mutter, R., and Derrick, P.J., *Analyst*, 128, 2003, 1452-1457.
- ² Meng, J.-C., Averbuj, C., Lewis, W.G., Siuzdak, G. and Finn, M.G., *Angew. Chem. Int. Ed.*, 43, 2004, 1255-1260.
- ³ Mouradian, S., Nelson, C.M. and Smith, L.M., *J. Am. Chem. Soc.*, 118, 1996, 8639-8645.
- ⁴ Huang, J. and Hemminger, J.C., *J. Am. Chem. Soc.*, 115, 1993, 3342-3343.
- ⁵ Voivodov, K.I., Ching, J. and Hutchens, T.W., *Tetrahedron Lett.*, 32, 1996, 5669-5672.
- ⁶ Hutchens, T.W. and Yip, T.-T., *Rapid Comm. Mass Spectrom.*, 7, 1993, 576-580.
- ⁷ Ching, J., Voivodov, K.I. and Hutchens, T.W., *J. Org. Chem.*, 61, 1996, 3582-3583.
- ⁸ Martic, S., Chen, Y., Brennan, J.D. and Brook, M.A., *Anal. Chem.*, submitted
- ⁹ Brook, M., *Silicon in Organic, Organometallic, and Polymer Chemistry*.(Chapter 12). New York: Wiley, 2000
- ¹⁰ Zenobi, R. and Knochenmuss, R., *Mass. Spectrom. Rev.*, 17, 1998, 337-366.
- ¹¹ a) Krause, J., Stoeckli, M. and Schlunegger, P.U., *Rapid Comm. Mass Spectrom.*, 10, 1996, 1927-1933; b) Chiarelli, M.P., *Anal. Chem.*, 65, 1993, 307-311; c) Kovi, P.J., *Anal. Chim. Acta*, 61, 1972, 7-13; d) Liao, P.C., *J. Mass Spectrom.*, 30, 1995, 408-423; e) Knochenmuss, R., *J. Chem. Phys.*, 91, 1989, 1268-1278; f) Gimon, M.E., Preston, L.M., Solouki, T.M., White, A. and Russell, D.H., *Org. Mass Spectrom.*, 27, 1992, 827-832.
- ¹² a) Dai, Y., Whittal, R.M. and Li, L., *Anal. Chem.*, 68, 1996, 2494-2500; b) Vorm, O., Roepstorff, P. and Mann, M., *Anal. Chem.*, 66, 1994, 3281-3287; c) Amado, F.M.L.,

Domingues, P., Santana, M.G., Ferrer, A.J. and Tomer, K.B., *Rapid Comm. Mass Spectrom.*, 11, 1997, 1347-1352.

¹³ Voivodov, K.I., Ching, J. and Hutchens, T.W., *Tetrahedron Lett.*, 37, 1996, 5669-5672.

¹⁴ Karas, M., Ehring, H., Nordhoff, B., Stahl, K., Hillenkamp, M.G. and Krebs, B., *Org. Mass Spectrom.*, 28, 1993, 1476-1481.

¹⁵ Xiang, F and Beavis R.C., *Rapid Comm. Mass Spectrom.*, 8, 1994, 199-204.

¹⁶ Dreisewerd, K., *Chem. Rev.*, 103, 2003, 395-425.

¹⁷ Loboda, A.V, Ackloo, S. and Chernushevich I. V., *Rapid Comm. Mass. Spec.*,17, 2003, 2508-2516.

4 CHAPTER 4. CASE STUDY OF SILICON-BASED MATRIX

4.1 Introduction

In conventional MALDI, the matrix in the free state absorbs and transfers energy from the laser to the analyte, and can also be vaporized into gas phase as a carrier of the analyte.

A number of different approaches have been developed to minimize the extent to which matrix-related interferences are present in the low molecular region of the spectrum. Alternative methods which utilize inorganic over organic matrices were discussed in Chapter 1-Chapter 3.^{1,2,3}

An alternative method to achieve minimal matrix interference and permit analysis over a large mass range exploits sol gel-based silica supports in which the matrix is immobilized via non-covalent or covalent interactions.^{4,5,6,7,8} Recent attempts to completely remove matrix-related signals from the mass spectrum have led to improved S/B in spectra,^{5,9} but the technology is highly dependent on the matrix concentration used, that is, the matrix interference background can only be obtained upon carefully adjusting the matrix concentration to an appropriate range.⁵ Even in the best cases, matrix signals usually confound analyte analysis. There are other analyte specific problems with current technology. For example, there is an analyte signal variability observed upon subsequent laser irradiation which renders the use of non-covalent sol-gel methods unreliable.^{5,9} Moreover, the appearance of the matrix background became unavoidable when larger

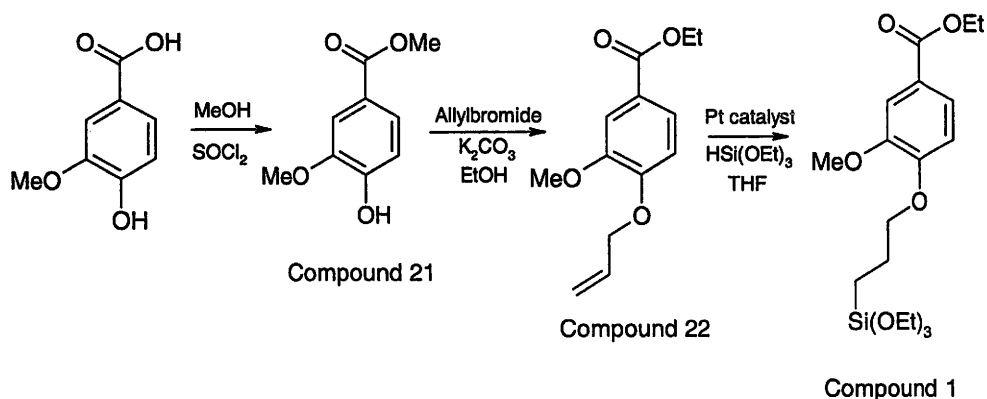
analytes were analyzed, since higher laser power was needed to ionize molecules of higher molecular weight.

Herein, we report the use of a high surface area MALDI support material containing silicon-based matrices that were covalently tethered to a silica network, which proved to be highly analyte selective and effective at suppressing interfering low molecular weight matrix signals. The material produced is stable, easily processable and can be fabricated as thick films. The matrix-free spectrum was obtained reproducibly without the evident dependence on the sol gel precursor concentrations used.

4.2 Results

2,5-Dihydroxybenzoic acid (DHB) is a commonly used MALDI matrix. We prepared, using the route shown in Scheme 4-1, an analogue to DHB that additionally possesses a trialkoxysilyl group that can be used to tether the matrix to a silica surface. All the compounds were identified by FTIR, ^1H and ^{13}C NMR and mass spectrometry. Thus, the methyl ether of 3,4-dihydroxybenzoic acid was protected as the methyl ester (**21**). Treatment with base and allyl bromide provided the requisite allyl synthetic handle. Due to the sensitivity of the methyl ester to pH changes, we have performed a transesterification step where the methyl ester was replaced with an ethyl ester in order to ensure the ester stability during the sol gel processing under acidic conditions. The resulting allyl ether **22** was subjected to platinum catalyzed hydrosilylation with $\text{HSi}(\text{OEt})_3$, which produces the DHB analogue **1**.

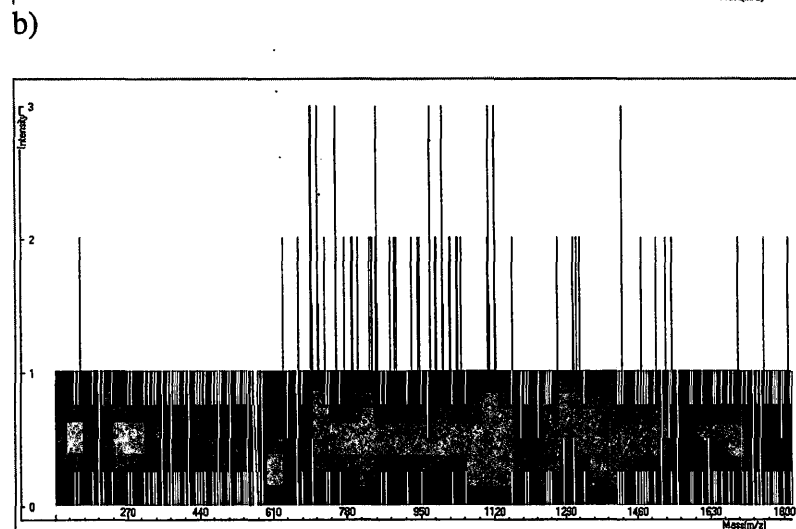
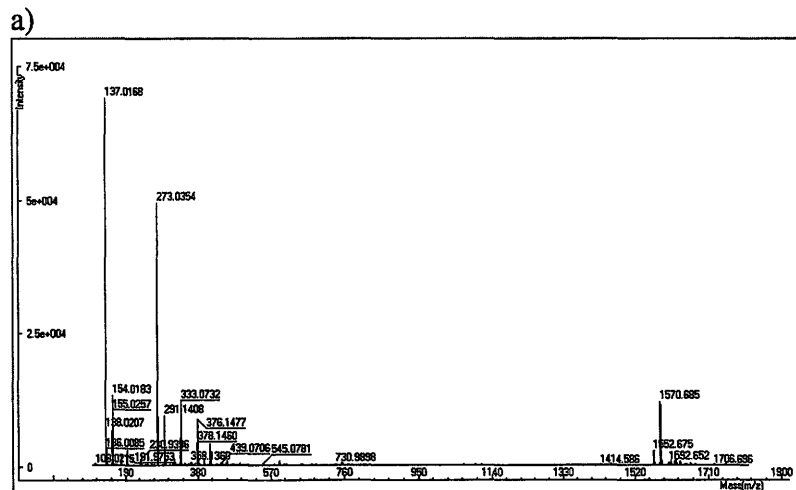
Scheme 4-1. Synthesis of triethoxysilylated derivative.

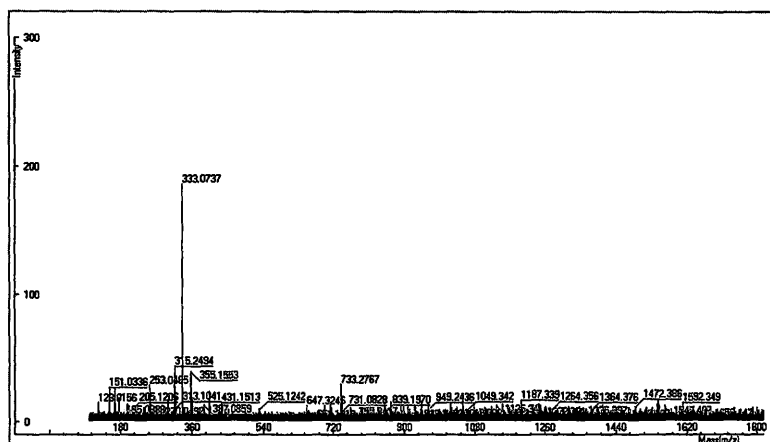


Herein, we prepared porous materials by doping silica with precursor molecules that were subsequently tethered into the monolith. Compound 1 was incorporated in silica in three distinct ways: i) compound 1 was itself used as a matrix and a high surface area support (T resin); ii) compound 1 was mixed with TEOS and then cured into a mixed TQ resin;¹⁰ or iii) compound 1 was cured into a porous silica film. These different supports were then compared in the MALDI experiments that examined four representative analytes: Glu¹-fibrinopeptide (*m/z* 1570), haloperidol (*m/z* 376), fluorescein (*m/z* 333) and trimethoprim (*m/z* 291).

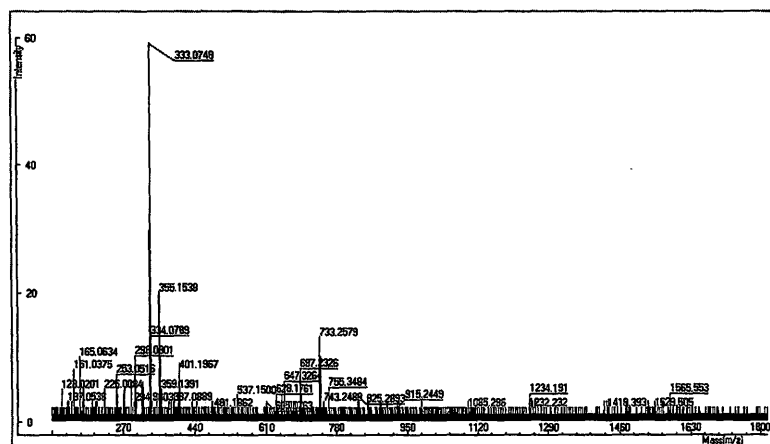
The typical MALDI spectrum obtained using standard DHB as the matrix (Figure 4-1a) is compared in with the spectra obtained on the three supports that incorporated compound 1 (Figure 4-1a-d).

Figure 4-1. MALDI MS using a) DHB, b) T resin, c) Compound 3/TEOS TQ resin, d) Cured silica with Compound 3 as MALDI support (analyte on top).





d)

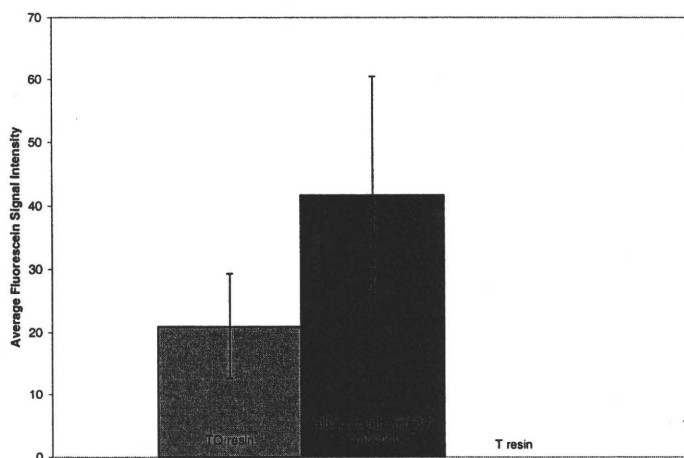


It can be seen that the silsesquioxane support prepared by sol-gel its condensation alone did not lead to any desorption or ionization in the MALDI experiment (Figure 4-1b). However, co-hydrolysis and co-condensation of **1** with TEOS gave rise to a support that afforded a selective desorption and ionization of exclusively fluorescein; where fluorescein intensity was predominant while those of TMP and haloperidol were negligible (Figure 4-1c). Similar results were obtained when compound **1** was subsequently chemisorbed on a mesoporous silica surface rather than being co-

hydrolyzed with TEOS (Figure 4-1d). These data are consistent with those shown for compound **5**, **6** (see Chapter 3).

On the basis of MALDI results, it was concluded that the ability to desorb and ionize analytes is enhanced by incorporating **1** into the silica network rather than by employing it alone. In this manner, a morphology is engineered which possesses key characteristics for MALDI performance: UV absorbance and higher surface area. The mesoporous silica derived from compound **1** did not result in analyte ionization, while the mesoporous TQ resin effectively led to the appearance of fluorescein (Figure 4-2).

Figure 4-2. Average signal intensity using compound 1 as T, TQ resin or when coated over silica.

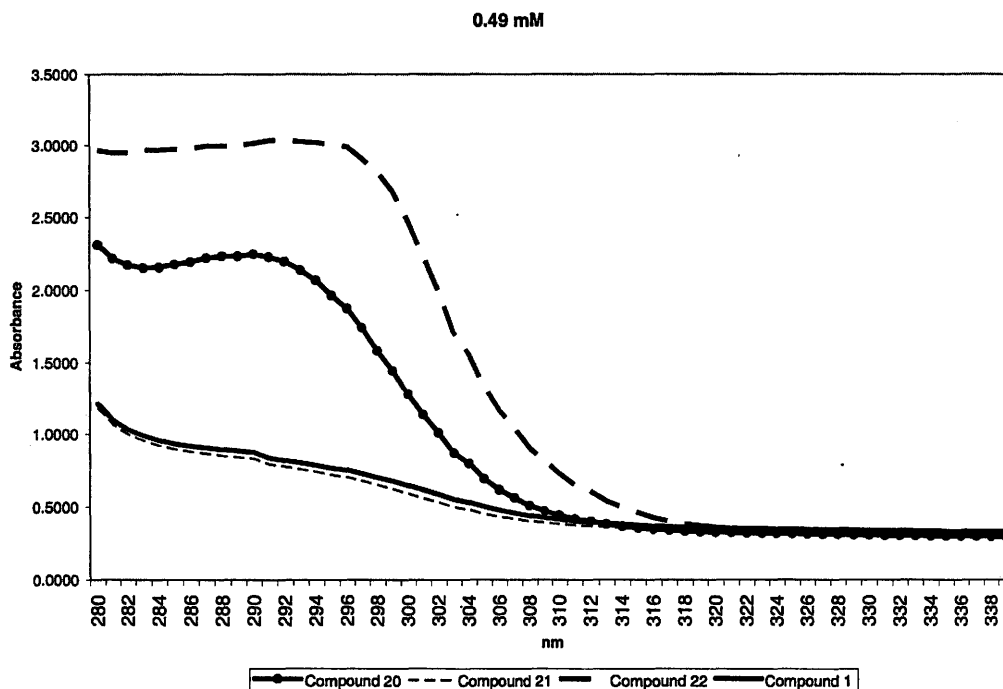


The proton source in our systems does not reside in free phenol or carboxylic acid groups, but is rather a result of more complex ionization mechanisms (thermal ionization and desorption of preformed ions)¹¹ in MALDI, which are still not completely known.

The prerequisites for a substance useful as a MALDI matrix are its ability to absorb at the wavelength of laser used and its ability under those conditions to transfer energy to analytes. We have studied the effect of functional group modification on UV

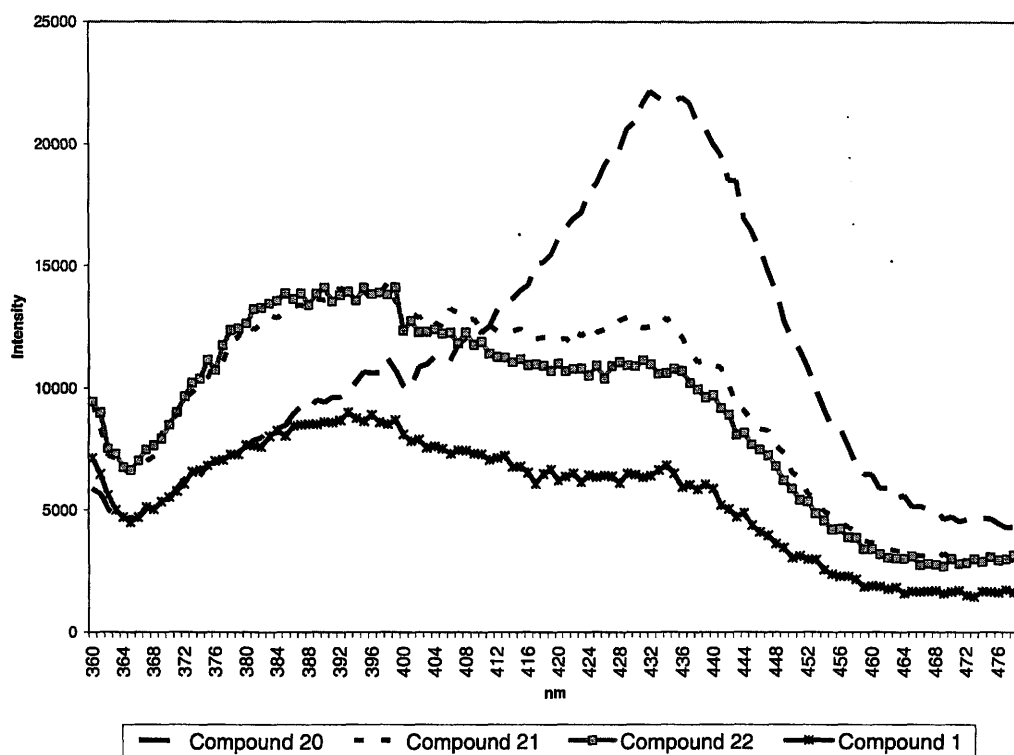
absorbance for the compounds presented in Scheme 1. UV spectra were obtained by dissolving compounds of interest in methanol. The UV spectra of starting material and compounds **1**, **21**, **22** are presented in Figure 4-3. From UV studies it is apparent that all four compounds shown in have absorption maxima near 292 nm. The absorption coefficients observed at 337 nm for 4-hydroxy-3-methoxybenzoic acid, **1**, **21**, **22** were 1065.93, 1054.94, 1076.60 and 1053.69 L/mol·cm, respectively. The UV study suggested that all of the compounds of interest could be used as UV-MALDI matrices, since the absorptivity coefficients observed are comparable to that for DHB (4139.77 L/mo·*cm). Thus, the efficacy of allyloxy-derivative as a matrix might be expected. It was concluded from the UV spectrum of a silicon based compound that the introduction of triethoxysilyl functionality has no dramatic effect on the absorbance.

Figure 4-3. UV spectra of the compounds from Scheme 4-1.



A change in the electronic behaviour of a matrix as a function of functional group modification was investigated by fluorescence spectroscopy (Figure 4-4). From the emission spectrum, a major peak (432 nm) was observed for the starting material containing free phenol and carboxylic group. Masking of the phenol and an acid by an allyloxy and ester group led to a decrease in the 432 nm peak and the appearance of an additional peak at 386 nm. Introduction of a Si(OEt)₃ group resulted in a decrease in the UV absorbance, but with retention of the two signature peaks.

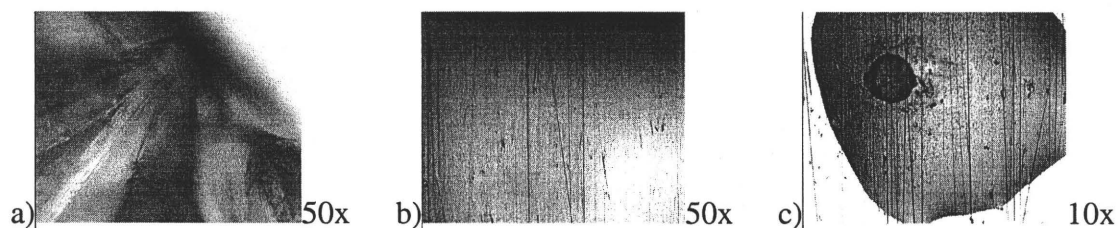
Figure 4-4. Fluorescence spectra of the compounds from Scheme 4-1.



We have performed a MALDI study of 4 analytes (glu-fib, trimethoprim, fluorescein, haloperidol) comparing surface-bound with unbound matrices as presented in Scheme 1-1, in order to study the effect of crystallization on signal intensity. A series of

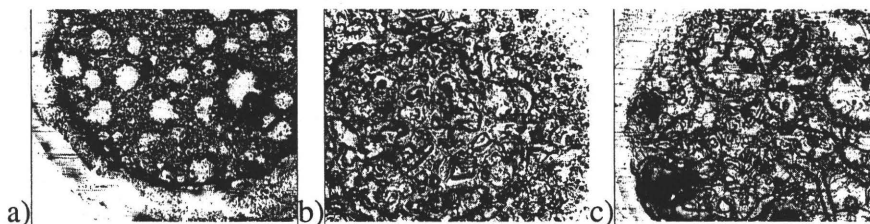
matrix solutions was prepared by dissolving **1**, **22**, **22** respectively, into methanol. We observed ionization of TMP and fluorescein when **20** was used that possessed both a free phenol and carboxylic acid, which could be ascribed to its high crystallization behaviour and a required functionality (Figure 4-5a). Similarly, when a methyl ester derivative was used as a matrix, analyte ionization could be associated with its free phenol group despite the absence of crystals (Figure 4-5b). In this case, TMP and fluorescein were observed, as well. The poor performance of allyloxy-derivative **22** can be ascribed to two factors; its poor crystallization and the absence of relevant acidic functionality (Figure 4-5c). An optical micrograph of droplet residues deposited on steel plates revealed large crystalline domains for matrices with free phenolic and carboxylic acid groups. However, the level of crystallization was dramatically reduced when such groups were protected, such as in **22**. Masking of carboxylic acid by an ester and/or masking of a phenol by an allyloxy group severely reduced compound's ability to form crystals. While the ester derivative is a solid, an allyloxy ester derivative is a liquid under standard conditions. Analogously, when silicon-based derivative was treated as a standard matrix (dissolved in the solvent and spotted) without further processing to give a T-resin, it exhibited poor performance as MALDI matrix.

Figure 4-5. Optical micrographs of a) 4-hydroxy-3-methoxybenzoic acid, b) compound 21 and c) compound 22



We suspected that MALDI performance also depended on the localization of the matrix and its inherent environment. Matrix-analyte interactions will affect the final ion yield of protonated fluorescein. Several trends were apparent from the optical images presented in Figure 4-6a-c. Irrespective of whether sol gel was made up of pure compound **1** T resin, or whether it had been converted by sol gel processes into a TQ resin, crystalline domains were not observed: the surfaces were smooth and appeared homogeneous. However, since the pure silicon-based derivative did not work alone as a matrix, it is expected that its excess over TEOS would be undesirable. As can be seen in Figure 4-6b, the compound **1** did not crystallize on its own, nor did it appear to have any highly ordered domains. Hence, no crystalline domains were observed for the surface support that worked as MALDI matrix for fluorescein. Notably, all of the silicon based covalently tethered matrices developed have failed to ionize peptides such as glu-fib, despite the previous reports on ionization of the higher mass peptides (>2000 Da) from the covalently bound absorbing surface.

Figure 4-6: Optical microscope images: a) Compound 1 T resin, b) TQ resin, c) silica coated with 1.



A comparison of the MALDI signal intensity between two kinds of supports, were made, a TQ resin and TEOS film coated with compound **1**: higher fluorescein ion intensity and better reproducibility were observed when the latter support was used. This may be due to the limited matrix-analyte interactions when compound **1** was embedded within silica. However, the analyte signal was found everywhere on the sol-gel derived film, suggesting that the analyte molecules were evenly distributed on the film. Such an observation suggests it is possible to eliminate the “sweet spot” phenomenon, which is commonly observed when standard MALDI matrices are used. On the basis of the results obtained, we have concluded that the necessity for crystallization was not an important concern in MALDI experiments.

When compared with free DHB, grafted **1** offers minimal interference in the low mass region and has led to the superior signal-to-background ratios, particularly for the desorption and ionization of fluorescein (m/z 333, $[M+H]^+$), for reasons which are being further investigated. In terms of average signal intensity, significant decrease was observed with grafted **1** when compared to free DHB. The higher signal intensity observed with DHB occurs at ‘sweet-spots’ which are absent from our systems: away from sweet spots, DHB is inferior.

Although there exists the belief that an exchangeable phenolic or carboxylic acid proton is needed for proton transfer in MALDI process, it is clear that such an exchangeable proton is not required for the formation of protonated analyte ions from **1**. Matrices that did not possess any free phenol or carboxylic groups were used successfully in MALDI analysis of certain analytes, in this case fluorescein.¹² The results obtained with our silica support are very much consistent with the model of photoinduced chemical or thermal ionization¹³ rather than with the model of excited-state species being the source of protons for MALDI, which is predictable for phenolic systems.¹⁴

In terms of analytical parameters, the limit of detection (LOD) for fluorescein was found to be about 2.5 nm/ μ L (\sim 3 pmol/ μ L), which is somewhat higher than the LOD observed for solid, acidic matrices. Our support allowed for far greater S/B ratios where the protonated molecular analyte ion was the predominant peak in the mass spectrum. So far, no clear relationship has been established between the nature of the analyte and the tethered matrix itself. Thus, it is not currently possible to generalize these results for different analytes.

No single matrix currently exists that can be used for all the analytes of interest ranging from the biomolecules and synthetic polymers to small molecules. Hence, the analyte selectivity of our silica support did not come as a surprise, since its behaviour does not deviate from that observed for standard MALDI matrix. The selectivity of **1** for fluorescein could be a result of the interactions between the organic residues in silica and analytes, and due to its inherent surface morphology. For example, the anionic analyte may be more effectively ejected from an anionic silica surface than other analytes. Glu-

fib, also an anionic molecule, needs more effective energy transfer because of its larger size.¹⁵ We suspect that by changing the sol gel precursors, by introducing different chemical functionalities, we will be able to develop other supports of varying selectivity. Subsequently, the correlation studies can be developed in order to further probe the correlation that exists between the MALDI support and the analytes.

We have demonstrated that surface morphology and inherent microstructure are important factors for MALDI performance. Our new material is a combination of mesoporous silica and covalently tethered matrix. Such a unique combination results in the efficient UV absorbance, efficient energy transfer and intimate analyte-to-matrix contact. Our supports offer a minimal interference in the low mass region and lead to an excellent signal-to-background ratio and greater instrumental signal-to-noise ratio. Interestingly, our sol gel acts as a selective support, which allows for the desorption and ionization of fluorescein exclusively for reasons which are being further investigated. In this manner, engineered morphology possesses the key characteristics for MALDI performance, i.e. the higher surface area and UV absorbance. The superior signal-to-background values and preferential binding of analytes observed using our support can be used to develop bioaffinity MALDI support that could lead to selective ionization within the complex mixture.

4.3 Summary

It was believed that the intrinsic matrix properties needed for optimal MALDI performance included UV absorbance, crystallization and chemical functionalities. We developed and tested silicon-based compounds (free of phenols and acid) as an alternative

matrices. Selective matching of analyte and matrix was possible by use of TEOS as an additional precursor. The TQ resin system offered a possibility of performing the standard MALDI analysis with less matrix amount required than when the standard matrix (CHCA) was used. In addition, silicon-based matrix was highly selective for fluorescein over TMP, haloperidol and glu-fib.

4.4 References

- ¹ Wei, J., Buriak, J.M. and Siuzdak, G., *Nature*, 399, 1999, 243-246.
- ² Paterson, D.S., Luo, Q., Hilder, E.F., Svec, F. and Frechet, J.M.M., *Rapid Comm. Mass Spectrom.*, 18, 2004, 1504-1512.
- ³ Zhang, Q., Zou, H., Guo, Z., Zhang, Q., Chen, X. and Ni, J., *Rapid Comm. Mass Spectrom.*, 15, 2001, 217-223.
- ⁴ Cohen, J.L. and Cox, J.A., *J. Sol-gel Sci. Tech.*, 28, 2003, 15-18.
- ⁵ Lin, Y-S. and Chen, Y-C., *Anal. Chem.*, 74, 2002, 5793-5798.
- ⁶ Lin, Y-S, Yang, C-H. and Chen, Y-C., *Rapid Comm. Mass Spectrom.* 18, 2004, 313-318.
- ⁷ Chen, C-T. and Chen, Y-C., *Anal. Chem.*, 76, 2004, 1453-1457.
- ⁸ Chen, W-Y and Chen, Y-C., *Anal. Chem.*, 75, 2003, 4223-4228.
- ⁹ Chen, C.-T. and Chen, Y.-C., *Anal. Chem.*, 18, 2004, 1956-1964.
- ¹⁰ Brook, M. A. *Silicon in Organic, Organometallic, and Polymer Chemistry*, Wiley: New York, 2000, Chap. 1.

- ¹¹ Zenobi, R. and Knochenmuss, R., *Mass Spectrom. Rev.*, 17, 1998, 337-366.
- ¹² Grigorean, G., *Eur. J. Mass. Spectrom.*, 2, 1996, 139-143.
- ¹³ Hilenkamp, F., Karas, M., Beavis, R.C. and Chait, B.T., *Anal. Chem.*, 63, 1991, 1193A-1202A.
- ¹⁴ Gimon, M.E, Preston, L.M., Solouki, T., White, M.A. and Russell, D.H., *Org. Mass. Spectrom.*, 27, 1992, 827-830.
- ¹⁵ Liao, P.C., *J. Mass Spectrom.*, 30, 1995, 408-423.

Conclusions and Future Directions

Initially, our objective was to effectively remove matrix-related signals while preserving the overall signal intensity in MALDI-TOF spectrum. By doing so we would maintain advantages associated with MALDI and extend this technique to the study of low mass compounds. With the development of optimal mesoporous supports (with DHB) we enhanced S/B ratios for cationic, anionic and neutral analytes by varying the sol gel composition. However, under the conditions used we were unable to completely remove matrix signals without impinging on the signals intensity of analytes. Notably, a macroporous silica (with DHB) was highly ineffective matrix in terms of overall signal intensity.

The next step would be to perform similar studies with other MALDI matrices. Since any two standard matrices perform differently in MALDI, it would be expected that their performance will vary even when they are introduced in silica. By performing such a study, a further understanding of the role of silica can be established. More general trends are expected to appear when sol gel system is applied to different matrices.

For example, use of structural analogues of 2,5-DHB, such as sinapinic acid, and its derivatives will offer a better understanding of processes which take place in silica-based supports. Since it is well known that DHB and sinapinic acid undergo different protonation mechanisms, a photoinduced ionization and ESPT reaction, respectively, it would be interesting to study the extent of silica effect on both such processes; moreover, this information could then be used to develop materials with enhanced sensitivity and

higher S/B ratios. One could also imagine to use other sol gel precursors (e.g., DGS, TMOS etc) in order to study the effect of silica's nature on matrix performance.

Another line of analysis was to develop different types of silica supports, by using silsesquioxanes rather than PEO-doped silica. Here, covalently linked organic UV absorbing compounds were permanently linked to the surface rather than entrained by simple physisorption. It has been shown that all of the silsesquioxanes developed failed to work as matrices when in their free state. It is well known that free matrices behave differently from when they are immobilized on the surface. In the light of our success with mesoporous silica we decided to develop other mesoporous supports with high surface area. It has been demonstrated that a removal of low mass interference signals was obtainable by using chemically tethered silicon-based matrices which allowed for highly selective desorption and ionization. In this study, a drastic difference was observed for T and TQ resins. However, most of the TQ resins (co-hydrolyzed and co-condensed TEOS with silsesquioxane) have led to a selective desorption of low or moderate signal intensities. Moreover, a higher selectivity was observed for an anionic type analyte (fluorescein). Alternative approaches one can take in order to optimize such mesoporous TQ resins would be to vary the molar ratio of silsesquioxane and TEOS.

There are many possibilities for chemically derivatized standard MALDI matrices. One might conceive of modifying a cinnamic acid type molecule which is another typical MALDI matrix. It is not inconceivable to assume that a tethered matrix of the higher absorbance could undergo a more efficient energy transfer, which would lead to higher sensitivity and possibility of analyzing molecules of higher molecular weight; hence,

further development of chemically different silsesquioxanes is needed to develop desirable ideal matrix.